'Effect of Ethanol and Biodiesel Addition on the Movement and Biodegradation of Volatile Petroleum Hydrocarbons in the Subsurface'

ABDULMAGID ELAZHARI M. ALI

BSc. MSc MRSC

Thesis submitted to Newcastle University in partial fulfilment of the requirements of the degree of Doctor of Philosophy

April 2011

Department of Environmental Engineering
School of Civil Engineering and Geosciences

Abstract

The microbial degradation of typical volatile petroleum hydrocarbons in an aerobic sandy soil was studied with and without the blending of 10 percent ethanol (E10) or 20 percent biodiesel (B20) in batch microcosms and mini-lysimeters. In the head-space of the mini-lysimeters all volatile compounds remained above the analytical detection limits over 92 days except toluene in the pure petroleum hydrocarbon mixture (PP) and ethanol in E10. The mass percentage of each petroleum hydrocarbon compound remaining at the end of the experiments was comparable for all fuel mixtures, except for m-xylene, which was significantly less reduced in E10 as compared to PP and B20. Total cell counts at the end of the experiments were highest for E10 and lowest for PP. DGGE analysis revealed a distinct microbial community structure for each fuel mixture. Batch studies confirmed these observations, in particular slower degradation of toluene in the presence of ethanol. Inorganic nutrient addition to the batch systems resulted in higher total cell counts, more rapid microbial degradation rates and more similar microbial community structures. Under aerobic conditions, competition for scare inorganic nutrients seems to be the most plausible reason for slower monoaromatic hydrocarbon biodegradation in the presence of more readily degradable biofuel.

Key words: Natural attenuation, VOCs, biofuels, microbial ecology, soil.

Declaration

I, the undersigned, hereby declare that this thesis entitled, "EFFECT OF ETHANOL AND BIODIESEL ADDITION ON THE MOVEMENT AND BIODEGRADATION OF VOLATILE PETROLEUM HYDROCARBONS IN THE SUBSURFACE" is my own work and that it has not been submitted for fulfilment of a degree at this or any other university, and that all the sources I have used or quoted have been indicated or acknowledged by means references.

Abdulmagid Elazhari Ali.

Acknowledgements

This thesis would have never been completed without the will and blessing of Allah, the most gracious, the most merciful. AL HAMDU LELLAH

It is a pleasure to thank those who made this thesis possible such as my Family and my parents who gave me an invaluable and moral support I required and my Organisation, Petroleum Training & Qualifying Institute, Tripoli, Libya, for the invaluable financial support.

I am heartily thankful to my supervisory team, who are responsible for the successful completion of my dissertation Dr David Werner and Dr Russell Davenport, whose encouragement, supervision and support from the preliminary to the concluding level enabled me to develop an understanding of the subject. Their untiring effort, commitment, encouragement, guidance and support helped me greatly in the understanding and writing of the dissertation without their corporation I could not have gotten such relevant work.

I am grateful to my thesis examiners, Prof Patrick HÖHENER and Dr Neil Gray. Their comments and feedback have significantly improved this thesis.

I also would like to make a special reference to Professor Ian. M. Head and Dr Arvind Singh for the help with some molecular analyses.

I would like to take this opportunity to thank all those who have contributed in any way, shape or form to the completion of this project report. Those at Environmental Engineering and Geosciences laboratories for their advice and support, friends for their ideas and criticisms.

Contents

List of Figures

List of Tables

1 Introduction

1.1 Overview

The overall quality of the environment is inextricably linked to the quality of life on Earth. Nowadays many countries face problems associated with contaminated sites. In the past when awareness of the health and environment effects connected with production, use, and disposal of hazardous substances were less well recognised than today, industrial activities have resulted in contaminated land, and the estimated number of contaminated sites is a global problem (Vidali, 2001).

The universally recognised concerns over air, soil and water pollution, whose effects have been clearly seen even to casual observers for centuries is in a sharp contrast to this situation. It has been reported that water pollution worries have been recorded in ancient Rome. For instance, the effect of the city's untreated sewage on the River Tiber were recognised as dangerous to human health (Halstead and Ebooks Corporation., 1998). Another example of a concern which has a long history are the smoke clouds that covered Elizabethan London which were clearly related to various human aliments, and quite serious efforts have been made to find a successful solution, for instance to ban the use of coal for domestic fuel (Evelyn et al., 1933).

In the late 1970s, land contamination was first identified in a few of the industrialized nations, and the hazard this could pose was still unknown. Some governments concerned, thus had to react in a state of too little, incomplete and partial information available, these governments are in the United States, the Netherlands, West Germany and the United Kingdom. However, other industrialised countries chose to do nothing and not to treat land contamination as a problem of real concern (Cairney and Hobson, 1998).

Further convincing proof has been given of the links between air, soil and water pollution events and related declines in the quality of life seen as the loss of fish in some rivers adjacent to industrialised sites, the destruction of trees and crops lying downwind of smelters and industrial chimneys, and the reduced life expectancies likely to occur in many industrial employments, as a result of the

continuous growth in industrialisation in West Europe, in the 18th and 19th centuries (Trevelyan, 1952).

It is now widely recognised that contaminated land is a potential threat to human health, and this discovery over recent years has led to international efforts to remedy many of these sites, either in response to the risk of adverse health or environmental effects caused by contamination or to enable the site to be redeveloped for new uses.

1.1.1 What is contaminated land?

The Environmental Protection Act 1990, Part II (a) details the legislation framework for dealing with contaminated land. This statutory guidance was brought into force in England on 1st April 2000 and defines contaminated land as:

"Any land, which appears to the Local Authority in whose area it is situated, to be in such a condition, by reason of substances either in, on or under the land, that:

i. Significant harms is being caused or there is the significant possibility such harm being caused; or,

ii. Pollution of controlled waters is being, or is likely to be caused".

The guidance has defined harm as "harm to the health of living organisms or other interface with the ecological systems of which they form part and, in the case of man, also includes harm to his property". Moreover, the statutory guidance also identifies how the regime operates and includes guidance on the identification of contaminated land and special sites, remediation, exclusion from (and appointment of) liability for remediation and recovery of costs of remediation (Environmental Agency, 2006).

In order for contaminated land to exist, the Local Authority must satisfy itself a POLLUTION LINKAGE exists in relation to the land. A pollution linkage comprises three separate components:

i. a SOURCE of contamination;

ii. a RECEPTOR for that contamination to affect, and;

iii. a PATHWAY capable of exposing a receptor to the contaminant source.

Consequently, land can only be designated as contaminated where it is causing unacceptable risk to human health or other specific receptors. Therefore, under this legal definition, contaminated land does not cover all land where contamination is present (Environmental Agency, 2006).

1.1.2 Contaminated land in the UK

The contaminated land in the UK arises largely as a result of past industrial processes which have left a legacy of many hazardous substances in the ground, including heavy metals, organic compounds, oils and tars, and soluble salts. These substances can represent an actual or potential threat to the environment, to humans, or occasionally to other targets. Although much of the contaminated land is the result of past activities associated with the industrial revolution many contaminative uses are still in operation today (Hestor and Harrison, 1997).

There is no doubt that the presence of land contamination in the UK is an invisible legacy of its industrial past. Moreover, it has been argued that the UK has seen human activities leaving contamination, either concentrated or altered in its chemical form, at least since the time of Roman lead mining, and an increasing range of new compounds have been manufactured and added to the list of contaminants and as a result the affected area of land has increased dramatically. Current estimates suggest between 100’000 and 220‘000 ha of land are contaminated, which represents between 0.4 and 0.8% of the UK land area (Hestor and Harrison, 1997).

1.2 Land pollution by petroleum hydrocarbons in the UK and worldwide

The releases of petroleum hydrocarbons to the soil environment may pose potential risks to human health, water resources, ecosystems, property and other environmental receptors. Managing the potential risks requires an understanding of the impact of exposure to petroleum on each of these receptors, enabling the development of a structured risk assessment framework. Unacceptable risks to human health and the environment from past and current contamination are being addressed in the UK by part IIA of the Environmental Protection Act 1990. Implementation of Part IIA provides the opportunity to develop a framework for the risk assessment of petroleum contamination in soils that addressed UK legislation and its supporting guidance and provides clarity in the process (Environmental Agency, 2003).

The removal of deleterious compounds from the environment is an area of focus at the forefront of environmental protection agencies worldwide.

On a global scale, it has been shown that, petroleum hydrocarbons are some of the most common pollutants in soil and groundwater. Recently there has been significant interest in research and development of new remediation approaches to remediate petroleum hydrocarbons polluted soil and groundwater. The petroleum hydrocarbons reach soil through spills, leaks from ruptured tanks and other disposal and storage facilities (Hinchee et al., 1995b).

1.3 Environmental concerns about blended fuels

Search for renewable transportation fuels, also called biofuels, resulted from the negative environmental consequences of fossil fuels. Hill et al. (2006) have reported that compared with ethanol, biodiesel releases just 1.0%, 3.8% and 13% of the agricultural nitrogen, phosphorus, and pesticides pollutants respectively, per net energy gain, and relative to the fossil fuels they displace, green house gas emissions are reduced 12% by the production and combustion of ethanol and 41% by biodiesel. Biodiesel also releases less air pollutants per net energy gain than ethanol (Hill et al., 2006). Owsianiak et al. (2009) have

reported that biodegradation of diesel/biodiesel blends in liquid cultures by a petroleum degrading microbial consortium showed that for low amendments of biodiesel (10%) the overall biodegradation efficiency of the mixture after seven days was lower than for petroleum-only diesel fuel. Preliminary laboratory studies have shown that ethanol can enhance the solubilisation of benzene, toluene and xylene (BTX) in water, and it might exert diauxic effects during BTX biodegradation (Corseuil and Alvarez, 1996). Similar findings have been reported by Hunt et al. (1997), who have found that at 500 mg/L ethanol, ethanol is likely to exacerbate the biochemical oxygen demand and exert a diauxic effect that would inhibit in situ BTX degradation. Moreover the inhibition of BTEX biodegradation and the possible decrease in sorption-related retardation suggests that ethanol is likely to increase BTEX plume lengths, as has been reported by Powers et al. (2001). Thus, while blending petroleum hydrocarbons with biofuels should achieve the primary aim of reducing greenhouse gas emissions, the implications for environmental pollution risks in a spill scenario need to be carefully assessed.

1.4 Physical properties of organic contaminants

Physical properties of organic contaminants which are important in determining their environmental fate have been reported as water solubility, octanol/water partition coefficient, vapour pressure, and Henry's Law constants.

The octanol/water partition coefficient is defined as the ratio of a compound's concentration in the octanol phase to its concentration in the aqueous phase of a two-phase system. Measured values for organic compounds range from 10^{-3} to 10^{7}. Compounds with low values (<10) are hydrophilic, with high water solubilities, while compounds with high values (>10^{4}) are very hydrophobic. Compounds with low water solubilities and high octanol/water coefficients will be adsorbed more strongly to solids and are generally less biodegradable in the environment. Highly soluble compounds tend to have low adsorption coefficients for solids and tend to be more readily biodegradable, but also more mobile in the environment (Crawford and Crawford, 1996).

Henry's Law states the distribution of a compound at the air/water interface. Henry's law constant depends on a compounds vapour pressure and solubility and is highly temperature sensitive. Temperature changes of 10^{o} C can give threefold increase in H_A (Crawford and Crawford, 1996).

Chemical or photochemical reactions are the main two reactions that most environmental contaminants are subject to. The removal of many hazardous organics from the environment can be achieved by biological organisms - particularly microorganisms play an important role as catalysts. Due to kinetic limitations, thermodynamically feasible contaminant transformations often do not occur in the absence of a biological catalyst, and lowering the activation energy that must be overcome for a reaction to proceed is possible via microbial enzymes (Mitchell, 1992).

1.5 Pollution remediation approaches

Despite over 25 years of development of subsurface remediation technologies and an increasing number of recourses dedicated to disseminate information about what has been learned in the process, cleanup of subsurface environments remains as one of the most difficult challenges for the environmental community today. A recent report by the U.S. Environmental Protection Agency has estimated that between 235,000 and 355,000 sites are contaminated by hazardous waste in the United States and will require between 30-35 years for clean-up (U.S.EPA, 2004) .

Methods which prevent soil and groundwater contamination are undoubtedly the most effective techniques for aquifer protection. However, contamination has occurred and continues to occur in thousands of sites due to leaching from waste disposal areas, spills, and leaks from thousands of underground storage tanks (Boopathy, 2000). Once contamination occurs, a suitable remediation technique must be applied. There are a number of techniques that may be used to either contain the pollutant, or treat the groundwater and at least partially clean up the aquifer (Wilson et al., 1986). These techniques range from removal of the polluted material with subsequent physical, chemical or

biological treatment on the surface, to physical containment and in situ treatment with chemicals or microorganisms (Wilson et al., 1986).

The clean-up of environmental pollution involves a variety of techniques, ranging from simple biological processes to advanced engineering technologies. Clean up activities may also address a wide range of contaminants. Technologies to remediate contaminated soil fall into two principals clean up approaches: in situ (which involves the treatment of contamination onsite without removing materials from the ground), and ex situ treatment (which requires the removal of contaminated soil for treatment or land filling). Selecting and designing the right clean up approach require skills and innovations (Lin et al., 1996).

Treatment type	Cost/yd^3	Required time (months)	Additional factors or expenses	Safety issues
Incineration	250-800	6-9	energy	air pollution
Fixation	90-125	6-9	transportation, monitoring	leaching
Coal-oil agloflotation	63-210	5-8	transportation	air pollution
Solvent extraction	220-460	6-10	transportation, energy	air pollution, solvent disposal
SCF	200-500	Variable	transportation, energy	high temp and pressure
Wet wet oxidation	75-250	Variable	transportation, energy	high temp and pressure
Landfill	150-250	6-9	monitoring	leaching
Bioremediation	40-250	9-60	time commitment of land	Interm. Metabolites

Table 1-1 .Comparison of Treatment Methods for Contaminated Soil (Lin et al., 1996)

1.6 Bioremediation

Since 1970s bioremediation has been a commercially technology. It has been reported that, bioremediation has gained increasing acceptance and publicity since the U.S. Environmental Protection Agency (EPA) and Exxon Company, USA, demonstrated its effectiveness and success on Alaskan beaches contaminated by the Valdez oil spill (Hinchee et al., 1995a).

In bioremediation studies, for determining the rate of natural attenuation or for designing and maintaining an active treatment system, the degradation rate for the pollutants is often the most important parameter (Van De Steene and Verplancke, 2007).

Microorganisms have been used to remove organic matter and toxic chemicals from domestic and manufacturing waste effluents for many years (Crawford and Crawford, 1996). Relatively new, over the past few decades, is the emergence and expansion of bioremediation as an industry, and its acceptance as an effective, economically viable alternative for cleaning soils, surface and groundwater contaminated with a wide range of toxic, often recalcitrant chemicals. Bioremediation is becoming the technology of choice for remediation of many contaminated environments, particularly sites contaminated with petroleum hydrocarbons. Bioremediation has also become an intensive area for research and development in academia, government, and industry (Crawford and Crawford, 1996).

Bioremediation refers to the productive use of biodegradative processes to remove or detoxify pollutants that have found their way into the environment and threaten public health, usually as contaminants of soil, water or sediments. These organic chemical pollutants are subject to enzymatic attack through the activities of living organisms. Most of modern society's environmental pollutants are included among these chemicals and the actions of enzymes on them are usually lumped under the term biodegradation (Crawford and Crawford, 1996).

1.6.1 Principles of bioremediation

Microorganisms (mainly bacteria) are able to destroy hazardous contaminants or transform them to less harmful products. This is the most important principle

in bioremediation. When the process takes place without human intervention it can be called intrinsic bioremediation or natural attenuation. If the technique requires the construction of engineered system in order to supply microbe-stimulating materials, then the process is called engineered bioremediation (National Research Council (U.S.). Water Science and Technology Board, 1993). When deciding whether bioremediation is the appropriate clean up for a site, a critical factor must be considered, which is the contaminants are susceptible to biodegradation by the indigenous organisms or by organisms that could be successfully added to the site. It has been shown that among the compounds most easily degraded in the subsurface are petroleum hydrocarbons (National Research Council (U.S.). Committee on Ground Water Cleanup Alternatives, 1994).

1.6.2 Factors influencing bioremediation

Like other technologies, bioremediation has its limitations, and for bioremediation to be effective where environmental conditions permit microbial growth and activity, its application often involves the manipulation of environmental parameters to allow microbial growth and degradation to take place at a faster rate (Autry and Ellis, 1992). Many factors may inhibit the biodegradation process and as a result the bioremediation technology will be affected, these factors include: the existence of the indigenous microbial community members capable of degrading the pollutants in a sufficient amount; the availability of contaminants to the microbial population; the soil type; temperature, pH, the presence of oxygen or any other electron acceptors, and the availability of inorganic nutrients mainly nitrogen and phosphorus (Vidali, 2001).

2 Literature Review

2.1. Overview

This chapter presents a review of the relevant literature for the remediation of petroleum hydrocarbons polluted soil. The main focus will be on intrinsic bioremediation and monitored natural attenuation (MNA) of petroleum hydrocarbons in the subsurface. Key parameters affecting fate, transport, and biodegradation of VOCs in the subsurface will be investigated. Moreover, the effect of available inorganic nutrients on the biodegradation of petroleum VOCs and the application of biostimulation techniques will be reviewed.

Finally a review related to the history of fuel oxygenate use up to its current status, will be presented and ends the chapter, including a discussion of fuel oxygenates fate and transport in the environment, as well as their biodegradation characteristics and their effect on the fate, transport and biodegradation of petroleum hydrocarbons. The fuel oxygenates that will be blended as a biofuel components, are mainly ethanol and biodiesel.

2.2. Petroleum hydrocarbon bioremediation

Due to accidental spills of fuels and other petroleum products from pipelines or underground storage tanks, petroleum hydrocarbons have become the most frequent groundwater contaminant. A residual held by capillary force in the unsaturated zone, can result from the fuel release to the subsurface (Hohener et al., 2006).

There is an urgent need to clean up polluted groundwater supplies and soils. Clean-up methods often employ the treatment of contaminants aboveground after pumping the contaminants to the surface by flushing the subsurface with water so that contaminants can dissolve. However, contaminants are not readily leached from soil, because organic contaminants generally sorb to soils, and therefore such aboveground treatment systems are generally inefficient and slow. Furthermore, most aboveground technologies involve physiochemical treatment processes that simply sequester the contaminants or transfer them to another environmental medium (Mitchell, 1992). Bioremediation offers a

potentially more effective and economical clean-up technique through partial or complete destruction of the contaminants, see Figure 2.1. The in situ process stimulates the growth of either indigenous or introduced microorganisms in the region of subsurface contamination and thus provides direct contact between microorganisms and the dissolved and sorbed contaminants for biotransformation. Use of in situ bioremediation for treatments of subsurface regions is challenging because these regions are difficult to characterize and the introduction of chemicals and microorganisms is not easy. Coupling this with our limiting understanding of factors controlling biotransformation pathways and reactions rates of many organic contaminants of concern makes establishing the utility of in situ bioremediation an important scientific and engineering problem (Mitchell, 1992).

Natural attenuation (passive remediation) refers to the observed reduction in contaminant concentrations and contaminant mass as contaminants migrate from their source into environmental media. Natural attenuation is a feasible approach to the remediation of soils and groundwater at many petroleum fuels contaminated sites. Monitored Natural Attenuation (MNA) is a remediation technique which relies on naturally occurring biodegradation processes that decreases the concentration and mass of contaminating substances over time in a specific environment i.e. soil, sediment, marine and water. However, it has to be demonstrated that the degradation process by the indigenous microorganisms are taking place through monitoring, when (MNA) is used as a remediation strategy (USEPA, 1999).

It has been shown that for determining the rate of natural attenuation, when designing and maintaining an active treatment system, the degradation rate of the pollutants must be taken into account, because it is the most important parameter (Van De Steene and Verplancke, 2007). It has been argued that natural attenuation of VOCs in the unsaturated zone can only be predicted when information about microbial biodegradation rates and kinetics are known (Hohener et al., 2006; Hohener et al., 2003).

For bioremediation to be successful, the bioremediation methods depend on having the right microbes in the right place with the right environmental factors for degradation to occur (Boopathy, 2000).

2.3. Monitored natural attenuation

Several studies have revealed that it is not just environmental factors which act on the fate and transport of petroleum hydrocarbons in the unsaturated zone, but also the experimental design plays an important role. Biodegradation of petroleum hydrocarbons has been investigated through many different methods such as:

2.3.1. Microcosm laboratory studies

Closed batch studies are widely used to investigate biodegradation and also the sorption of petroleum hydrocarbons. For instance, the aerobic biodegradation of 14 hydrocarbons in two soils was determined using a simple microcosm/respirometric method based on oxygen consumption, the depletion of oxygen over time in the headspace of microcosms containing soil and test chemicals concentrations (Miles and Doucette, 2001). In another study, eleven soil samples contaminated and non-contaminated top soils and aquifers from seven locations in Belgium were examined in lab-scale batch microcosms simulating in situ conditions for their indigenous biodegradation capacity (Moreels et al., 2004). Another approach to evaluate biodegradation in laboratory microcosms applies carbon isotope fraction as an indicator for in situ biodegradation of the fuel oxygenates (Somsamak et al., 2005).

2.3.2. Laboratory columns

The mobility and natural attenuation of petroleum hydrocarbon pollutants can be studied in column experiments. For instance, a study has reported the results of a series of experiments on toluene movement through soil columns of different length in sterilized, pre-exposed and unexposed soil (Jin et al., 1994). Another column study of the biodegradation of vapour-phase petroleum hydrocarbons used an intact soil core from the site of an aviation gasoline release (Moyer et al., 1996). Hohener et al. (2003) used a laboratory column study to investigate the rates and kinetics of petroleum hydrocarbon vapours

degradation in the unsaturated zone, and reported that a column approach is preferable for determining biodegradation rate parameters to be used in risk assessment models.

2.3.3. Large scale field lysimeter

More complex, but also more representative of field conditions are large-scale lysimeter studies. Oudot et al. (1989) used a large lysimeter to study the hydrocarbon infiltration and biodegradation of medium molecular weight hydrocarbons, and their results have shown that the potential for leaching of unmodified hydrocarbons towards the groundwater was slight, whereas the input of total organic carbon resulting from microbial activity could account for more than 1% of the initial carbon load. Freijer et al. (1996) investigated the mineralization rate of petroleum hydrocarbons in lysimeter studies with five different contaminated soils with initial HC contents ranging from 0.1 to 13 g kg^{-1}. They have found that, carbon dioxide production rates are strongly related to hydrocarbon consumption rates for hydrocarbon contents > 1.0 g kg^{-1}, and for hydrocarbon contents < 1 g kg^{-1} the mineralization quotient increases steeply with decreasing hydrocarbon contents, which demonstrated that the share of hydrocarbon mineralization in total CO_2 production decreases.

Pasteris et al. (2002) reported the evaluation of the natural attenuation of 13 fuel compounds with MTBE in the unsaturated zone during a period of 70 days. They concluded that estimated first-order biodegradation rates in the unsaturated zone range from <0.05 d^{-1} for MTBE up to 8.7 d^{-1} for octane and the aerobic biodegradation of degradable fuel compounds to CO_2 started without lag phase and removed about 3 times more fuel mass than volatilization. The lysimeter results illustrated the recalcitrance of MTBE vapours in comparison with fuel vapours and confirmed a significant groundwater pollution risk for MTBE.

Dakhel et al. (2003) investigated the impact of the additives MTBE and ethanol on groundwater quality, during a period of 10 months to investigate the fate of spilled blended-gasoline. They found that, all soluble petroleum hydrocarbons including ethanol were transported to the groundwater and all the petroleum constituents disappeared concomitantly except isooctane from the aerobic

groundwater due to biodegradation. The results reported suggest that MTBE-free gasoline would be less harmful for groundwater resources and that ethanol is an acceptable substituted.

Finally, a recent lysimeter study conducted by Song et al. (2010) involved an approach for estimating microbial growth and biodegradation of hydrocarbon contaminants in subsoil. They report kinetic parameters of hydrocarbons degrading microorganisms estimated on the basis of measurements conducted during an initial 92 days post hydrocarbons contamination and noted that the prediction was in good agreement with the measured reduction in hydrocarbons concentration.

2.3.4. Field experiment

The most relevant, but also most complex and expensive experiments investigate the fate of petroleum hydrocarbons after accidental or designed spills under field conditions. In a field experiment with an emplace source during a period over three months to study the microbial community response to PHCs contamination in the unsaturated zone, (Kaufmann et al., 2004) concluded that significantly elevated CO_2 concentrations were observed after contamination, and reported that total cell numbers were strongly correlated with soil organic carbon and nitrogen content but varied little with the degree of contamination.

More results from field experiments have been reported by Christophersen et al. (2005), in their study of the transport of hydrocarbons from an emplaced fuel source experiment in the vadose zone at Airbase Vaelose, Denmark. The source consisted of 13 hydrocarbons and CFC-113 as a tracer, and the study has concluded that for the first days after source emplacement, the transport of CFC-113, hexane and toluene was successfully simulated using a radial gas-phase diffusion model for the unsaturated zone and only the most water-soluble compounds were detected in the groundwater and concentrations decreased sharply with depth, providing evidence for effective natural attenuation.

Ultimatively, the fate of petroleum hydrocarbons in the unsaturated zone can only be assessed through a complete natural attenuation monitoring process (MNA). Sorption, diffusion, evaporation and biodegradation are the main processes affecting the presence of a VOC contaminant. It is necessary to consider all of them when evaluating or determining the movement and the fate of degradable VOCs in the unsaturated zone (Atlas and Philp, 2005).

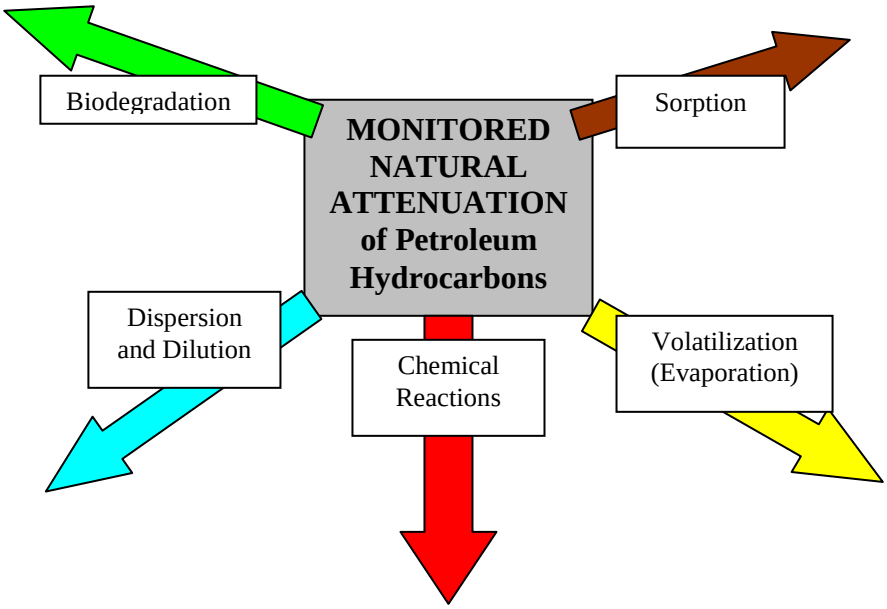

Figure 2.1 Monitored Natural Attenuation Parameters

2.4. The main key points affecting MNA

The main processes are briefly explained here:

1) Biodegradation: breakdown of contaminants by microorganisms in the environment, the goal being the formation of non-toxic by-products like CO_2 and H_2O. It can be determined by the reduction in dissolved oxygen and hydrocarbon concentrations, and the production of CO_2.
2) Chemical transformation: The reduction in concentration of the target contaminant as a result of abiotic chemical processes.

3) Dispersion: the process of mixing which takes place when fluids flow through a porous medium and clean groundwater is mixed with and dilutes contaminated water.
4) Sorption: the attachment of compounds to soil or rock by physical or chemical attraction.
5) Volatilization: the transportation of a chemical from the liquid to the vapour phase.

Moreover, MNA involves modelling, sampling and analysis, and for the best prediction of VOCs natural attenuation rate in the unsaturated zone, information about microbial biodegradation and kinetics rate should be known (Hohener et al., 2006; Hohener et al., 2003).

To monitor the migration of VOCs in vadose zone soil-gas monitoring is an important tool. Werner et al. (2005) reported a new approach on the basis of the combination of soil-gas monitoring technique with natural gradient tracer methods, for the measurement of diffusive contaminant fluxes, and the detection and rough quantification of NAPL.

2.4.1. Volatilization and its effect on the natural attenuation of VOCs in the unsaturated zone

Volatilization is the mechanism of the partition of non-aqueous phase liquids (NAPLs) to the vapour phase and can be quantified by using Raoult's Law:

$$C = \frac{X_i P^0}{RT} \qquad \textbf{Equation 2-1}$$

Where,

X_i is the mole fraction of the pure compound in NAPL mixture [-]

P^o is the pure compound vapour pressure, atm

R is the universal gas constant, $\frac{m^3 \ atm}{mol \ K}$

T is the temperature, K

C is the constituent concentration mol m^{-3}

Vapour phase is the dominant transport pathway of petroleum hydrocarbon VOCs in the unsaturated zone and the evaporation of VOCs occurs from the NAPL phase. Gas-phase diffusion is a much more rapid process than liquid-phase diffusion.

In VOCs mixture as a result of the evaporation of the more volatile VOCs, the mixture composition will change (Wang et al., 2003).

Many studies shown that gas-phase diffusion is the dominating transport process for the migration of VOCs in the unsaturated zone (Pasteris et al., 2002; Conant et al., 1996; Silka, 1988).

Transient diffusion through a soil layer can be described by Fick's Second Law:

$$\frac{\partial C}{\partial t} = \frac{D_{eg}}{\alpha} \frac{\partial^2 C}{\partial X^2} \qquad \textbf{Equation 2-2}$$

Where:

D_{eg} is the effective diffusion coefficient ($cm^2\ s^{-1}$),

α is the capacity factor,

C is the concentration in the soil air ($g\ cm^{-3}$), and

X and t are the distance (cm) and time (s).

α accounts for the distribution of a compound in the three phases systems.

Pasteris et al. (2002) described the diffusive vapour transport, through a modified form of a mathematical model proposed by Jin et al. (1994). Their model is based on the following assumptions:

i. Diffusion is the dominant transport process;
ii. The sorbed and dissolved phases undergo reversible linear sorption;
iii. The dissolved and the gaseous phases obey Henry's Law;
iv. Biodegradation rates are constant with time and space, and

v. The soil diffusion coefficients for the gaseous and dissolved phases are modified from their values in air and water by tortuosity factors τ described by the model of Millington and Quirk (1961)

$$\tau_a = \frac{\theta_a^{2.33}}{n_{tot}^2} \qquad \textbf{Equation 2-3}$$

$$\tau_w = \frac{\theta_w^{2.33}}{n_{tot}^2} \qquad \textbf{Equation 2-4}$$

Where θ_a is the volumetric soil air content (cm^3 gas cm^{-3}), θ_w is the volumetric water content (cm^3 water cm^{-3}), n_{tot} is the total porosity in the sand. From the above assumption they expressed the chemical transport equation in terms of the soil air concentration C_a as (Jin et al., 1994)

$$R_a \frac{\partial C_a}{\partial t} = D \frac{\partial^2 C_a}{\partial x^2} - r(C_a) \qquad \textbf{Equation 2-5}$$

Where R_a is the capacity factor. R_a and D is defined as follows:

$$R_a = \frac{(\rho_b K_d + \theta_w + \theta_a H)}{H} \qquad \textbf{Equation 2-6}$$

$$D = \frac{(\theta_a \tau_a D_a H + \theta_w \tau_w D_w)}{H} \qquad \textbf{Equation 2-7}$$

Where:

ρ_b is the soil bulk density (g cm^{-3}), K_d is the distribution coefficient between dissolved and solid phase (cm^3 g^{-1}), H is the dimensionless form of Henry's law coefficient (g cm^{-3} air/g cm^{-3} water), D is the effective diffusion coefficient of any fuel compound in soil air (cm^2 s^{-1}), and D_a is the molecular diffusion coefficient in air (cm^2 s^{-1}), D_w is the molecular diffusion coefficient in water (cm^2 s^{-1}), and $r(C_a)$ is the degradation term (g cm^{-3}s^{-1}).

The linear concentration profile of a conservative compound volatilized from an artificial mixed NAPL source in a large-scale field lysimeter experiment suggested the compound was transported upward and downward at almost same rate, indicating that vapour phase diffusion is the only dominant transport mechanism (Pasteris et al., 2002).

Dakhel et al. (2003) in a small volume release of gasoline in a large scale lysimeter, quantitatively assessed the volatilisation. Diffusive fluxes (F) across the lysimeter surface for each compound on a carbon mass basis (g of C cm^{-2} s^{-1}) were calculated by using Fick's law

$$F = \tau \theta_a D_a \frac{\partial C_a}{\partial Z}\Big|_{Z=0} \qquad \textbf{Equation 2-8}$$

$\frac{\partial C_a}{\partial Z}$ is the vapour concentration gradient (g cm^{-4})

D_a is the molecular diffusion coefficient in air, and can be determined according to the method of Fuller as outlined in (Schwarzenbach et al., 1993).

$$D_a = 10^{-3} \frac{T^{1.75}\left[\left(\frac{1}{m_{air}}\right)+\left(\frac{1}{m}\right)\right]^{\frac{1}{2}}}{P\left[V_{air}^{1/3}+V_i^{1/3}\right]^2} \quad (cm^2\ s^{-1}) \qquad \textbf{Equation 2-9}$$

Where:

T is the absolute temperature (K),

m_{air} is the average molecular mass of air (28.97 g mol^{-1}),

m is the organic chemical molecular mass (g mol^{-1}),

P is the gas phase pressure (atm)

V_{air} is the average molar volume of the gas in air (~ 20.1 cm^3 mol^{-1}),

V_i is the molar volume of the chemical of interest (cm^3 mol^{-1}).

2.4.2. Sorption and its effect on the natural attenuation of VOCs in the unsaturated zone

Sorption as defined by Schwarzenbach et al. (1993) is "The process in which chemicals become associated with solid phases (either adsorption onto a two-dimensional surface, or absorption into three-dimensional matrix)".
The prediction of sorption values from soil organic carbon partition coefficient (K_{oc}) is especially successful for hydrophobic VOCs. Values can be estimated using empirical regressions from the compound solubility or its distribution coefficient in the octanol-water system.

Schwarzenbach et al. (1993) cited in Pasteris et al. (2002) described the determination of the distribution (sorption) coefficient of compound between liquid and solid phases for soils having an f_{oc} of more than 0.1% as:

$$K_d = f_{om} * K_{om}$$ **Equation 2-10**

$$f_{om} = 1.72 * f_{oc}$$ **Equation 2-11**

$$\log K_{om} = 0.82 \log K_{ow}$$ **Equation 2-12**

However, Piwoni and Banerjee (1989) cited in Christophersen et al. (2005) have shown that K_d for soils having f_{oc} less than 0.1% can be estimated as:

$$\log K_d = 1.04 * \log K_{ow} + \log f_{oc} - 0.84$$ **Equation 2-13**

From the above equations it can be seen that the adsorption of organic chemicals is strongly influenced by the organic carbon content of the solid.

2.4.3. Biodegradation and its effect on the natural attenuation of VOCs in the unsaturated zone

The literature reviewed showed that biodegradation of the petroleum VOCs is the key parameter in natural attenuation; biodegradation rates can be estimated through:

2.4.3.1. Monod and Michaelis-Menten Kinetics

Monod kinetics describes the growth of microorganisms on a limiting substrate . They are represented mathematically by:

$$\mu = \mu_{\max} \frac{S}{S + K_S} - k_d \qquad \textbf{Equation 2-14}$$

Where
μ is the growth rate [T^{-1}],
μ_{max} is the maximum growth rate [T^{-1}],
S is the growth-limiting substrate concentration [ML^{-3}],
K_s is the half-saturation constant or the substrate concentration that allows the bacterial population to grow at half of the maximum growth rate [ML^{-3}], and
K_d is the microbial decay rate [T^{-1}], (Suarez and Rifai, 1999).

The change in substrate concentration using Monod kinetics is given by:

$$\frac{dS}{dt} = -\frac{\mu_{\max}}{Y} B \left[\frac{S}{S + K_S} \right] \qquad \textbf{Equation 2-15}$$

Where:

Y is a yield coefficient that represents the mass of biomass produced per substrate utilized [MM^{-1}], and
B is the biomass concentration [ML^{-3}].

2.4.3.2. Zero-Order Kinetics

When the substrate concentration is much greater than the half saturation concentration (**S>>Ks**), Equation 2-15 may be re-written as:

$$\frac{dS}{dt} = -\frac{\mu_{\max}}{Y}\mathbf{B} \qquad \textbf{Equation 2-16}$$

OR (for a constant biomass concentration)

$$\frac{dS}{dt} = -V_m = K_0 \qquad \textbf{Equation 2-17}$$

Where

V_m is the substrate utilization rate [$ML^{-3}T^{-1}$], also known as the zero-order biodegradation rate (Suarez and Rifai, 1999).

2.4.3.3. First-Order Kinetics

If the substrate concentration is much smaller than the half-saturation concentration (S<<Ks), the expression (S/S+Ks) approximates (S/Ks) and Equation 2-15 may be expressed as:

$$\frac{dS}{dt} = -\frac{\mu_{\max}}{Y} B\left[\frac{S}{K_S}\right] = -\frac{V_m}{K_S} * S \qquad \textbf{Equation 2-18}$$

The expression $\frac{V_m}{K_S}$ represents the first-order biodegradation rate constant (λ) [T^{-1}].

Consequently, Equation 2-18 is written as:

$$\frac{dS}{dt} = -\lambda S \qquad \textbf{Equation 2-19}$$

While biodegradation is taken into account in many approaches to evaluate natural attenuation of petroleum VOCs in the unsaturated zone, biodegradation alone does not tell the whole natural attenuation story, so further attention is required to be taken into account the effects of the other natural attenuation mechanisms, in particular sorption and volatilization.

2.5. Prediction of natural attenuation of VOCs in the unsaturated zone

Hohener et al. (2006), identify two major problems connected with the prediction of natural attenuation of volatile organic compounds in the unsaturated zone, the first one concerns the difficulty of verifying critically information about microbial biodegradation rates, which may lead to an unpredictable natural attenuation scenario; the second is the difficulty of finding the right mechanism for describing the biodegradation kinetics.

What we know about groundwater contamination due to accidental spills of fuels is based on empirical studies that investigate how hydrocarbon NAPLs and vapours migrate to groundwater tables.

Squillace et al. (1999), investigated the occurrence, distribution, and status of 60 VOCs in untreated ambient groundwater of the conterminous United States, on the basis of samples collected from 2948 wells between 1985 and 1995. They have reported that VOC concentrations generally were low; 56% of the concentrations were less than 1 µg/L. In urban areas they have found that, 47% of the sampled wells had at least one VOC, and 29% had two or more VOCs; furthermore U.S. EPA drinking-water criteria were exceeded in 6.4% of all sampled wells and 2.5% of the sampled drinking-water sampled wells. On the basis of the same study it has been reported that in rural areas, 14% of the sampled wells had at least one VOC; furthermore, drinking-water criteria were exceeded in 1.5% of all sampled wells and 1.3% of the sampled drinking-water wells.

Several studies have shown that a serious threat for groundwater quality has been identified from diffusive spreading of gaseous constituents of fuels in the unsaturated zone. Baehr et al. (1999), in a study for the evaluation of the atmosphere as a source of VOCs in shallow groundwater, have reported that if the VOCs originated from a point source(s) concentrations in groundwater could potentially increase over time to levels of concern as groundwater plumes evolve, whereas if the atmosphere is the source, then groundwater concentrations would be expected to remain at low-level concentrations not to exceeding those in equilibrium with atmospheric concentrations. Another study conducted by Pasteris et al. (2002), reported that the recalcitrance of MTBE vapours compared to other fuel vapours leads to a significant groundwater pollution risk.

A recent key study in the literature for groundwater risk assessment has been reported by Hohener et al. (2006) in a European Framework Project entitled Groundwater risk assessment at contaminated sites (GRACOS). A field experiment was designed to investigate the natural attenuation potential for petroleum hydrocarbons in the unsaturated zone and to derive biodegradation rate coefficients for 13 VOCs at the field site. The method which has been used to achieve this aim was by interpreting vapour plume extensions and comparing them to an analytical solution of a reactive transport model. Furthermore, comparison between rates measured in the same soil in two different laboratory experimental systems and rates obtained from numerical models was undertaken, and the main study interest was the comparison of biodegradation rate data obtained at the field scale and lab-derived rate data.

2.6. Assessing hydrocarbons natural attenuation

Natural attenuation in the unsaturated zone is difficult to assess for biodegradable compounds, because aerobic biodegradation can lead to vertical gradient of oxygen in the unsaturated zone of few meters thickness. Baehr and Baker (1995) used a reactive gas transport model to determine rates of hydrocarbons biodegradation in unsaturated porous media. They reported that data from column experiments or from field sites can be analyzed by applying

their one-dimensional model, where gas transport in the unsaturated zone is approximately vertical.

Another study conducted by Lahvis et al. (1999), have quantified aerobic biodegradation and volatilization rates of gasoline hydrocarbons near the water table under natural attenuation conditions. They concluded that transport of the hydrocarbons in the unsaturated zone can be limited relative to that of oxygen and carbon dioxide and the hydrocarbons were nearly completely degraded within 1 m above the water table and the biodegradation rates exceeded the prediction rates of solubilisation to groundwater, demonstrating the effectiveness of aerobic biodegradation and volatilization as a combined natural attenuation pathway.

Correct and proper designs of experimental approaches taking into account the possibility of oxygen concentrations reduction are required for the prediction of natural attenuation. Some field studies have investigated the natural attenuation of hydrocarbons vapours above different petroleum products floating on groundwater tables. In a study of petroleum hydrocarbon bioventing in soil core, microcosm and tubing studies have concluded that biodegradation reduced low influent concentrations of individual hydrocarbons by 45 to 92 percent over a 0.6-m interval of an intact soil core and the estimated total hydrocarbon concentration was reduced by 75 percent from approximately 4.7 x 10^{-4} to 1.2 x 10^{-4} kg/m^3 (Moyer et al., 1996).

The distribution of oxygen and carbon dioxide gases in the unsaturated zone can provide a geochemical signal of aerobic hydrocarbon degradation at petroleum product spill sites, and the fluxes of these gases are proportional to the rate of aerobic biodegradation and may be quantified by calibrating a mathematical transport model with the oxygen and carbon dioxide gas concentration data (Lahvis and Baehr, 1996). Another study conducted by Franzmann et al. (2002), using geochemical evidence from a plume of hydrocarbon-contaminated groundwater showed that sulphate reduction rapidly developed as the terminal electron accepting process and toluene degradation was linked to sulphate reduction.

Different ways and different methods have investigated the natural attenuation of VOCs vapours above various petroleum products floating on groundwater tables. Some studies related to the in situ biodegradation rates as well as coupled one-dimensional constituent concentration models for hydrocarbons and oxygen, have been published.

The time-averaged concentration of hydrocarbon and oxygen vapours in the unsaturated zone above the residually contaminated capillary fringe at the U.S. Coast Guard Air Station in Traverse City, have been investigated and measured (Ostendorf and Kampbell, 1991).

The calibration of a mathematical transport model to the oxygen and carbon dioxide gas concentration data reported the rate of aerobic biodegradation which is proportional to the fluxes of these gases (Lahvis and Baehr, 1996). In addition the method application was successful in quantifying the significance of naturally occurring process that can effectively contribute to plume stabilization. However, it can be argued that, only upward transport of vapours was studied at those sites, and as a result of fuel spills which were not recent, and the initial acclimatization phase of the microbial community could therefore not be studied.

Pasteris et al. (2002) measured successfully the first-order biodegradation rate for 11 VOCs. The microbial degradation started on the first day after contamination in a large scale lysimeter field experiment after placing an immobile gasoline source in alluvial sand. The flow of the oxygen in this experiment was just in one direction according to the cylindrical geometry of the experiment, which may have lowered the oxygen concentration in comparison to a real field site where oxygen can diffusive in three dimensions. This as well as the disturbance of the sand during lysimeter filling may have accelerated degradation rates (Pasteris et al., 2002).

A limited number of laboratory experiments studies simulating the unsaturated zone, have provided experimental evidence for biodegradation rates and

kinetics of VOC vapours. Some of these experiments have simulated the unsaturated zone through laboratory microcosm experiments. English and Loehr reported the removal coefficients for three VOCs in a fine sandy loam soil, and determined the sorption coefficients and degradation removal rates from batch reactors. Their results indicated that organic vapours are sorbed and then removed by biodegradation in the unsaturated soil systems (English and Loehr, 1991).

Allen-King et al. (1994) investigated the rate of toluene biodegradation using lab microcosm tests with soils from three different horizons, and the maximum utilization rate (μ_{max}) for soil from all three depths was 2.0 d^{-1}. Toluene biodegradation was rapid, occurring at a time scale comparable to the rate of sorption in many of the microcosms and demonstrated the potential for biodegradation of these contaminants in the unsaturated zone.

Kinetic studies conducted to study the biodegradation of petroleum hydrocarbons under various conditions (different soil cores, oxygen concentrations, and nutrients) showed that if oxygen was supplied to the soil microorganisms, the microbial community could adapt to the contaminated environment through selective enrichment and degrade the petroleum hydrocarbon at relatively fast rates (Zhou and Crawford, 1995).

Freijer et al. (1996) investigated the mineralization rates of petroleum hydrocarbons in five different oil-contaminated soil with initial hydrocarbon contents ranging from 0.1 to 13 g kg^{-1} was estimated as function of environmental factors, by applying two different laboratory experimental scales (30-50 cm^3 soil volume) in closed-jars under constant environmental conditions and in lysimeters (0.81 m^3 soil volume) under dynamic climate and hydrological conditions. Oxygen concentration and hydrocarbon content affected the mineralization rates, but water content could not be identified as a direct governing environmental factor, and the CO_2 production rate seems to be a good quantity to express the mineralization rate of the hydrocarbons.

The usage of biodegradation rates obtained in the laboratory to predict the biodegradation rates under field conditions is sound, when differences in environmental conditions have been taken into account (Freijer et al., 1996).

Estimation of biokinetic parameters for unsaturated soils through a Bayesian parameter estimation model describing biodegradation of organic compounds in unsaturated soils was collected from microcosm studies (Sleep and Mulcahy, 1998). The gas phase concentrations of both carbon dioxide and substrate were the main model parameters, allowing estimation of both yield and initial variable biomass concentrations. Application of the model to the microcosm data demonstrate the ability of the model to estimate biokinetic parameters in unsaturated soils, including both yield and initial biomass levels, and it has been found that differences in biokinetic parameters for the moisture contents of 8 and 12% (by mass) were not significant at the 95% level (Sleep and Mulcahy, 1998).

Moreover, Franzmann et al. (1999) applied laboratory microcosms experiments to study and measure the rate of microbial mineralisation of benzene in a soil profile above groundwater from the surface and three different depths (0.25-0.35m, 0.5-0.6m and 2.6-2.8m) from a site which was known to have experienced gasoline contamination of groundwater. Their results showed that the fastest microbial mineralisation rate of [14C] benzene was 18±13 μmol kg^{-1} day^{-1} with a half life ($t_{1/2}$) of 11±1 days in soil from a depth of 0.25 m below the ground surface. Microbial mineralisation rates in soil from depth 0.5 meter were reported to be slower which is 27±6 μmol kg^{-1} day^{-1}, $t_{1/2}$ = 72±16 days, as were mineralisation rate in surface soils 52±13 μmol kg^{-1} day^{-1}, $t_{1/2}$ = 26±7 days. In the anoxic soil just above the groundwater table, the situation was extremely different and microbial mineralisation rates were extremely slow 0.04±0.01 μmol kg^{-1} day^{-1}, $t_{1/2}$ = 173±31 years. It has been concluded that, at the study site the diffusion of oxygen from the surface, volatile aromatics from the contaminated groundwater and the metabolic capability of the microbial population would seem to be in a dynamic equilibrium that prevents appreciable

breakthrough of aromatic hydrocarbons to the atmosphere (Franzmann et al., 1999).

Another study applied an open microcosm method (stainless steel bioreactors) for quantifying microbial respiration and estimating biodegradation rates of hydrocarbons in gasoline-contaminated sediment samples (Baker et al., 2000). Respiration rates and estimated hydrocarbon biodegradation rates were compared to those obtained using an in situ method based on measuring the transport of carbon dioxide in the unsaturated zone. It has found that results of the two methods were similar, demonstrating that the bioreactor method can be used to produce meaningful and cost-effective estimates of in situ hydrocarbon degradation.

Ostenford et al. (2000) reported the use of soil microcosms to assess the potential of aerobic microorganisms to degrade petroleum hydrocarbon vapours in the unsaturated zone. The live microcosm's soil samples degraded hydrocarbons much faster than the leakage rate, except for 2.2.4-trimethylpentane, which was recalcitrant.

Rate determination of hydrocarbon biodegradation in unsaturated porous media was done by using a reactive gas transport mathematical model by Baehr and Baker (1995). The one-dimensional model can be applied to analyze data from column experiments or from field sites were gas transport in the unsaturated zone is approximately vertical, and the model allows for the determination of constituent production/consumption rates as a function of the spatial coordinate. It has been reported that, the model can be applied in a predictive mode to obtain the distribution of constituent concentrations and fluxes on the basis of assumed values of model parameters and biodegradation hypothesis. Another laboratory column study for the prediction of natural attenuation of volatile organic compounds in the unsaturated zone by studying the rates and kinetics of VOCs in unsaturated alluvial sand was performed at room temperature under aerobic conditions (Baehr and Baker, 1995).

The study of Hohener et al. (2003), has coupled a reactive transport model for VOC vapours in soil gas to Monod-type degradation kinetics for data interpretation, in order to determine kinetics rate laws for the aerobic biodegradation of 12 VOCs and MTBE. The first notable observation was that, an acclimatization of 23 days took place before steady-state diffusive vapour transport through the horizontal column was achieved, and from the concentration profiles of toluene, m-xylene, n-octane and n-hexane Monod kinetic parameters K_s and μ_{max} were provided as a result of substrate saturation. However, the situation was extremely different with other VOCs, in particular the removal of cyclic alkanes, isooctane, and 1,2,4-trimethylbenzene which followed first-order kinetics over the whole concentration range applied, but MTBE, n-pentane and chlorofluorocarbons (CFCs) were not visibly degraded, and it was concluded that, the column approach was preferable for biodegradation rate determination to be used in risk assessment models.

Another laboratory column experiment was performed to study the transport and biodegradation of toluene in unsaturated soil, where toluene was added to 25-cm diameter soil columns through an inlet chamber and it was diffused through the soil to an outlet chamber at the top of the column, and soil gas diffusion coefficient was measured under sterilized conditions, and subsequent experiments in which biodegradation will take place were used to estimate rate coefficient by fitting the outflow to a mathematical model (Jin et al., 1994).
It was reported that the biodegradation rate was very rapid under both pre-exposed and unexposed soil conditions, corresponding to a half- life of 2 hours when bacterial activity reached high levels, and the volatilization flux prior to this stage was reported to be very erratic, which demonstrate that growth rates of bacteria was out of phase with the transport process. The removal of toluene during the transport has greatly increased as a result of the pre-exposure of the soil to the substrate prior the transport experiment (Jin et al., 1994).

Moyer et al. (1996) determined the bioventing kinetics of petroleum hydrocarbons in a soil core. The first biodegradation evidence was the low influent hydrocarbon concentrations which were decreased by 45 to 92 percent

over a 0.6-m interval of an intact soil core, and the estimated hydrocarbon concentration was reduced by 75 percent from 26 to 7 parts per million. Steady-state concentrations were input to a simple analytical model balancing advection and first-order biodegradation of hydrocarbons, and the model has been calibrated to the concentration profiles by using the first-order rate constants for the major hydrocarbon compounds. It has been concluded that the rate constants for some individual hydrocarbon compounds varied by a factor 4, and compounds with lower molecular weights, fewer methyl groups, and no quaternary carbons tended to have higher constants.

2.7. Biodegradation kinetics experiments

2.7.1. First-order kinetics

Among different unsaturated experimental systems conflicting findings of biodegradation kinetics were obtained. For instance, Jin et al. (1994) reported first-order rates, even though the first-order kinetics was not well described until the population stabilized in their study. Another study conducted by Moyer et al. (1996), have used first-order rate biodegradation constant for the major hydrocarbon compounds within their study to calibrate a model to the concentration profiles. They concluded aerobic biodegradation kinetics in the unsaturated zone were approximately first-order. Lahvis et al. (1999) in their study have found that first-order rate constants near the water table were highest for cyclohexane (0.21-0.65 d^{-1}) and nearly equivalent for ethylbenzene.

2.7.2. Zero-order kinetics

A recent study has investigated the influence of nonionic surfactant on biodegradation of toluene dissolved in the water phase and biodegradation kinetic behaviours of toluene in a biofilter (Chan and You, 2010). The study illustrated that toluene dissolution in the water phase was enhanced by the addition of surfactant into the aqueous solution and the maximum amount of toluene dissolved in the water phase occurred at the surfactant concentration of

34.92 mg L^{-1}. Zero-order kinetics with diffusion limitation was regarded as the most adequate biochemical reaction kinetic model.

Transport and biodegradation of BTX compounds in sandy soil was modelled by Mohammed and Allayla (1997). The study used a finite difference model for simulating one dimensional BTX transport allowing equilibrium sorption given by linear isotherm and biodegradation given by zero-order kinetics under a variety of initial and boundary conditions. The model considers time-dependent groundwater velocity and spatially variable initial concentration and the observed data suggested that the fits to zero-order model are good for the range of the concentration of BTX compounds studied.
Effects of microcosm preparation on rates of toluene biodegradation under denitrifying conditions has been investigated (Hutchins, 1997). The study examined the effects of preparation methods on rates of toluene biodegradation under denitrifying conditions with substrate material from two aquifers. The study concluded that in both cases, the data fit a zero-order kinetics plot.

Biotransformation rates for dissolved toluene in unsaturated sandy soil were determined by Allen-King et al. (1996), in dynamic infiltration experiments to study the fate of dissolved toluene during steady infiltration. The study demonstrated that transformation rates under N-limited conditions were 8 to 35 mg (kg d^{-1}) and appeared to follow zero-order kinetics

2.7.3. Monod-kinetics

A Bayesian parameter estimation model was developed for estimation of biokinetic parameters describing biodegradation of organic compounds in unsaturated soils (Sleep and Mulcahy, 1998). The model was based on gas-phase measurements of both substrate and carbon dioxide concentrations allowing estimation of both yield and initial variable biomass concentrations.

Another study for determining the kinetic rate laws for aerobic biodegradation of a mixture of 12 volatile organic compounds and methyl tert-butyl ether

(MTBE) in unsaturated alluvial sand, Hohener et al. (2003) found that Monod kinetic parameters K_s and μ_{max} could be derived from concentration profiles of toluene, m-xylene, n-octane, and n-hexane, because substrate saturation was approached with these compounds under some of the experimental conditions.

A major landmark in the study of determining biodegradation rate coefficients for the aerobic biodegradation of volatile petroleum hydrocarbons in the vadose zone is the work developed by Hohener et al. (2006), because he was the first to use a comparison of three different experiments, laboratory column, microcosm experiments with the sandy soil at room temperature under aerobic conditions and a field experiment in an unsaturated sandy soil in order to compare biodegradation of hydrocarbon vapours obtained from these three different sources with three models. The study has illustrated that degradation rates in laboratory microcosms were underestimated by up to factor of 5 due to lack of sensitivity for slowly degrading compounds and all field models suggested a significant higher degradation rate for benzene than the rates measured in the lab.

2.8. Effect of inorganic nutrients addition on the fate, transport and biodegradation of volatile organic compounds

Since microorganisms require nitrogen, phosphorus and other mineral nutrients for incorporation into biomass, the availability of these nutrients within the area of hydrocarbon biodegradation is critical and low concentrations of available nitrogen and phosphorus in soil may severely limit microbial hydrocarbon degradation (Leahy and Colwell, 1990; Atlas, 1981).

A considerable amount of published studies describe the role of inorganic nutrients on the biodegradation of petroleum hydrocarbons. The Exxon Valdez spill, which is the spill of more than 22,000 barrels of crude oil from oil tanker Exxon Valdez in Prince William sound, Alaska, as well as a smaller spill in Texas, formed the basis for a major study on bioremediation through fertilizer

application and the largest application of this emerging technology (Atlas, 1995).

Walworth and Reynolds (1995) tested the effects of phosphorus and nitrogen levels on the bioremediation of a cryic entisol contaminated with diesel fuel, treated with different nitrogen levels (0, 400, 800, or 1200 mg/kg of soil) and phosphorus (0, 60, 120, or 1800 mg/kg of soil) at two different temperature $10^{o}C$ and $20^{o}C$. Their results have shown that, at $10^{o}C$, bioremediation rates were not affected by the fertility treatments, and at $20^{o}C$, reaction rates were increased by the addition of phosphorus, but not affected by the nitrogen addition.

It has conclusively been shown that addition of phosphorus without nitrogen to study the oil bioremediation in a high and a low phosphorus soil amended with 3, 6, and 9% crude oil by weight for 120 days at $25^{o}C$ did not enhance biodegradation, but addition of nitrogen without phosphorus approximately tripled the quantity of oil degraded (Chang et al., 1996). However, addition of nitrogen and phosphorus together did not increase biodegradation of oil more than addition of nitrogen alone when oil concentration was 3%, and at 6 and 9% oil concentrations. CO_2 evolution increased for both soils by adding phosphorus and nitrogen in comparison to the addition of nitrogen alone and total petroleum hydrocarbons biodegradation increased by 30% by day 60 and the results demonstrated that, addition of phosphorus to soil to enhance oil degradation was only beneficial for oil concentrations above 3% (Chang et al., 1996).

Brook et al. (2001) point out the role of the nitrogen sources and concentrations to study the effect of various nitrogen addition regimes on the biodegradation rates of diesel fuel in nutrient limited soil at two carbon-to-nitrogen ratios. The several different nitrogen sources were ammonium nitrate, ammonium sulphate, potassium nitrate, urea, and urea oligomers. It has been shown that for both carbon-to-nitrogen ratio tested, hydrocarbon degradation rates were the highest for the ammonium sulphate (20:1 at 0.032 d^{-1}; 40:1 at 0.019 d^{-1}) and urea treatments (20:1 at 0.025 d^{-1}; 40:1 at 0.011 d^{-1}). A degradation rate correlation as a function of nitrate and ammonia

concentrations was developed and the correlation suggests the occurrence of nitrate inhibition at elevated nitrate concentrations.

In another study conducted by Ferguson et al. (2003) investigated the effects of nitrogen and phosphorus amendments on microbial mineralisation using radiometric microcosm experiments and gas chromatography. The investigation involves testing the hydrocarbon mineralisation at nine different inorganic nitrogen concentrations (ranging from 85 to over 27,000 mg N kg-soil H_2O^{-1}) during 95 days. Total 14C-octadecane mineralisation increased with increasing nutrient concentration peaking in the range 1000-1600 mg N kg-soil-H_2O^{-1}, and the mineralisation of aliphatic hydrocarbons constituents of special Antarctic blend diesel in the contaminated soil showed good agreement with the 14-C-octadecane mineralisation outcomes.

Nutrients have been identified as major limiting factor for mineralization of hexadecane in an arctic soil. Ammonium chloride was added to give nitrogen concentrations ranging from 0 to 1000 mg NH_4^-N kg^{-1} soil after 36 days incubation the total hexadecane mineralization was reduced. The results demonstrated that the highest mineralization rates were found in soil samples amended with 50-200 mg NH_4-N kg^{-1} at 10% moisture, where 50-58 mg hexadecane/kg/day was mineralized (Borresen and Rike, 2007).

The effectiveness of nitrogenous nutrient (nitrogen) amendments in enhancing biodegradation of petroleum contaminants in soil by using a solid-phase circulating bioreactor (SCB), in a bench-scale SCB, has been demonstrated by Fallgren and Jin (2008). The total petroleum hydrocarbons (TPH) concentration was 5000 mg kg^{-1} in soil decreased 92% within 15 days, while in a scaled-up SCB system containing 120 kg petroleum contaminated soil with TPH at about 125,000 mg kg^{-1}, a degradation rate of 365 mg kg^{-1} d^{-1} was obtained from the poultry manure-amended treatment during a 200-day period of operation. It has been concluded that treatments with the same amount of nitrogen as ammonium nitrate attained a TPH degradation rate of 469 mg kg^{-1} d^{-1} during the same period and a control SCB unit, which was maintained under the same aerobic conditions but without nitrogen addition, had a TPH degradation rate of 273 mg kg^{-1} d^{-1}. These results indicated that poultry manure appears to be a

preferred nitrogen amendment that can further enhance the biodegradation of petroleum contaminants in soils (Fallgren and Jin, 2008).

Moreover, effects of inorganic nutrients (sulphate, phosphate, and ammonium chloride) levels on the biodegradation of benzene, toluene, and xylene (BTX) by *Pseudomonas spp* in a laboratory porous media sand aquifer model in a glass tank, have been investigated by Jean et al. (2008), the experimental results indicate that BTX compounds could be effectively removed when optimal concentrations of phosphates (650-1250 mg/L), ammonium chloride (10-50 mg/L), and sulphate (10-20 mg/L) were amended into the simulated aquifer.

In another study for the effect of biostimulation with nitrogen and phosphorus was analyzed by using microcosms set up on metal trays containing 2.5 kg of contaminated soil from Marambio Station. At the end of the experiment (45 days) , it has been shown that all biostimulated systems showed significant increase in total heterotrophic and hydrocarbon-degrading bacteria counts, and results confirmed the feasibility of the application of bioremediation strategies to reduce hydrocarbon contamination in Antarctic soils and showed that, when soils are chronically contaminated, biostimulation is the best option (Ruberto et al., 2009).

The evaluation of nutrient addition to BTEX compounds and hydrocarbon content biodegradation in diesel contaminated soils has been investigated with three different treated and non-treated soils, clay, loam, and sea sand, and the significant enhancement of diesel degradation was observed soon after the addition of nutrients in loam and sea sand, but no significant differences was observed in clay soil. The fertilizer supplements stimulated higher degradations, but no significant differences in contaminated sea and loam soil after 60 days incubation period were observed. An inhibitory effect of the nutrient addition was observed in the clay soil, and the mineralization of hydrocarbon C>(16) were relatively faster than the shorter chain compounds such as C-9 (Singh and Lin, 2009).

In a recent study to evaluate the nutrients addition effect on the bioremediation at the crude oil contaminated Alang sea coast, it has been shown that, addition

of optimum concentrations of nitrogen (1%), phosphorus (0.5%) and potassium (0.01%) in combination significantly enhanced biodegradation by 22 to 32% (Vyas and Dave, 2010).

It can be concluded that the success of the addition of nutrients to enhance the biodegradation of petroleum hydrocarbons in the unsaturated zone, depends on the amount and form of the added nutrient. Moreover, the literature discussed clearly suggests that the levels of effect in biostimulation are also based on the soil type, water content, the availability of nutrients and the structure and the mass of the fuel constituents, as well as the microbial community present in the soil.

2.9. Effect of biofuel components addition on the fate, transport and biodegradation of volatile organic compounds

The substitution of fossil fuels with biofuels in the European Union (ELF) is a part of a strategy to mitigate greenhouse gas emission from road transport (Ryan et al., 2006). A review covering EU strategy for biofuels until 2025 has been provided by Kulczycki (2006).

Biofuels are believed to be environmentally sound and competitive fuels. It has been reported that the European governments intend to increase the share of biofuels in total EU fuel consumption to 5.7% by 2010 and bioethanol is the primary candidate (Frondel and Peters, 2007; Kozakowski, 2006). It is also a substitute for MTBE.

2.9.1. Effect of ethanol addition on the fate, transport and biodegradation of volatile organic compounds

Solubilisation of ethanol in water and of gasoline components in ethanol leads to the wetting effect of ethanol on the more hydrophobic soil components, and the enhancement of the downward migration of gasoline components. If this is true, as a result of ethanol addition, then the risk of contamination of

groundwater by gasoline is greatly increased. Furthermore, ethanol is increasingly likely to be encountered in groundwater plumes containing VOCs (BTEX), and a better understanding of its effect on VOCs biodegradation is warranted.

In comparison to the numerous literature studies of the fate and transport of VOCs in the unsaturated zone, the effect of ethanol addition on the fate and transport of VOCs in the unsaturated zone has been investigated by only a limited number of studies. Corseuil et al. (1996) have investigated the implications of the presence of ethanol on intrinsic bioremediation of BTX plumes in Brazil, and have reported that ethanol can enhance the solubilisation of BTX in water, and it might exert diauxic effects during BTX biodegradation.

Powers et al. (2001) reported that ethanol can increase the aqueous concentration of BTEX compounds due to a cosolvent effect, and it can inhibit BTEX biodegradation by preferentially consumption of electron accepters and nutrients. Two main mechanisms related to the presence of ethanol are generally considered to impact BTEX transport and fate. The first mechanism was that, ethanol can increase the aqueous concentration of BTEX constituents due to a cosolvent effect, and the second is, it can inhibit BTEX biodegradation by preferentially consuming electron acceptors and nutrients.

Adam et al. (2002) have investigated the effect of ethanol addition on the movement of petroleum hydrocarbons fuels in soil. The movement of diesel fuel was followed in a 1-m soil column. It has been shown that, an aqueous ethanol concentration above 10% was required for any movement to occur, and at 25% aqueous ethanol, the majority of constituents were mobilised and the retention behaviour of the soil column lessened, and at 50% aqueous ethanol, all the constituents were found to move through the columns. The results suggest a greater possibility of groundwater contamination by petroleum hydrocarbons in ethanol additive petrol and diesel fuel spills, and the addition of 51% ethanol to diesel fuel was found to enhance the downward transport of the diesel fuel constituents and thereby to increase the risk of groundwater contamination.

In another study for the evaluation of the impact of ethanol addition on groundwater quality in a large-scale field lysimeter experiment under outdoor conditions, it was concluded that, within a first period of 30 days with 5-mm daily recharge, all soluble compounds including ethanol were transported to the groundwater, and ethanol disappeared concomitantly with benzene and all other petroleum hydrocarbons except isooctane from the aerobic groundwater due to biodegradation. Therefore it was found that ethanol is an acceptable substitute for MTBE (Dakhel et al., 2003).

Lahvis et al. (2003) have investigated the small-volume release of ethanol-blended gasoline (gasohol) at underground storage tank sites as a function of soil type, biodegradation rate, groundwater infiltration rate, and depth to groundwater. The model results indicate that migration of ethanol in the vadose zone is limited to less than 100 cm from the source for releases occurring in coarse-grained soil (sand) assuming highly conservative biodegradation and infiltration rate approximations. While, in fine-grained soil (sandy clay), ethanol transport is limited to less than 50 cm under equivalent biodegradation and infiltration conditions. It was concluded that ethanol addition in gasoline does not significantly affect benzene transport and mass loading to groundwater.

The mechanisms affecting the infiltration and distribution of ethanol-blended gasoline in the vadose zone has been studied in one and two-dimensional experiments to examine the behaviour of gasoline and gasohol (10% ethanol by volume) as they infiltrate through the unsaturated zone and spread at the capillary fringe (McDowell and Powers, 2003). It has been found that, ethanol in the spilled gasohol quickly partitions into residual water in the vadose zone and is retained there as the gasoline continues to infiltrate. Under the conditions tested the results demonstrated that over 99% of the ethanol was initially retained in the vadose zone. However, the main two factors affecting this scenario are, the volume of the gasoline spilled and the depth to the water table, which causes an increase in the aqueous-phase saturation and relative permeability, and as a result allowing the ethanol-laden water to drain into the gasoline pool. Under the same conditions, the presence of ethanol does not have a significant impact on the overall size or shape of the resulting gasoline

pool at the capillary fringe (McDowell and Powers, 2003). In the case of a high aqueous ethanol concentration, ethanol can facilitate the transfer of fuel constituents into the aqueous phase, results in enhancing contaminant concentrations in groundwater a process called cosolvency.

The effect of ethanol on the aqueous solubility of mono- and polycyclic aromatic hydrocarbons have been investigated (Corseuil et al., 2004). Experiments were carried out in batch reactors under equilibrium conditions for pure mono- and polycyclic aromatic hydrocarbons, gasohol and diesel. Initial signals have shown that, a linear relationship between cosolvency power and K_{ow} was determined, which allows predictions of the increase of aromatics solubility due to presence of ethanol. The results indicated that cosolvency would be significant and critical only under two circumstances, for high aqueous ethanol concentrations (higher than 10%) and in case of large gasohol spills or in simultaneous releases of neat ethanol and other fuels. Under these conditions it can be demonstrated that the hydrophobic and toxic aromatic hydrocarbons, which are usually present in minor aqueous concentrations in non-blended fuel spills may dissolve in large amounts in groundwater (Corseuil et al., 2004).

Osterreicher et al. (2004) have studied the evaluation of bioventing treatment of a gasoline-ethanol contaminated undisturbed residual soil from Rio de Janeiro. The results of culturable bacteria population counts show the effect of contamination and bioventing on the microbiota of gasoline and gasoline-ethanol contaminated soil, and the bacterial counts showed a delay in soil population reaction to contamination in gasoline-ethanol contaminated soil in comparison with gasoline-contaminated ones. These observations indicate a possible preferential degradation of ethanol as compared to BTEX.

The impact of fuel-grade ethanol and transport to groundwater in a pilot-scale aquifer tank have been evaluated (Cápiro et al., 2007). They have tested fuel-grade ethanol (76 L of E95, 95% v/v ethanol, 5% v/v hydrocarbon mixtures as a denaturant) released at the water table in an 8150-L continuous-flow tank packed with fine-grain masonry sand. It was found that, ethanol quickly migrated upwards and spread laterally in the capillary zone, and the horizontal migration of ethanol occurred through a shallow thin layer with minimal vertical

dispersion, and was one order of magnitude slower than the preceding bromide tracer. Two dyes Sudan-IV as a hydrophobic and Fluorescein as a hydrophilic tracer provided evidence that the fuel hydrocarbons phase separated from the E95 mixture as ethanol was diluted by pore water and its cosolvent effect was diminished. These results are in a great and significant disagreement with a study conducted by Corseuil et al. (2004) about the cosolvency effect in subsurface systems contaminated with PHCs and ethanol.

Their results indicated that cosolvency would be significant only for high aqueous ethanol concentrations higher than (10%), as (Cápiro et al., 2007) have used 95% v/v.

Osterreicher-Cunha et al. (2007) have reported a study of biodegradation processes of BTEX-ethanol mixtures in tropical soil and found that ethanol delays BTEX biodegradation, and the presence of ethanol caused a higher and longer-lasting boost in enzymatic activity. Their results suggest that ethanol could delay BTEX degradation because of its constitutive degradation by soil microbial communities.

In a more recent study conducted by Osterreicher-Cunha et al. (2009) investigated the effect of ethanol on the biodegradation of gasoline in an unsaturated tropic soil, the ethanol amounts varying from 20 to 26% v/v. The results have shown that, the presence of gasoline and gasohol in soil enhanced microbial enzymatic activity but suppressed culturable bacterial population. Bacterial counts showed a delay in soil populations reactions to contamination in gasoline-ethanol contaminated soil when compared to gasoline-contaminated soil in agreement with their previous study (Österreicher-Cunha et al., 2004). These findings suggest that ethanol enhances BTEX retention in soil, boosts microbiological activity but delays BTEX biodegradation.

Another recent study for the evaluation of ethanol addition on the volatilization of monoaromatic compounds (benzene, toluene, and xylenes BTX) from gasoline vapours from two rivers sand columns contaminated with gasoline and gasoline-ethanol were monitored for 77 days. The main observations were that, for ethanol concentrations higher than 10%, no important changes in the

benzene concentration were observed. The toluene exponentially increases between 20 and 30% ethanol concentration, and the maximum concentration of xylenes was observed when the ethanol concentration was 20% (v/v). These results suggest that the benzene evaporation behaviour is preferentially affected by the interactions among ethanol and other aromatic compounds rather than the ethanol concentration itself, and the evaporation behaviour of toluene and xylenes are directly dependent on the ethanol content (Jóice et al., 2009).

Having investigating the effect of ethanol addition it can be concluded that the effect of ethanol addition on the natural attenuation of VOCs in the subsurface is likely to increase BTEX plume lengths in groundwater and the net effect of its addition is likely to be system specific, depending mainly on the release scenario and the assimilative capacity of the aquifer. Under aerobic conditions, it can be concluded that the preferential degradation of ethanol by indigenous microorganisms in the subsurface and groundwater tend to deplete oxygen and nutrients thereby hindering BTEX biodegradation (Corseuil et al., 1998; Hunt et al., 1997b).

2.9.2. Effect of biodiesel addition on the fate, transport and biodegradation of volatile organic compounds

The chemical composition of biodiesel is monoalkyl esters of long chain fatty acids derived from renewable feed stock like vegetable oils and animals fats. Its production process is called transesterfication in which, fat or oil is reacted with a monohydric alcohol in the presence of a catalyst usually NaOH or KOH (Meher et al., 2006). Moreover, biodiesel is a clean renewable fuel, and its physico-chemical properties are similar to those of fossil diesel fuel in compression ignition engines.

Biodiesel is a part of the family of biofuels. ASTM International defines a biodiesel blend as "a blend of biodiesel fuel with petroleum based diesel fuel". Biodiesel blends are often designated with the abbreviation **BXX**, where **XX** represents the volume (in percent) of biodiesel fuel in the blend. According to the definition a blend of 80% diesel fuel and 20% biodiesel is designated as

B20, and if a fuel consisting of pure biodiesel then it will designated as **B100** (Stauffer and Byron, 2007).

Biodiesel is currently defined in the European Union in the technical regulation EN 14214 or in the USA in ASTM 6751-02 as Fatty Acid Methyl Esters (FAME), which is the result of reaction of fatty acids with methyl alcohol (Lois, 2007).

Most of the recent studies in the field of biodiesel have been focused on the methods of the preparation and purification of biodiesel, (Di Serio et al., 2007; Hama et al., 2007; Issariyakul et al., 2007; Shumaker et al., 2007), others have focused on the analysis of the biodiesel, (Felizardo et al., 2007; Jin et al., 2007; Kwanchareon et al., 2007; Oliveira et al., 2007). Unfortunately neither the first group nor the second have focused or discussed the biodegradation of the biodiesel and its effects on the other fuels.

A limit amount of literature has been published discussing biodiesel addition on the fate and transport of petroleum hydrocarbons in the unsaturated zone. These papers will be briefly reviewed.

Synergic effects of biodiesel on the biodegradability of fossil-derived fuels have been studied, and the possibility of using biodiesel to cometabolically degrade two fossil-derived fuels, diesel fuel and gasoline (Pasqualino et al., 2006). The results have shown that, for all the mixtures, the synergic effect was positive, showing that biodiesel improves the biodegradation of both diesel and gasoline by means of cometabolism, and the biodegradability of pure biodiesel reached nearly 100% during the test period, while diesel fuel and gasoline reached 50% and 56% respectively. These results demonstrated that the biodegradability of the mixtures increased when biodiesel was added due to the effect of cometabolism.

The primary aerobic biodegradation of a B20 fuel (20% soybean fatty acid methyl esters, 80% petroleum diesel) by unacclimated innocula from a rainwater detention pond has been studied by Prince et al. (2008). The results have shown that biodegradation was rapid and essentially complete, with an overall median half-life at ~ 100 ppm B20, of 6.8 days (n=34).

The fatty acids methyl esters, n-alkanes and iso-alkanes, and simple and alkylated aromatic compounds were the most readily degraded compounds and it has been concluded that the last identified compounds to be degraded were ethylalkanes, trisubstituted cycloalkanes and declalines, but even these disappeared with an apparent half-life of <30 days, and their results seem to contrast with those of (Penet et al., 2006), who studied the biodegradation of diesel in soil containing systems. They found only 19 soil samples exhibited almost complete biodegradation of diesel added at 400 ppm in 28 days at 30^{o}C; the mean was 80% for samples contaminated soils, 64% in uncontaminated soil and 60% with activated sludge, when they added 5 g soil per litre of incubation.

It has been conclusively shown that for low amendments of biodiesel (10%) the overall biodegradation efficiency of the mixture after seven days was lower than for petroleum diesel fuel (Owsianiak et al., 2009). During their study biodegradation of the lowest fraction was favoured by rhamnolipids supplementation, whereas the biodegradation of the highest fractions was somehow inhibited, and their results demonstrated that for analyzed microbial consortium biodiesel was more favoured carbon source than diesel fuel, but there was a concentration for which the overall biodegradation rate of the mixture is lower than for pure diesel fuel. Finally the results might indicate that for a specialized microbial consortium, a rapid change from favoured hydrocarbons to methyl esters influences assimilation of organic carbon (Owsianiak et al., 2009).

3 Research Hypothesis, Aims and Objectives

3.1. Introduction

Because of growing concerns about the gasoline additive MTBE it is likely to be phased out of the fuel supply. Concerns include its pollution of public drinking water since the 1980s (Tiemann, 2006), and its potential harmful effects, such as, MTBE is much more soluble in water than petroleum hydrocarbons, has a low taste and odour threshold, has a higher transport rate and often requires more time to be remediated. MTBE is extremely soluble and, once released, it moves through soil and into water more rapidly than other fuel constituents and once in groundwater, it is slow to biodegrade and is more persistent than other gasoline constituents (Tiemann, 2006). On the basis of its environmental effects, the search has started for capable, actual and useful oxygenate alternatives. One of the key issues to selecting the most appropriate alternative will be its readily biodegradability in the environment. In the U.S., the fuel additive MTBE has been replaced with ethanol (Deeb et al., 2003; Powers et al., 2001; Harley et al., 2000).

The UK has scaled back its plans to introduce biofuels such as ethanol and biodiesel, after a government-commissioned report warned of their wider social and environmental impacts. The UK government will now review its renewable transport fuel obligation, which required suppliers to ensure 5 per cent of all their fuel comes from renewable sources by 2010. That is now likely to be pushed back to at least 2013 as part of a 'more cautious approach' to biofuels (http://www.rsc.org/chemistryworld/News/2008/July/08070802.asp). Nevertheless, biofuels are increasingly blended with petroleum because of environmental concerns about MTBE and concerns about the combustion of fuel from non-renewable sources (Dakhel et al., 2003).

3.2. Scope of the study

This study will look at the aerobic biodegradation of VOCs in the presence of biofuel components in particular ethanol and biodiesel. This will be compared with the biodegradation of a pure VOCs fuel. The fate, transport and biodegradation of volatile organic compounds (VOCs) in the unsaturated zone,

in the presence or absence of biofuel components with and without nutrient addition will be investigated.

3.3. Approach

The present study aims to provide a comprehensive understanding of the environmental effects of the addition of biofuels to petroleum on the natural attenuation of VOCs in the unsaturated zone, by examining the effect of ethanol and biodiesel addition on the fate, transport and biodegradation of petroleum VOCs in the unsaturated zone in the first phase, while the second phase investigates the availability and the role of inorganic nutrients.

Laboratory experiments were conducted employing gas chromatography to evaluate gaseous transport of VOCs in unsaturated, aerobic soil lysimeters and batches, and gas chromatography mass spectrometry was applied to evaluate the production and consumption of CO_2 and O_2 in unsaturated soil lysimeters and batches.

Molecular biological analyses were conducted as well (Wolicka et al., 2009; Stelzer et al., 2006) employing total cell count (Gray et al., 2009; Kepner and Pratt, 1994), denaturing gradient gel electrophoresis (Tzeneva et al., 2008) and band sequencing in order to identify hydrocarbon-degrading bacteria in soil and evaluate the effect of soil pollution with petroleum containing biofuels on microbial activity and community structure under aerobic conditions.

Finally, the chemical and geochemical, and microbiological information was comprehensively evaluated to assess the effect of biofuel addition by analyzing chemical and microbiological data and looking at the microbial community structures.

3.4. Research hypothesis

The initial hypothesis was that, in the presence of readily degradable additives, such as ethanol and biodiesel, petroleum hydrocarbons degradation is slower.

3.5. Knowledge gaps

The substitution of fossil fuels with biofuels in the European Union (ELF) is part of a strategy to mitigate greenhouse gas emission from road transport (Ryan et al., 2006). A review covering EU strategy for biofuels until 2025 has been reported by (Kulczycki, 2006).

Biofuels are believed to be environmentally sound and competitive fuels. It has been reported that the European governments intend to increase the share of biofuels in total EU fuel consumption to 5.7% by 2010 and bioethanol is the primary candidate (Frondel and Peters, 2007; Kozakowski, 2006).

As mentioned in the literature review, a considerable amount of literature has been published discussing the biodegradation and transport of petroleum hydrocarbons in unsaturated zone, but there are only a few reports in the literature regarding the effect of ethanol on VOCs biodegradation (Osterreicher-Cunha et al., 2009; Wu et al., 2009; Cápiro et al., 2007; Hansen et al., 2005; Dakhel et al., 2003; He et al., 2003; Adam et al., 2002; Leong et al., 2002).

There are also only a few studies in the literature regarding the effect of the addition of biodiesel on the migration and biodegradation of VOCs under aerobic conditions (Owsianiak et al., 2009; Prince et al., 2008; DeMello et al., 2007; Kwanchareon et al., 2007; Oliveira et al., 2007; Stauffer and Byron, 2007; Bay et al., 2006; Meher et al., 2006). Significant gaps remain in our understanding of the role of new petroleum additives (ethanol and biodiesel) on the whole natural attenuation process, and a better understanding of such roles and effects is warranted for the selection and design of appropriate remedial strategies in places where biodiesel and ethanol are used as additives and for future recommendations about the use and the addition of biofuels.

Gaps remain in particular in our understanding of the role of ethanol and biodiesel in the natural attenuation of hydrocarbons and their vapour plumes in the unsaturated zone. Whilst significant inhibition of BTEX biodegradation has been reported for fuels containing ethanol in groundwater contamination

scenarios (Jóice et al., 2009; Osterreicher-Cunha et al., 2009; Guo et al., 2007; Osterreicher-Cunha et al., 2007; Hansen et al., 2005; LAHVIS, 2003; Alvarez and Hunt, 2002; Powers et al., 2001), this inhibition has mainly been attributed to the depletion of dissolved oxygen by the rapid ethanol biodegradation. In the unsaturated zone oxygen availability may be less of a concern, because it can be more rapidly supplied from the atmosphere via the air-filled soil pores.

Furthermore, most of the published literature has been focused either on just the BTEX group or assessing the role of ethanol on the natural attenuation of the hydrocarbons as total petroleum hydrocarbons rather than discussing the effect of biofuel components on each fuel constituent. Gaps also remain in our understanding of the effect of biofuels on soil microbial community structures responsible for the degradation of petroleum hydrocarbons.
This study represents a first step towards closing these gaps in our knowledge and this gives to the study its innovation.

3.6. Research aims

This project aims to provide an integrated and comprehensive understanding of the environmental effects of the addition of ethanol and biodiesel on the natural attenuation of VOCs in the unsaturated zone, in particular soil and groundwater pollution risks for ethanol-blended fuel and biodiesel-blended fuel retained in the unsaturated zone. It uses a multidisciplinary approach, measuring the sorption-distribution coefficient and retardation factor and determining the biodegradation rate of the 12 VOCs in unsaturated soil samples and applying modern molecular microbial methods, in order to investigate the influence of biofuels on petroleum hydrocarbon degradation, with and without nutrients addition.

3.7. Research objectives

3.7.1. Monitor the vapour phase concentration of the constituents of three fuel mixtures, containing either no biofuel or 10% ethanol (E10) or 20% biodiesel (B20) in closed batch and semi-open mini-lysimeter systems.

3.7.2. Measuring oxygen consumption and carbon dioxide production for each system.

3.7.3. Measuring the sorption-distribution coefficient K_d

3.7.4. Calculating the retardation factor $R_{a.}$

3.7.5. Determining the biodegradation rate of the 12 VOCs, $k_{app.}$

3.7.6. Quantifying the diffusive volatilization flux for the mini-lysimeters.

3.7.7. Measuring the NAPLs residual for each mixture constituents at the end of batch and mini-lysimeter experiments.

3.7.8. Determining the total cell numbers for each system.

3.7.9. Performing denaturing gradient gel electrophoresis (DGGE) in order to study changes in the microbial community structure for each system.

3.7.10. Sequencing bands from the DGGE in order to identify dominant members of the microbial communities.

3.7.11. Quantifying the final carbon mass balance for each system

3.7.12. Statistical data analysis and interpretation of results.

3.8. Modelling framework

In order to establish a comprehensive understanding of the soil and groundwater risks for PP, E10 and B20, it is useful to assess the degradation rate by including it in an analytical model that can calculate the attenuation of the vapour concentration C_a with radial distance r, from the source zone. For this purpose Equation (1) from Hohener et al (2006) is applied.

For a constant spherical source with radius r_0 in an homogenous infinite porous Medium, the attenuation of the vapour concentration C_a with radial distance r is:

$$C_a(r,\infty) = \frac{C_{a0} r_0}{r}\, e^{-\sqrt{\frac{k_{app}}{D'}}\,(r-r_0)} \quad \textbf{Equation 3-1}$$

Where:

$Ca\,(r,\infty)$: The steady-state vapour concentration as a function of distance from the source

C_{a0} : The concentration near the source

r_0 [cm]: The radius of the source

r [cm]: The distance from the source

K_{app} [s^{-1}]: the apparent biodegradation rate in the batch experiments

$D^{'}$: The sorption-affected gas-phase diffusion coefficient can be calculated as:

$$D^{'} = f_a\, \tau_a\, D_a \quad \textbf{Equation 3-2}$$

Where:

τ_a denotes the tortuosity factor τ described by the model of (Millington and Quirk, 1961)

$$\tau_a = \frac{\theta_a^{2.33}}{n_{tot}^2} \quad \textbf{Equation 3-3}$$

$D_a \left[\frac{cm^2}{s}\right]$ the molecular diffusion coefficient in air can be calculated according to the method of Fuller as outlined in (Schwarzenbach et al., 1993).

f_a: the mass fraction of the compound in the soil air can be calculated according to the method of (Werner and Hohener, 2003):

$$f_a = \frac{1}{1 + \frac{\rho_s (1-\theta_t)}{K_s \theta_a} + \frac{\theta_w}{H\theta_a}}$$ **Equation 3-4**

Where θ_a, θ_w and θ_t denote the air-filled, the water filled, and total porosity respectively, and ρ_s denotes the density of the solids.

$K_s \left[\frac{mol\ cm^{-3}\ (air)}{mol\ g^{-1}\ (solid)} \right]$ denotes the air-solid partitioning coefficient, which can be defined as the ratio between the Henry's law constant and the solid-water partitioning coefficient K_d.

3.9. Research questions

The specific research questions to be addressed are:

3.9.1. What is the impact of ethanol and biodiesel on the biodegradation rate of the petroleum hydrocarbons in aerobic soil?

3.9.2. What are the biodegradation rates of aerobic micro-organisms degrading VOCs in the presence of ethanol and biodiesel?

3.9.3. How strongly are the VOCs absorbed by soil?

3.9.4. How easily are the VOCs to evaporate from the soil?

3.9.5. How strongly does the addition of ethanol and biodiesel affect the natural attenuation of small petroleum hydrocarbon spills in the unsaturated zone?

3.9.6. Are microorganisms degrading the biofuel component different species from those degrading petroleum hydrocarbons?

3.9.7. Is competition for inorganic nutrients a potential explanation for the inhibition of petroleum hydrocarbon degradation in the presence of biofuels in aerobic soil?

3.9.8. Are blended fuels containing a biofuel component a lesser or greater environmental risk than pure petroleum when small spills are retained in the unsaturated zone?

4 Materials and Methods

4.1. Introduction

The fate of volatile organic carbons (VOCs) in petroleum-contaminated soil was investigated at the laboratory scale, using two different approaches. The first approach used a laboratory mini-lysimeter system. The second approach looked at the intrinsic biodegradation in batch systems and the effect of nutrients; both approaches were investigating indigenous microorganism under aerobic conditions.

4.2. Experimental designs

4.2.1. Solid-water distribution coefficient and biodegradation rate measurements

This part of the study produced the data to predict the migration and the fate of 12 VOCs vapours mixture in the unsaturated zone, by setting-up a laboratory batch microcosm experiment. The microcosm experiments were performed with the sandy soil at room temperature under aerobic condition. Vials of 40 ml volume (H x Φ = 97 x 27 mm, Sigma-Aldrich UK) closed with Teflon Mininert valves were used for the microcosm experiments. Mininert valves are Teflon closures that allow sampling through a valve, which contains a rubber septum to prevent leakage or exposure of vial contents during sampling. The sand was wetted to a volumetric water content θ_w of 0.18 and packed to a total porosity of 0.433 with leaving about 27 mm headspace in the bottle. Abiotic controls were prepared by autoclaving the sand three times at 120^{o}C for 20 min at intervals of 24 h (Hohener et al., 2003), using (ENSIGN 125, Rodwell Scientific Instruments, UK). Before adding the VOCs, the microcosms were stored at 25 ^{o}C for 24 h. Then, 1 ml of the headspace gas of a bottle containing the fuel mixture at 25^{o}C was injected. The decreases of the VOCs concentration in the microcosm were measured by GC-FID for up to 5 days for the normal soil microcosm and 7 days for the abiotic controls respectively. Decreases of concentration rates were determined by plotting the concentration vs. time. Partial pressure of CO_2, O_2 and SF_6 as a conservative tracer, were analyzed by GC-MS.

4.2.2. Mini-lysimeter experimental system

Stainless-steel mini-lysimeter buckets (height 20 cm, diameter 15 cm) were filled with sandy soil to a height of 15 cm. A volume of 35 mL of either pure petroleum hydrocarbons, PP, ethanol-blended fuel, E10, or biodiesel-blended fuel, B20, were mixed into the soil to obtain a source zone with a residual NAPL saturation θ_{NAPL} (-) of 4% (v/v), and the buckets were quickly filled with clean soil to a height of 15 cm, leaving 5 cm as headspace. Each step consisted of adding soil to the soil mini-lysimeter and compacting it to reach a thickness of 5 cm, before adding the subsequent layer. The mini-lysimeters were closed with stainless steel lids with a clay seal and had sampling ports to withdraw gas samples from the headspace, and an inlet and outlet in the lid which could be sealed with a nut or connected to a multi-channel pump (Watson-Marlow Bredel Pumps, UK) to purge the headspace. The bulk density of 1.58 Kg L^{-1} and the soil water content θ_w (-) of 0.23 ± 0.01 resulted in a water-filled pore space (WFPS) suitable to the optimal soil water content for aerobic microbial activity, which has been suggested by Aon (Aon et al., 2001; Linn and Doran, 1984). The soil-filled volume of the mini-lysimeters had a volumetric water content θ_w (-) of 0.23 ± 0.01 and a total porosity θ_t (-) of 0.49 ± 0.02. The headspace of the three mini-lysimeters was simultaneously flushed on day 11, 21, 24, 30, 38, 46, 58, 67 and 75 with air at a flow rate of about 100 ml per minute for 12 hours to keep the mini-lysimeters aerobic. VOCs, CO_2, and O_2 concentrations were monitored in the headspace.

Figure 4.1 Laboratory mini-lysimeters system, control, PP, E10 and B20 fuel mixtures respectively.

4.2.3. Batches experimental system

Batch experiments were performed in 65 ml amber vials (Jencons, a VWR Division, Bedfordshire, UK) closed with Teflon Mininert valves (Sigma-Aldrich Company Ltd. UK) containing 15.07 ± 0.12 g wet weight of sandy soil with a water content of 8.5 ± 1.3 weight %. VOC concentrations were monitored after injecting 0.030 mL of the fuels as liquid. To study the effect of inorganic nutrients, 1.8×10^{-3} g of N in the form of NH_4Cl and 1.8×10^{-4} g of P in the form of KH_2PO_4 was added to each nutrient amended batch. On day 14 about 40.0 mL of headspace air in the nutrient amended batches were replace with pure air to keep the batches aerobic using gas-tight syringes. The amount of CO_2 and VOC vapours removed with the syringe was measured and considered in the mass balance.

4.3. Materials

4.3.1. Fuel compound mixtures

A mixture of 12 typical fuel compounds shown in Table 4-1 was prepared from chemicals of at least 99% purity, all obtained from Sigma-Aldrich UK. The selected fuel compounds and their weight percentages are typical for major constituents of gasoline or kerosene, and closely resemble those used in previous studies (Dakhel et al., 2003; Pasteris et al., 2002). The mixture will be referred to as pure petroleum hydrocarbons, PP, in this study. It was blended with 10% (v/v) ethanol (Sigma-Aldrich Company Ltd. UK) to create ethanol blended fuel, E10, or with 20% (v/v) biodiesel to create biodiesel blended fuel, B20 as is shown in Table 4-2. The fuel compounds investigated here are more typical for gasoline and kerosene than diesel, but were also used as the petroleum hydrocarbon components of B20 in this study to allow for cross-comparison of results.

Compound	Formula	M.Wt g/mol	Density g/mL	Weight in VOCs mixture %	Initial concen-tration g/m^3
n-pentane	C_5H_{12}	72	0.626	3.2	83.354
n-hexane	C_6H_{14}	86	0.659	7.4	56.606
n-octane	C_8H_{18}	114	0.703	8.4	6.337
n-decane	$C_{10}H_{22}$	142	0.73	17.9	1.692
n-dodecane	$C_{12}H_{26}$	170	0.75	9.5	0.112
methyl cyclopentane	C_6H_{12}	84	0.749	6.3	43.543
methylcyclohexane	C_7H_{14}	98	0.77	10.5	22.393
Cyclohexane	C_6H_{12}	84	0.779	6.3	30.604
Isooctane	C_8H_{18}	114	0.692	15.8	36.078
Toluene	C_7H_8	92	0.865	3.2	4.479
m-xylene	C_8H_{10}	106	0.868	5.3	2.260
1,2,4,trimethylbenzene	C_9H_{12}	120	0.876	6.3	0.746
Total				100	

Table 4-1. Physiochemical properties of the VOCs pure solution and calculated volumes and concentrations

Lysi-meter	Name	Description	Composition	Mixture symbol
1	Pure petroleum	Pure highly and semi VOCs	12 petroleum hydrocarbons (VOCs)	**PP**
2	Ethanol-blended fuel	PP + ethanol	12 petroleum hydrocarbons + 10 %(V/V) Ethanol	**E 10**
3	Biodiesel-blended fuel	PP + biodiesel	12 petroleum hydrocarbons + 20% (V/V) biodiesel	**B 20**

Table 4-2 Fuel and blended fuel mixtures

4.3.2. Characterization of the soil

The sandy soil used in this study was obtained from a construction site on Newcastle University campus. It had the following grain size composition: 87.26% sand, 11.33% silt and 1.42% clay. The soil contained by dry weight 7.3 mg/kg ammonical (Kjeldahl) nitrogen, < 1.00 mg/kg total oxidized nitrogen, 550 mg/kg total phosphorus and 1570 mg/kg total organic carbon (all results from Derwentside Environmental Testing Services Limited, Durham, UK).

4.4. Sampling methods

4.4.1. Quality assurance and quality control (QA/QC)

All syringes were daily flushed with pure air or pure nitrogen prior to the sampling, they were then analysed by a blank run (injection of air) to ensure that no target pollutants were present. A new calibration curve was daily determined.

Any analytical measurement, no matter how carefully made, is subject to some uncertainty, which may arise from a number of possible sources not necessarily independent of one another. For instance, when the analysis of the VOCs vapours is made by injecting the headspace gas, the same procedure for the standards should be followed. As gaseous samples pass through the column, calibration should also be made identically by passing gaseous samples standards into the column.

Using liquid standards to calibrate gaseous samples collected from the headspace systems may yield a discrepancy, as the liquid phase standard typically has more sensitive response. Hence, the calibrated results of gas samples may be underestimated. According to (Demeestere et al., 2008), quantification of gaseous VOCs loaded on a sorbent tube using response factors obtained with liquid standards results in systematic deviation of 40-80%. On the other hand, using liquid standards solutions is a common and the most preferred method reported in the literature since accurate gas standards are expensive and not easy to generate; particularly in the case of reactive, polar or volatile analytes and at low concentrations (Demeestere et al., 2008). In this study, routine standards calibration was carried by injecting gaseous phase standards, which will be described later in this chapter.

4.4.2. GC-FID analysis of VOCs

For VOCs identification, 1.92 g of the PP solution was transferred to a 40 ml glass vial with a Teflon mininert valve for gas headspace analysis.
VOCs identification were analyzed using a headspace technique, by injecting 10 µL of gas headspace using a 25 µL Hamilton gastight syringe into a HP-7890 Series Gas Chromatography (Agilent Technologies, USA) equipped with a HP-5 capillary column (30 m * 0.249 mm * 0.25 µm) and Flame Ionization Detector FID. The injection used a split ratio of 10 and was heated to 200 ^{o}C. The column temperature was held at 30 ^{o}C for 5 min, increased to 120 ^{o}C at a rate of 10 ^{o}C min^{-1}, and then held constant for 6 min. The hydrogen carrier gas was adjusted to a flow rate of 2ml min^{-1}.

The chromatogram of the total PP VOCs headspace result is shown in Figure 4.2.

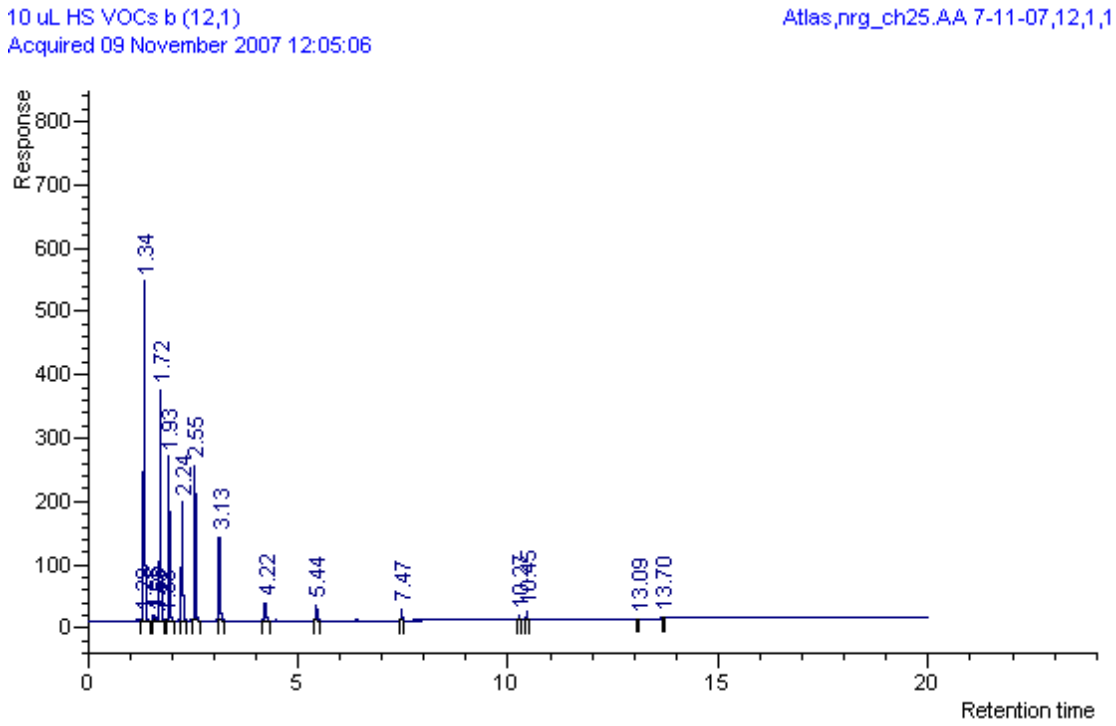

Figure 4.2 PP VOCs chromatogram

4.4.3. Identifying each VOC peak in the PP VOCs chromatogram

For the identification of each VOC peak, 10 µL gas from the headspace of the pure compound liquid was sampled with a 25 µL Hamilton gastight syringe and injected into the GC using and analysed with the method described above.
On the basis of the VOC chromatogram result, each VOC has been identified according to the retention time. A summary of each VOC retention time can be found in Table 4-3.

An example of n-octane, n-decane and toluene chromatograms are shown in Figure 4.3, Figure 4.4 and Figure 4.5 respectively.

No	Compound	Retention time (min)
1	n-pentane	**1.34**
2	n-hexane	**1.72**
3	Methylcyclopentane	**1.93**
4	Cyclohexane	**2.24**
5	Isooctane	**2.55**
6	Methylcyclohexane	**3.13**
7	Toluene	**4.24**
8	n-octane	**5.42**
9	m-xylene	**7.47**
10	1,2,4,trimethylbenzene	**10.27**
11	n-decane	**10.45**
12	n-dodecane	**13.70**

Table 4-3.VOCs retention time (min)

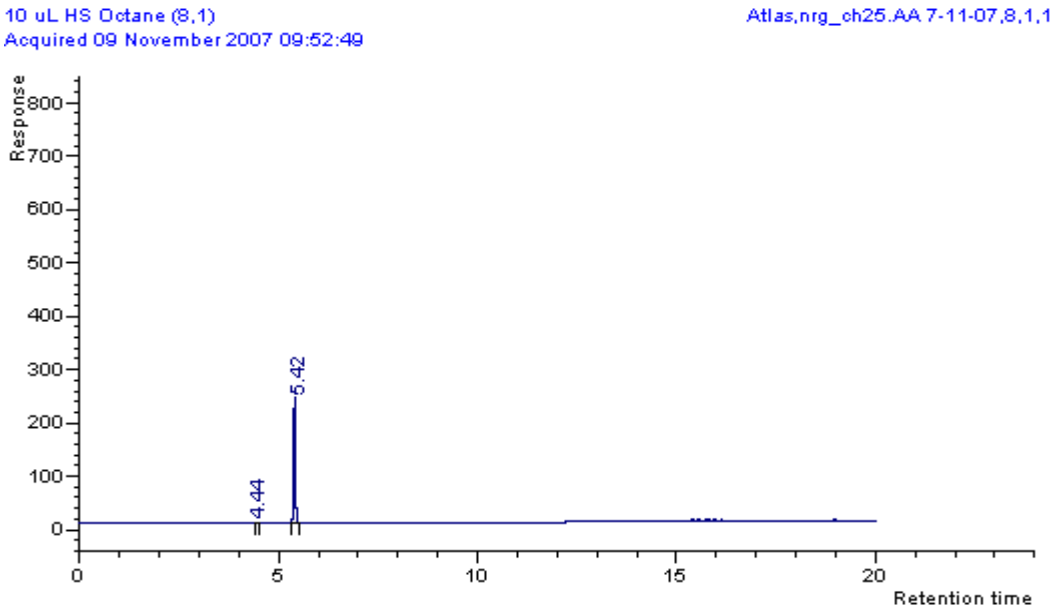

Figure 4.3. Chromatogram of 10 µL headspace n-octane.

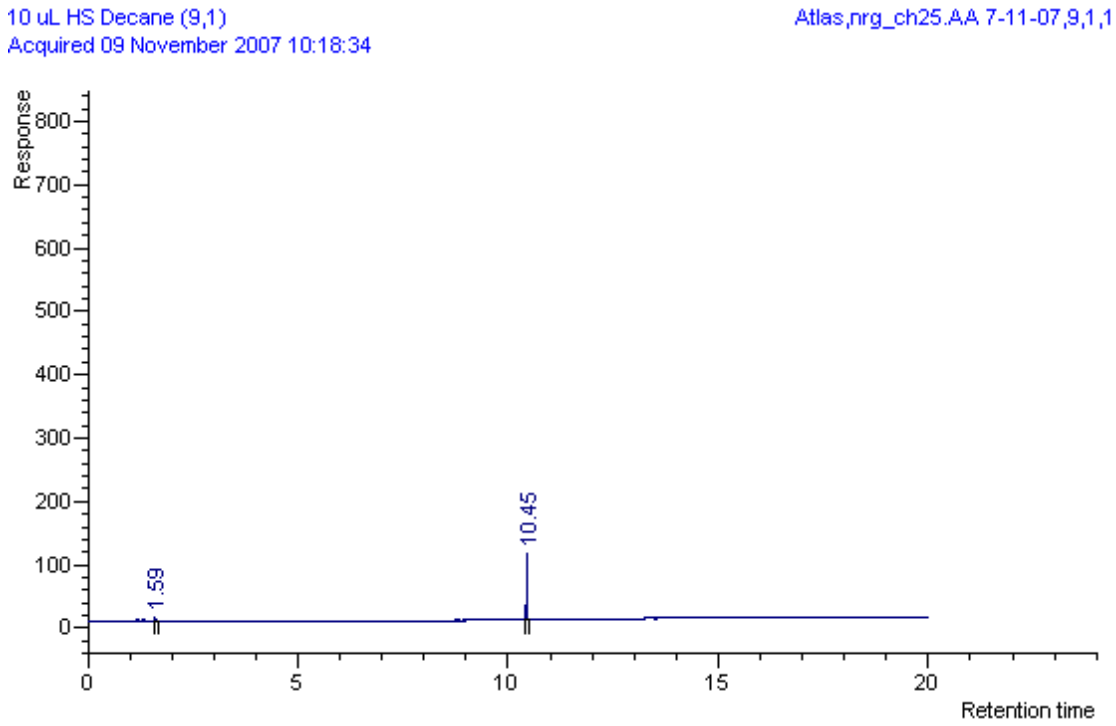

Figure 4.4. Chromatogram of 10 µL headspace n-decane.

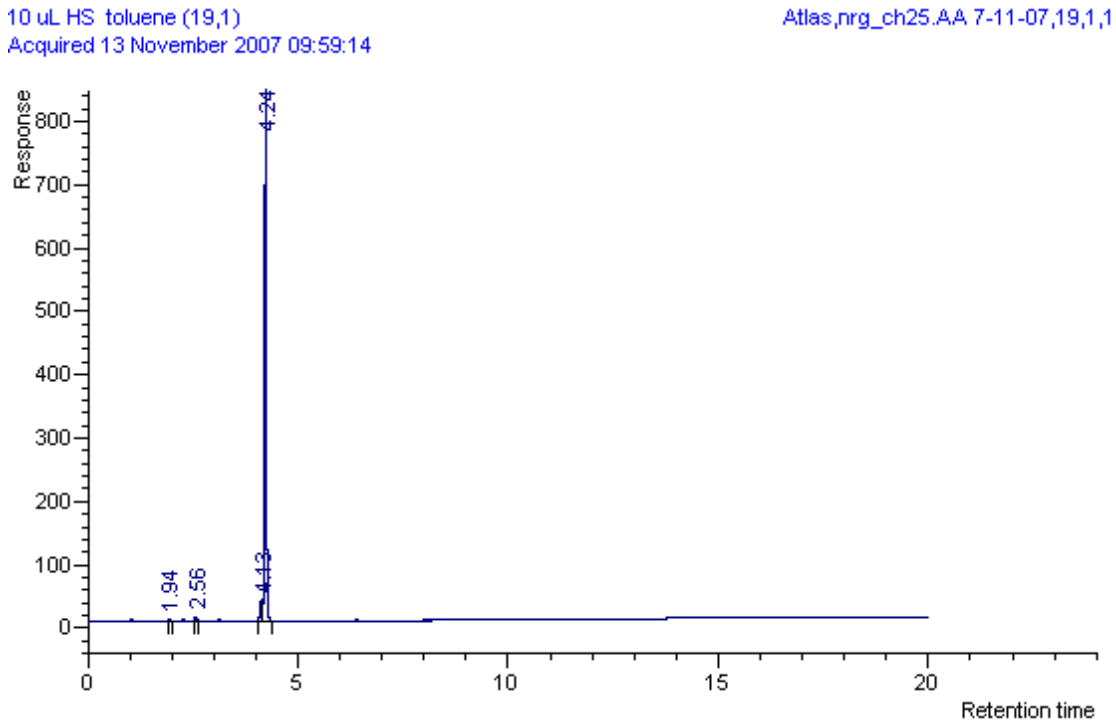

Figure 4.5. Chromatogram of 10 µL headspace toluene.

4.4.4. Preparing and identifying ethanol in the E10 mixture

For calibration and identification purposes a small volume of 10 mL of ethanol-blended fuel mixture was prepared by diluting 1mL pure ethanol in VOCs solution to make a final 10mL ethanol-VOCs solution. Then the solution quantitatively transferred into 40 ml glass vial with a Teflon Mininert valve for gas headspace analysis.

10 µL of E10 gas headspace was sampled using a 25 µL gastight syringe and injected into a HP-7890 Series Gas Chromatography, E10 headspace chromatogram is shown in Figure 4.6.

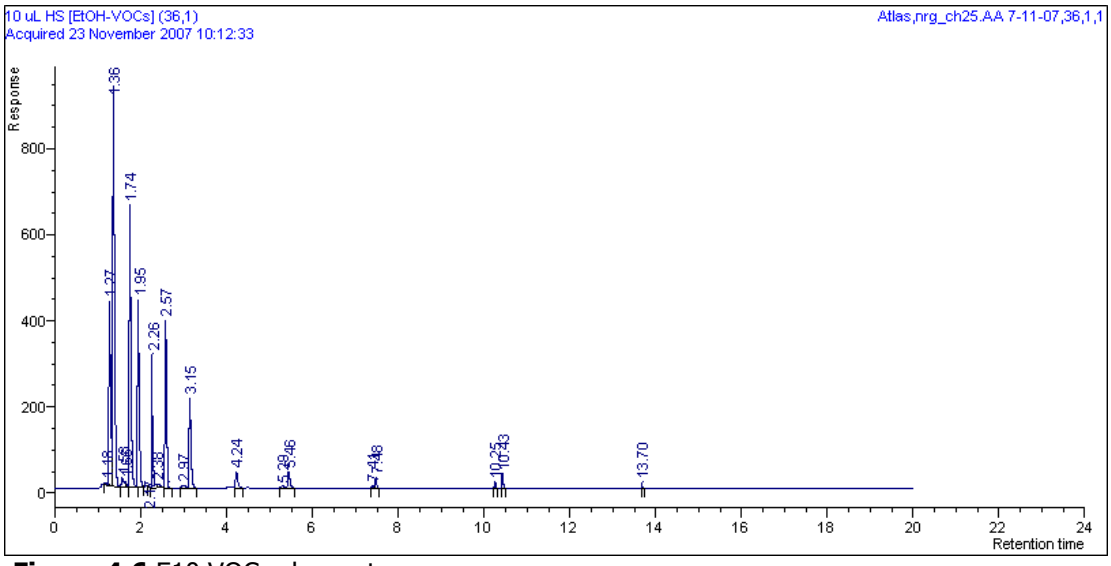

Figure 4.6 E10 VOCs chromatogram

4.4.5. Identifying the ethanol peak

The ethanol peak in the E10 headspace chromatogram has been identified by injecting 10 µL of gas sampled from the headspace of pure ethanol into the GC at the same conditions, the chromatogram of the pure ethanol is shown in Figure 4.7. It can be concluded that the peak with retention time of 1.27 in is Figure 4.6 the ethanol peak, according to the peak retention time in the pure ethanol chromatogram.

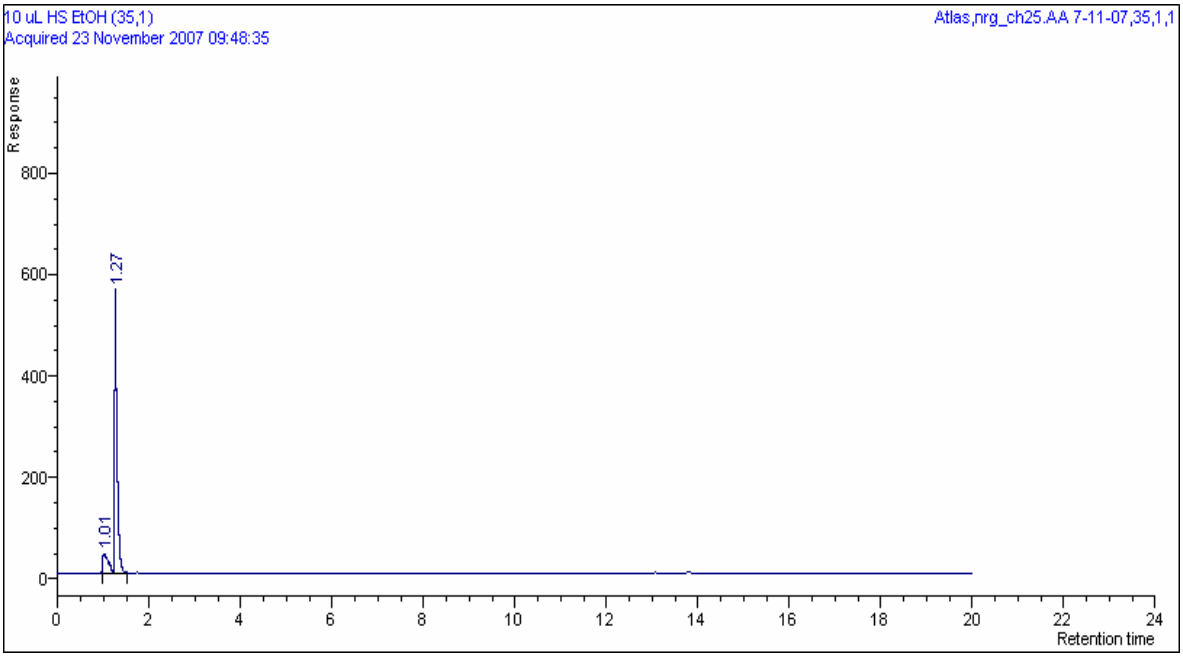

Figure 4.7. Chromatogram of 10 µL headspace ethanol.

4.4.6. Calibration mixtures curves

For calibration purposes, two standard VOCs calibration mixtures were prepared, calibration mixture 1 (CM1) includes the more volatile VOCs, these are the first six VOCs in Table 4-3.

Calibration mixture 2 (CM2) includes the less volatile VOCs, these are the compounds from 7 to 12 in same table.

The composition, quantities and initial vapour concentration of CM1 is shown in Table 4-4.

compound	Formula	M.Wt	weight in the mix, %	no of mol	mol fraction	(vapour concentration)[a] C g/m^3
n-pentane	C_5H_{12}	72	1.518	0.021	0.020	39.764
n-hexane	C_6H_{14}	86	5.314	0.062	0.059	40.505
Methylcyclopentane	C_6H_{12}	84	12.146	0.145	0.139	83.088
methylcyclohexane	C_7H_{14}	98	30.364	0.310	0.298	53.414
Cyclohexane	C_6H_{12}	84	18.219	0.217	0.208	87.599
Isooctane	C_8H_{18}	114	32.642	0.286	0.275	74.008
Total			100		1.0	

Table 4-4. Calibration Mixture 1 quantities and concentrations
[a] calculated based on mole fraction and Raoult's law.

1.0 ml gas headspace of CM1 was diluted into 40 ml air headspace in a 40 ml glass vial with a Teflon mininert valve, then 20, 40, 60, 80 and 100 µL of the gas headspace was injected into the GC-FID to construct a calibration curve and analyzed using the method described above.

An example of the 60 µL gas headspace chromatogram result of CM1 is shown in Figure 4.8.

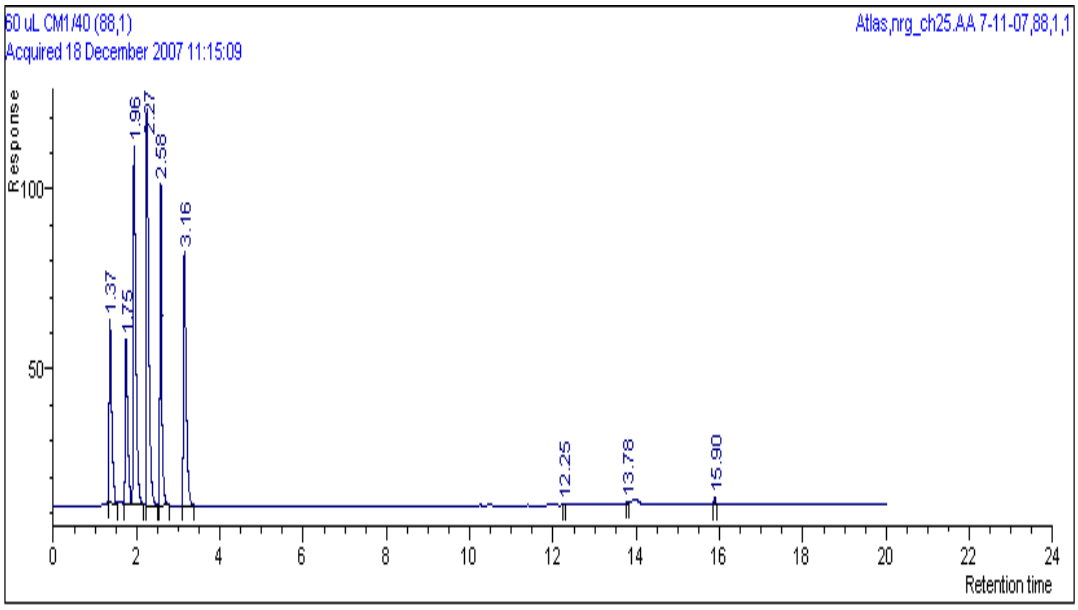

Figure 4.8. Chromatogram of 60 µL headspace CM1.

The calibration curve for each VOC in CM1 was obtained from the analysis of the CM1 headspace. Quantification was based on mass injected, peak area and data acquisition was performed using GC Atlas software.
The linearity of the CM1 calibration curves was usually good, with regression coefficients (R^2) of about 0.985.

An example of the n-pentane calibration curve calculations and calibration curve result are shown in Table 4-5 and Figure 4.9 respectively.

V uL injected	(C g/uL) [a]	(C/40) [b]	(mass injected in g) [c]	Area in mVs
20	3.98×10^{-08}	9.94×10^{-10}	1.99×10^{-08}	70.452
40			3.98×10^{-08}	151.961
60			5.96×10^{-08}	203.43
80			7.95×10^{-08}	305.297
100			9.94×10^{-08}	387.466

Table 4-5. n-pentane calibration curve calculations

[a] was calculated on the basis of the mole fraction of the pure VOC in CM1 and Raoult's law. [b] calculated as a/40. c calculated on the basis of the diluted concentration and the volume injected.

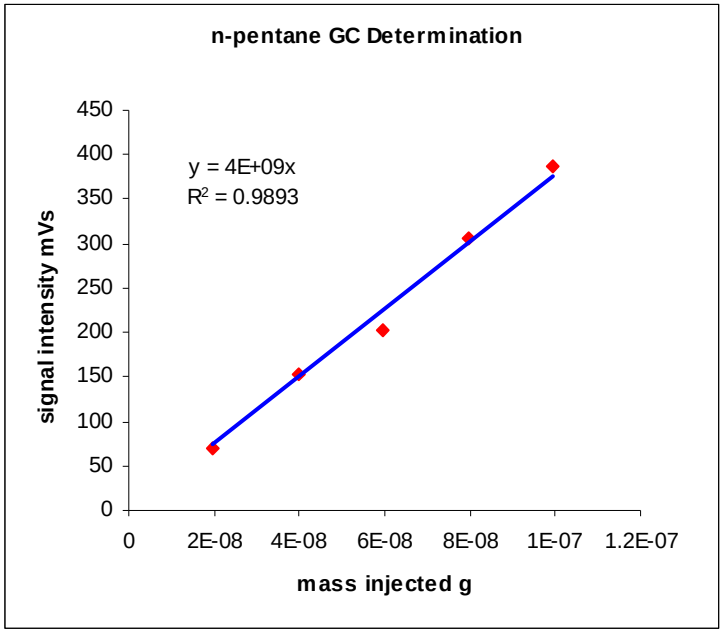

Figure 4.9. n-pentane calibration curve.

Calibration Mixture 2 (CM2) includes the less volatile VOCs these are the last six VOCs in the chromatogram. Quantities, volumes and concentrations of CM2 VOCs are shown in Table 4-6.

compound	Formula	M. Wt	weight in the mix, %	no of mol	mol fraction	(vapour concentration)[a] C g/m^3	(V)[b] ml
n-octane	C_8H_{18}	114	11.268	0.099	0.131	11.579	16.0
n-decane	$C_{10}H_{22}$	142	39.906	0.281	0.372	5.153	54.7
n-dodecane	$C_{12}H_{26}$	170	21.127	0.124	0.164	0.341	28.2
Toluene	C_7H_8	92	4.225	0.046	0.061	8.184	4.9
m-xylene	C_8H_{10}	106	9.390	0.089	0.117	5.506	10.8
1,2,4,TMB	C_9H_{12}	120	14.085	0.117	0.155	2.273	16.1
Total			100		1.0		130.6

Table 4-6. Quantities, volumes and concentrations of CM2

[a] calculated based on mole fraction and Raoult's law. [b] calculated based on weight in the mixture and the compound density.

After preparing CM2 as described about 5.0 ml of the solution was quantitatively transferred into a 40 ml glass vial with Teflon mininert valve, then 20, 30, 40, 50, 60 and 70 µL of the CM2 gas headspace was diluted into 100 µL syringe air, then all the volumes were respectively injected to the GC-FID and analyzed using the method described above.

The calibration curves and quantification for each VOC in CM2 was obtained by the same method described previously for CM1.

The linearity of the CM2 calibration curves was usually good, with regression coefficients (R^2) about 0.99 except for decane and dodecane the regression coefficient (R^2) was about 0.89 and 0.52 respectively. Because of the comparatively low volatility of decane and dodecane, probably due to condensation of vapours in batch bottles and syringes used for sampling (Hohener et al., 2003) the gas-phase analysis of this compound was difficult with the method employed in this study and decane and dodecane results are only semi-quantitative.

An example of the toluene calibration curve calculations and the calibration curve result is shown in Table 4-7 and Figure 4.10 respectively.

Constituent VuL	V injected uL	mass inj g	A mVs
20	100	$1.64x10^{-07}$	966.938
30	100	$2.46x10^{-07}$	1467.404
40	100	$3.27x10^{-07}$	2040.88
50	100	$4.09x10^{-07}$	2468.667
60	100	$4.91x10^{-07}$	3130.765
70	100	$5.73x10^{-07}$	3694.723

Table 4-7. Toluene calibration curve calculations

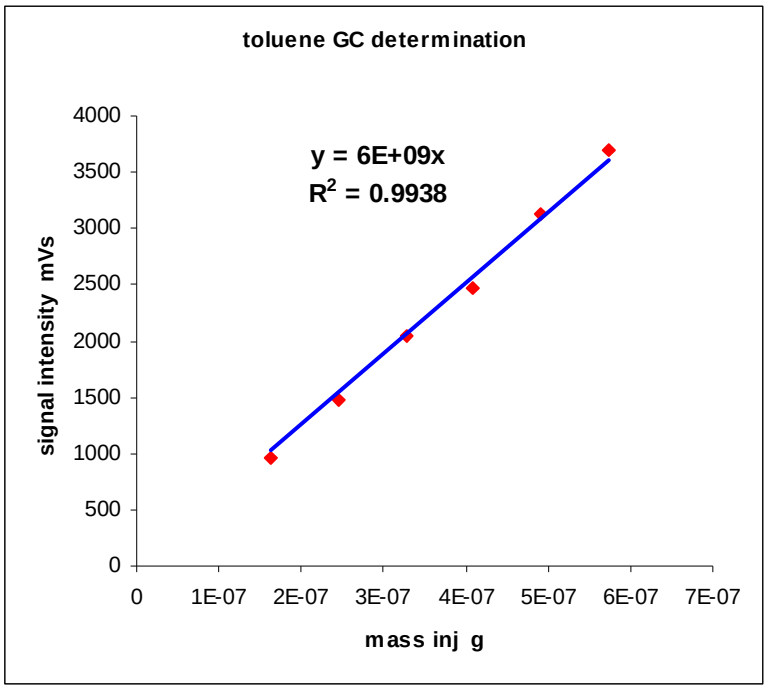

Figure 4.10. toluene calibration curve.

4.4.7. Ethanol calibration curve

Ethanol GC determination was obtained by diluting 1.0 ml gas headspace of pure ethanol in 40 ml air headspace in 40 ml glass vial with Teflon mininert valve, then 20, 40, 60, 80 and 100 µL of the gas headspace was injected respectively to the GC-FID using the conditions previously described for CM1. The result of ethanol calibration curve is shown in Figure 4.11.

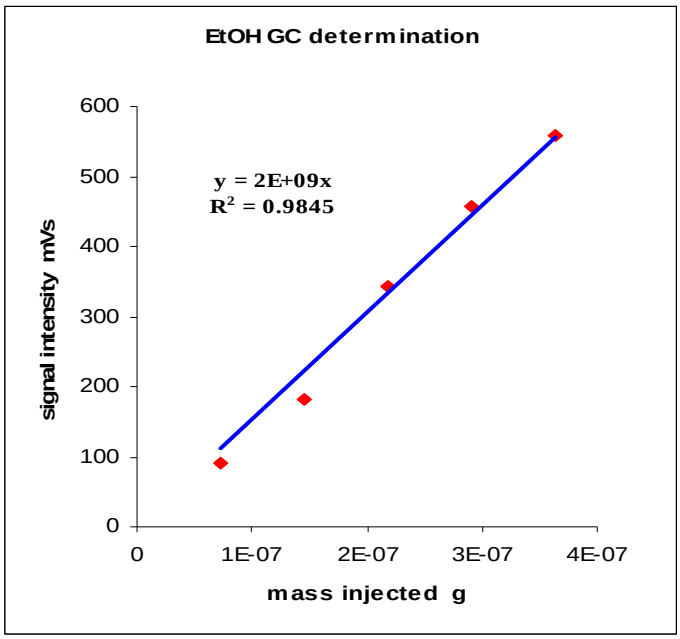

Figure 4.11 Ethanol calibration curve

4.4.8. Carbon dioxide and Oxygen analysis

GC-MS analysis of biogenic gases (CO_2 and O_2) was performed on a Fisons 8060 GC using split injection (150°C) linked to a Fisons MD800 MS (electron voltage 70eV, filament current 4A, source current 800uA, source temperature 200°C, multiplier voltage 500V, interface temperature 150°C). The headspace sample (40ul) was injected in split mode. Separation was performed on a HP-PLOT-Q capillary column (30m x 0.32mm i.d) packed with 20um Q phase. The GC was held isothermally at 35°C with helium as the carrier gas (flow rate of 1ml min^{-1}, pressure of 65 kPa, split at 100mls min^{-1}).

4.4.9. Non-aqueous phase liquid (NAPL) residuals quantification

10 g of soil were extracted twice for 24 h in 10 mL pentane/dichloromethane (6:4 by volume). The combined extracts were passed through a glass chromatographic column (45cm x 10 mm i.d.) pre-packed with 3g of activated silica gel topped by 1.0 g of sodium sulfate. Columns were flushed with an additional 20.0 mL of solvent and all solvent was collected in 40mL batches from which 1mL was transferred into a 1.0 mL GC-vials for analysis. Pentane and hexane could not be quantified by this method because of incomplete

separation from the solvent peak. The main esters of biodiesel which consisted of 8.2 ± 0.13 % (w/w) palmitic acid methyl ester C16:0, 3.5 ± 0.02 % (w/w) stearic acid methyl ester C18:0, 40.3 ± 0.32 % (w/w) oleic acid methyl ester C18:1, and 38.9 ± 0.20 % (w/w) linoleic acid methyl ester C18:2, 9.0 ± 0.59 % (w/w) linolenic acid methyl ester C18:3 could be quantified, but ethanol and biodiesel metabolites such as fatty acids could not be quantitatively recovered. Blank samples processed through the clean-up showed no background contamination.

Compounds in cleaned-up solvent extracts were identified and quantified by GC-MS analysis on a Agilent 6890/7890A GC in split less mode, injector at (280°C) linked to a Agilent 5973/5975C MSD. Separation was performed on an Agilent fused silica capillary column (30m x 0.25mm i.d) coated with 0.25um dimethyl poly-siloxane (HP-5) phase. The GC was temperature programmed from 50-310°C at 5°C min and held at final temperature for 10 minutes with Helium as the carrier gas (flow rate of 1ml/min, initial pressure of 50kPa, split at 30 mls/min).

4.5. Molecular Methods

4.5.1. Total microbial cell number

A fundamental aspect of many ecological investigations is the need for a reliable quantitative estimation of the microbiological populations that are present within its environment. However, the application of epifluorescence microscopy is now generally acknowledged to be the best method currently available for counting microorganisms in order to identify any microorganisms growth during a bioremediation process (Herbert et al., 1990). When compared to traditional culturing methods that may require incubation times of up to 3 days (Madrid and Felice, 2005), epifluorescence microscopy provides very rapid microbial enumeration, with an incubation period of less than 30 minutes with a DNA stain to allow the direct observation and total enumeration of organisms.

Mini-lysimeter soil samples used for measuring total cell number were collected from three different positions in each mini-lysimeter. Each mini-lysimeter was divided into three equal zones of 5 cm depth. 20 ± 1.8 g soil samples were randomly collected from depths 5 cm (top zone), 10 cm (middle zone) and 15 cm (source zone) from each mini-lysimeter. Samples were ground, suspended in (1:1 w/v 50% ethanol) and stored at -20^{o}C for later analysis.

Total cell counts in soil samples were determined by diluting 1 mL from previously fixed suspended cells' samples (1:1 w/v 50% ethanol) to a suitable dilution 10^{-2} in filter sterile 1 X Phosphate Buffered Saline (PBS). SYBR gold fluorescence dye (chemical number S-11494, Invitrogen Ltd, UK), diluted 100 x in filter sterile PBS, 50 uL was added to each sample to stain the nucleic acids in the cells. Staining was used to determine the total numbers of soil bacteria, the dilution factor 1:100 was used for the whole bacteriological counts. Because SYBR gold is light sensitive, samples were wrapped in foil and incubated at room temperature for 30 min, before filtration. 1mL of each sample was filtered. Bacteria were collected by filtration through a 0.2-mm-pore-size black polycarbonate filter (diameter, 25 mm; Millipore). The filters were mounted in paraffin oil (Gray et al., 2009).

Total bacteria were determined by direct count on black nuclepore filters using an Olympus BX40 Epi-fluorescence microscope, and a minimum of 30 of fluorescence cells with a clear outline and finite cell shape were counted under oil immersion (x100) in a minimum of 20 randomly chosen fields (Gray et al., 2009). Error between samples was estimated using the standard deviation of the mean from three replicate counting samples measured per each mixture and controls. Cell size was performed by analyzing photos taken by Olympus digital camera (E-400) and CellC freeware from http://www.cs.tut.fi/sgn/csb/cellc/.

Cell volume was calculated by assuming that the shape of bacteria was cylindrical (C) with hemispheric (H) ends as depicted below in Figure 4.12.

Figure 4.12 Assumed bacteria shape

To convert bacterial biovolume into carbon biomass, a conversion factor of 310 fg of C μm^{-3} has been used (Fry, 1990).

$$\frac{\frac{cell}{g\ (dry\ soil)} * Cell\ size\ \mu m^3\ * 310\ \frac{fg}{\mu m^3}\ \left(\frac{biomass\ carbon}{volume\ of\ cell}\right)}{10^{15}\ \frac{fg}{g}}$$

Equation 4-1

Sizes of bacteria were measured by using photographs of stained cells taken with an Olympus digital camera (E-400) system attached to an Olympus BX40 Epi-fluorescence microscope. The bacterial dimensions were measured by analysing the digital photographs using CellC freeware (Selinummi et al., 2005).

4.5.2. Denaturing gradient gel electrophoresis (DGGE)

Denaturing gradient gel electrophoresis (DGGE) is a method by which fragments of DNA of the same length but different sequence can be resolved electrophoretically (Head et al., 1998), and in the last decade, 16S rRNA gene fragments from environmental samples have been analysed by the application of this method. In this technique, a mixture of PCR-amplified fragments of different sequence is electrophoretically carried through a gradient of denaturant in a polyacrylamide gel (Kowalchuk et al., 1997). Sequence variations affect the exact position at which the fragments denature and cease migration through gel. The resulting banding pattern provides a representation of the structure of the most predominant members of the bacterial community. This approach allows a rapid visual comparison of communities members of which can subsequently be identified by excising and sequencing bands of interest (Malik et al., 2008).

Since DGGE was first used in a microbial ecology study of sea sediments (Muyzer et al., 1993), it has been used in a wide range of environments including hot springs (Ward et al., 1998; Ferris et al., 1996), and wastewater treatment plants (Godon et al., 1997), (Cocolin et al., 2001).

Total DNA was extracted from 0.5 g of frozen samples by using the FastDNA Spin Kit (Q-Biogene) and a ribolyser (Thermo) according to the manufacturer's instructions. The presence of sufficient DNA was determined by agarose gel electrophoresis (1% agarose gel in 1xTAE buffer).

Amplification of 16S rRNA gene fragments corresponding to position 341 to 534 of *E. coli* from bacterial population were performed in a total volume of 50 ul containing 0.2 µM of primer 2, (5'-ATTACCGCGGCTGCTGG-3') and 0.2 uM of primer 3, (5'-CGCCCGCCGCGCGCGGCGGGCGGGGCGGGG GCACGG GGG GCCTACGGGAGGCAGCAG-3') with an additional 40 nucleotide GC clamp at its 5' end (Muyzer et al., 1993), 1 X PCR buffer (Bioline), 1.5 mM MgCl2, 0.2mM dNTPs, 1U *Taq* DNA polymerase (Bioline) and buffer provided with *Taq* enzyme and using (10-15 ng) as template DNA.

Amplification was performed in a Techne thermal cycler with the following temperature cycle: 1 cycle 95ºC for 3 min followed by 30 cycles of 94ºC (1 min), 53ºC (1 min) and 72ºC (1 min) and a final extension at 72ºC for 10 min.

All PCR reactions were carried out in 200µl PCR tubes. PCR products were analysed by agarose gel electrophoresis (1% Agarose; 1xTAE buffer) against a marker with known fragment sizes (PCR marker, Sigma).

DGGE analysis was conducted with a D-code system (Bio-Rad) at a denaturing gradient of 30-55% (100% denaturant is defined as 7M urea plus 40% v/v formamide in 1xTAE) in 0.75 mm thick polyacrylamide gel with 16 cm by 16 cm dimension (10% acrylamide-N,N'-methylene-bisacrylamide, 37.5:1).
A standard mixture of cloned 16S rRNA gene fragments was added to four lanes of each gel in order to normalize the gels during analysis.

Electrophoresis was performed at 60ºC for 4.5 hours in 1xTAE buffer (40mM Tris-acetate, 1mM EDTA, pH 8.3) at a constant voltage of 200V, and stained for 30 minutes using SYBR gold diluted to 1/10000 in 1xTAE (Sigma).

4.5.3. Gel analysis

Stained gels were imaged using a UV trans-illuminator with associated software (Bio-Rad). DGGE gel images were analyzed using the Bionumerics software package (Applied Maths).

Bacterial community similarity comparisons were carried out by analysing DGGE patterns with BioNumerics software 5.1 (Applied Maths, 2008). A similarity matrix and cluster analysis was generated using the Dice coefficient and unweighted pair-group method average (UPGMA), respectively. MDS (multi-dimensional scaling) was performed using Primer6 (PRIMER-E Ltd, Plymouth, UK) (Clarke K.R, 2001), to produce a three-dimensional ordination plot in which the distance between data points is proportional to the relatedness between samples.

The structural diversity of the microbial community was examined by the Shannon index of general diversity H' (Shannon and Weaver, 1963). H' was calculated on the basis of peak height from the different bacterial taxa (DGGE bands) as a proportion of the total summed peak height intensity of all bands in a given lane (sample). The equation for the Shannon index is:

$$H = \sum_{i=1}^{N} P_i \, ln \, P_i$$

Equation 4-2

Where P_i is the proportional abundance (relative peak height band intensity) of i^{th} taxon, and N is the total number of bands.

The richness (S) of the bacterial community was determined from the number of bands in each lane.

The evenness (E) of the bacterial community (Pielou, 1969) was calculated as:

$$E = \frac{\sum_{i=1}^{s} P_i \, lnP_i}{ln\, S}$$

Equation 4-3

(E), Pielou's equitability, where S = band

$$1 - \lambda = 1 - \frac{\{\sum_i N_i(N_i - 1)\}}{\{N(N-1)\}}$$

Equation 4-4

Where,

$1 - \lambda$ is the Simpson's index

N_i is the abundance (band peak height) of i species

N is the total abundance of all taxa (sum of the band peak heights)

4.5.4. Sequencing of DGGE bands

To determine the identity of DNA fragments found in DGGE bands, the centre of some bands related to samples from the batch experiments only were stabbed with a 10µl disposable pipette tip. The gel fragment excised were then transferred to 50µl TE buffer and incubated overnight at 4^{o}C, 1µl of this suspension was re-amplified using the same primer pairs however without GC clamp. This amplicon was used in sequencing reaction after treatment with ExoSAP-IT PCR product clean-Up kit from USB corporation. The DNA fragments were sequenced using one of the primers and the Big Dye terminator (v3.1) cycle sequencing kit (ABI). Sequencing was conducted by the Proteomics and Molecular Biology Unit, University of Newcastle upon Tyne (with an Applied Biosystems 377 DNA sequencer).

4.5.5. Sequencing analysis

Searches in the GenBank with the Blast program (Cocolin et al., 2001; Altschul et al., 1997) were performed to determine the closest known relatives of the partial 16S rRNA sequences obtained. The GenBank accession for the nucleotide sequences obtained from the DGGE bands are shown in Table 9.4 in the appendix.

4.5.6. 16S rRNA gene sequences classification

Using a new classifier (Ribosomal Database Project) RDP to assign 16S rRNA gene sequences to the new phylogenetically consistent-order bacterial taxonomy, on the basis of a naive Bayesian rRNA classifier, hierarchial taxa can be obtained. The classifier allows classification of both bacterial and archaeal 16S rRNA (Wang et al., 2007).

5 Modelling Attenuation of Volatile Organic Compounds in the Unsaturated Zone

5.1. *Introduction*

An important topic in groundwater and soil quality management is natural attenuation. It has been reported that the efficiency of natural attenuation is impacted by three key processes, diffusion, sorption and biodegradation (Karapanagioti et al., 2001). Only a limited number of research papers has coupled the kinetics of these processes, because mostly each process has been studied individually. For accurate prediction of the magnitude of natural attenuation, research on the interplay of diffusion, sorption and biodegradation process is a necessity (Karapanagioti et al., 2001). Adoption of certain simplifications to the true complexity of the physical systems is always necessary, in order to be able to use mathematical and analytical models to simulate multiphase flow and multicomponents fate and transport of VOCs in the subsurface environments (Gaganis et al., 2002). Due to the uncertainty in the description of the natural attenuation processes and in the evaluation of controlling parameters, as well as the number of the constituents to be simulated, modelling natural attenuation of vapour plumes generated by VOCs mixtures in the unsaturated zone is complicated (Karapanagioti et al., 2004). Several models have been used in the literature for simulating the fate, transport and predicting the plumes extent generated by multicomponents mixtures (Werner et al., 2006; Jassal et al., 2004; Karapanagioti et al., 2004; Moldrup et al., 2003; Gaganis and Burganos, 2002; Schirmer et al., 2000).

The goal of the initial experiments was to:

i. Examine the ability and efficiency of the soil indigenous microorganisms in degrading specific fuel VOCs.
ii. Measuring the apparent biodegradation rate k_{app} for each VOCs constituent in the soil investigated.
iii. Measuring the soil-water distribution coefficient for each VOCs constituent, K_d.
iv. Applying the measured kapp and Kd parameter values in an analytical model to estimate the extent of the VOCs migration from a known source zone, and to compare the model analyses results based on batches

experimental data for the soil investigated in this study with results based on parameters determined in a field lysimeter experiment described in the literature (Pasteris et al., 2002).

5.2 Experimental

This part of the study simulated the migration and the fate of 12 VOCs vapours mixture in the unsaturated zone. In order to examine the efficiency of the indigenous microorganisms in degrading VOCs, the apparent biodegradation rates and the sorption coefficients were determined. The experiment was performed by setting-up two laboratory batch microcosm experiments. The first set contains live sand, and abiotic controls were prepared by autoclaving the sand for the second set. Then, 1 ml of the headspace gas of a vial containing the fuel mixture at 25^{o}C was injected into the batches and VOC concentrations were monitored for up to 7 days. For more details about the experimental part, please refer to chapter 4, part 4.2.1.

5.3 Results and discussions

5.3.1 Solid-water distribution coefficient determination

The concentrations of the VOCs, and the biogenic gases CO_2 and O_2 and the conservative tracer SF_6 concentrations in the microcosms were measured by GC-FID and GC-MS respectively, for up to 7 days.

Stable concentrations representing sorption equilibrium were determined by plotting the concentration vs. time in comparison with controls consisting of batches without soil. The tracer SF_6 stayed within 80% of its initial concentration during the experiment period. K_d values derived from the data are shown in Table 5-1.

Profiles of vapour-phase concentrations of the VOCs in the autoclaved soil are shown in Figure 5.1. It can be seen that the vapour concentration of these compounds remains relatively stable during the experiment which lasted for 7

days. Figure 5.1, demonstrates the concepts of a steady gas-phase concentration and solid-water distribution representing the sorption equilibrium.

The average of the measured concentration for each constituent was used to determine the solid-water distribution coefficient K_d as follows:

$$K_d = \frac{C_s}{C_w} \qquad L\ kg^{-1}$$

Where, C_w and C_s denotes as the constituent concentration in the soil water, and in the solid respectively, and can be calculated as:

$$C_s = \frac{m_s}{S_m}$$

$$C_w = \frac{m_w}{V_w}$$

Where, S_m is the total soil mass (kg), and m_s (g) is the constituent mass in soil, and can be calculated as:

$$m_s = (m_t) - (m_a + m_w)$$

Where, (m_t), (m_a) and (m_w) denotes as, total constituent mass, constituent mass in soil air and in soil water respectively.

$$m_a = C * V_a$$

$$m_w = \frac{C}{H} * V_w$$

Where, C (g/L) is the measured constituent concentration in the headspace of the batches

H, is Henry's law constant dimensionless

V_a , V_w (L) denotes the total system air and water volume respectively.

Results of the solid-water distribution coefficient can be seen in Table 5-1.

The measured K_d values ranged from 0.90 ± 0.6 for m-xylene to 377 ± 103 for n-octane. The K_d results demonstrate that the monoaromatics have the lowest measured K_d values because they are more soluble than alkanes. On the basis of the water solubility and volatility it is expected that each compound will be sorbed or partition into either soil solids, soil air and/or soil water (Christophersen et al., 2005; Karapanagioti et al., 2005). The normal and cyclo-alkanes have relatively high K_d values in comparison with the monoaromatics because of their high volatility and their low water solubility, see Table 5-1.

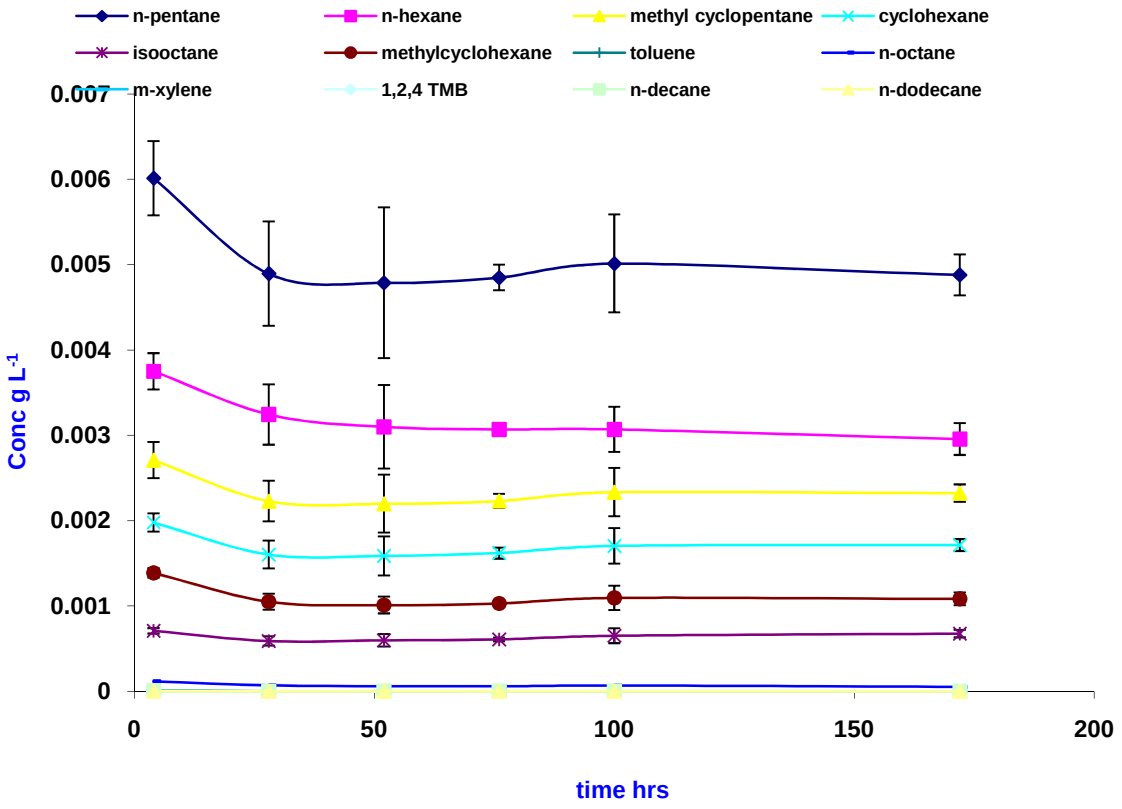

Figure 5.1 Comparison of PP vapour-phase concentration in the autoclaved sand batches, as a function of time. Error bars: ±1 standard deviation (SD, n=3)

5.3.2 Apparent biodegradation rate determination kapp

The measurement of biodegradation rates by indigenous microorganisms is the first step in microbiological characterization. These measurements can be complicated by low microbial population or by the absence of species capable of

degrading contaminants. Also, optimum conditions of temperature, oxygen nutrients supply, and contaminant availability due to low solubility or strong sorption can limit degradation rates, especially in early tests where these limiting factors are not well defined (Providenti et al., 1993).

The main objective of microbial degradation tests is to determine whether the indigenous microorganism are capable of bioremediation when condition are optimized (Crawford and Crawford, 1996).

A variety of mathematical expressions have been suggested to describe the kinetics of biodegradation reactions. These models have been increasing in complexity as they attempt to accommodate the numerous variables that can affect the biodegradation rate in the natural environment. However, the main limitation of some of the VOC transport models is that they have not included biodegradation at all (Gierke et al., 1992; Brusseau, 1991; Mendoza and Frind, 1990; Falta et al., 1989). Additionally, other transport models limitations have been using simplified representations such as first-order reaction kinetics (Frind et al., 1990; Jury et al., 1990; Jury et al., 1983), or Michaelis-Menten kinetics (Chen et al., 1992; Widdowson et al., 1988; Molz et al., 1986). First-order reactions, which assume a constant biomass, are normally observed in short incubation studies conducted at low chemical concentrations.

The data measured in the live microcosms were significantly different to those in abiotic soil within the first 5 days. The compounds showed a faster decrease in live microcosms compared to abiotic microcosms. Results of the first-order biodegradation are shown in Table 5-1.

Profiles of vapour-phase concentrations of the VOCs in live soil are shown in Figure 5.2. It can be seen that the vapour-phase concentration of these compounds decreased sharply within 50 hours.

The maximum vapour-phase concentration of the most VOCs was recorded just 4 hrs after incubation, and then most of the PP constituents' mixture decreased continuously until day 3. The differences between sterile and live soil

demonstrates that the vapour concentration of these compounds decreased because of biodegradation.

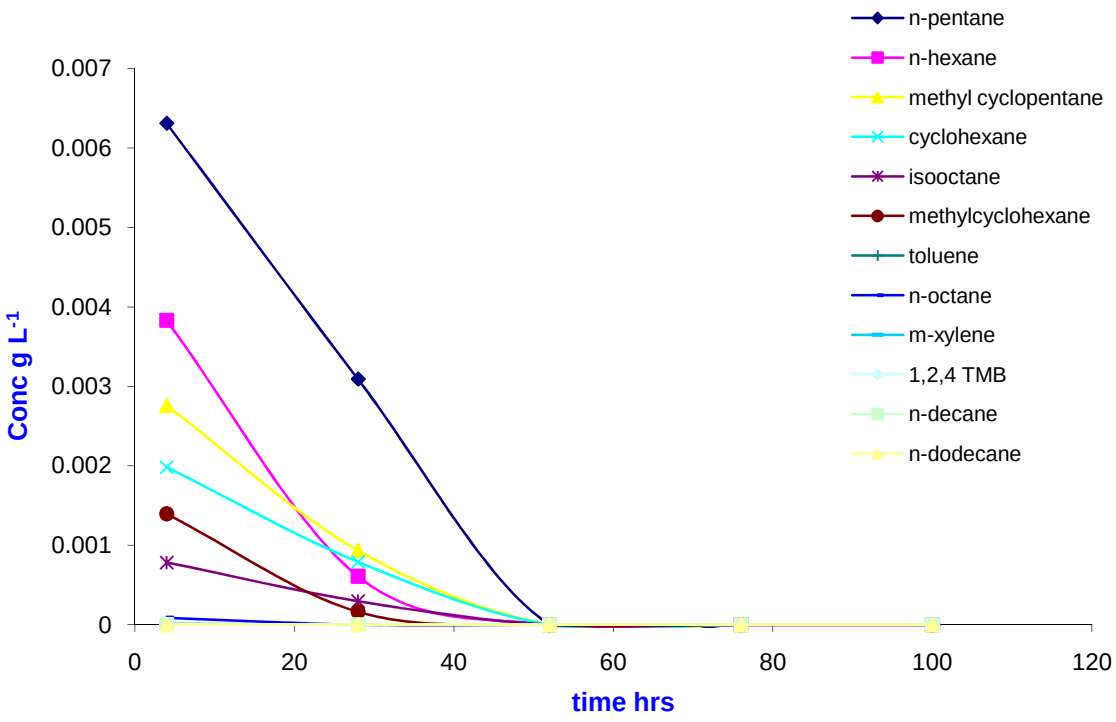

Figure 5.2 Vapour-phase concentration of VOCs in live sand batches.

The measured vapour-phase concentration in Figure 5.2 was used to estimate the half-life rate for each constituent. From the measured half-life, the first order apparent biodegradation rate was estimated.

Assuming first order decay from an initial concentration C_o to C in time t gives:

$$\mathbf{C = C_o \exp(-kt/R_a)} \qquad \textbf{Equation 5-1}$$

Where k is a rate constant and R_a [-] the retardation factor

From which k can be calculated as

$$\mathbf{k = \left\{\frac{-1}{t}\right\} \ln\left\{\frac{C}{C_0}\right\}} \qquad \textbf{Equation 5-2}$$

The half-life $t_{1/2}$ is then

$$\mathbf{t_{1/2} = \frac{0.693}{k}} \qquad \textbf{Equation 5-3}$$

This approach assumes first order decay and it does not allow for an initiation or lag period during which the microbial community becomes activated or acclimated.

First-order kinetics has been found to be a good approximation for most of the VOCs studied in both batch and column experiments by Hohener et al. (2003). Results of the measured k_{app} are shown in Table 5-1.

For all highly-volatile VOCs, the concentration decreased in the live sand was significantly different to that in abiotic sand within the first 7 days, indicating rapid biodegradation has occurred.

For less-volatile VOCs constituents, the concentration decreased even faster than the highly VOCs in the live sand, in particular the aromatics. This decrease was significantly different in comparison with that in abiotic sand within the first 3 days.

For the highly VOCs the apparent half-lives are in the order of 0.5-1.2 days, which translates into an apparent first-order biodegradation rate k_{app} of 1.2 to 0.6 per day, and for the aromatic VOCs the concentration decreases and biodegradation rates are even faster. This is comparable to the biodegradation rates determined by Pasteris et al. (2002) for sand in a lysimeter.

5.3.3 Oxygen and Carbon dioxide

Profiles of the concentrations of CO_2 in the batches for both live and abiotic sands are shown in Figure 5.3. CO_2 plots in the abiotic control were relatively stable through the incubation period and the concentration remained within 82 ± 26 % from its initial concentration. For the live sand batches a CO_2 production increase was clearly seen in the headspace, see Figure 5.3. From the plots it can be seen that CO_2 production started immediately after vapour injection without any significant lag phase period. On day 0 the CO_2 concentration in the live sand increased significantly from 0.0070 g/L, to reach a concentration of 0.017 g/L on day 7. The increasing of CO_2 in the live sand batches which were observed after the vapour injection illustrates metabolic

activity of soil microorganisms (Andre et al., 2009) and demonstrates the active biodegradation process (Hohener et al., 2006; Grathwohl et al., 2002). Both, VOCs biodegradation and background soil respiration contribute to the observed increase in CO_2.

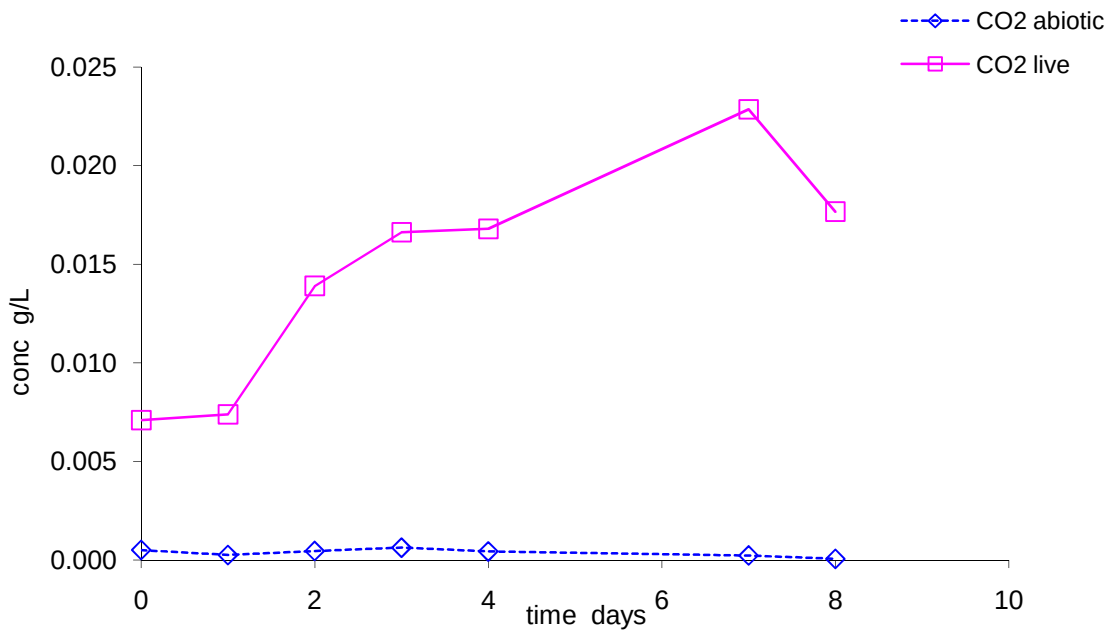

Figure 5.3 Concentration profiles of CO_2 in the live and autoclaved sand**.**

Compound	formula	Weight in mixture, %	Initial vapor concentration (20 °C),[a] g m^{-3}	Calc Da[b] (20°C) m^2 d^{-1}	Calc $K_{d,}$[c] L kg^{-1}	Measured K_d L kg^{-1}	Calc Capacity factor[d] R_a m^3 gas m^{-3}	measured Capacity factor[d] R_a m^3 gas m^{-3}	First –order biodegradation (k)[f] d^{-1}
n-pentane	C_5H_{12}	3.2	95.9	0.082	13.20	7.7 ± 2.7	0.62	0.05	0.59
n-hexane	C_6H_{14}	7.4	65.1	0.076	42.69	6.4 ± 2.0	1.11	0.15	0.98
n-octane	C_8H_{18}	8.4	7.29	0.067	553.48	377 ± 103	6.50	4.51	1.19
n-decane	$C_{10}H_{22}$	17.9	1.95	0.060	368.38	384 ± 41	1.97	43.81	1.19
n-dodecane	$C_{12}H_{26}$	9.5	0.129	0.055	5010.71	not quantified	23.51	0.26	1.11
methylcyclopentane	C_6H_{12}	6.3	50.1	0.081	3.80	5.2 ± 0.7	0.62	0.75	0.76
methylcyclohexane	C_7H_{14}	10.5	25.8	0.075	12.89	3.3 ± 0.5	4.44	1.35	1.04
cyclohexane	C_6H_{12}	6.3	35.2.	0.082	8.58	4.8 ± 0.5	1.87	1.17	0.72
Iso-octane	C_8H_{18}	15.8	41.5	0.066	20.01	24.67 ± 4.7	0.68	5.27	0.76
toluene	C_7H_8	3.2	5.15	0.082	1.42	3.75 ± 0	8.38	20.55	1.19
m-xylene	C_8H_{10}	5.3	2.6	0.076	4.28	0.90 ± 0.6	23.35	0.93	1.04
1,2,4-trimethyl-benzene	C_9H_{12}	6.3	0.858	0.071	14.19	1.4 ± 1.0	72.37	0.91	0.92

Table 5-1 Fuel Compounds, Calculated Model Parameters, and Resulting First-Order Biodegradation Rate Constants.

[a] Calculated based on initial mole fraction and Raoult's law. [b] Calculated according to the method of Fuller as outlined in (Schwarzenbach et al., 1993). [c] Calculated according to the method of (Abdul et al., 1987) as outlined in (Christophersen et al., 2005) log K_d = 1.04* log K_{ow} + log f_{oc} – 0.84. [d] Calculated as Ra = (ρb*Kd + θw + θaH)/H using ρb = 1.36 kg L^{-1}, θa = 0.257, and θw = 0.176 . [f] Calculated as k = ln (2)/$t_{1/2}$

5.4 Field framework

In order to establish a comprehensive understanding of the soil and groundwater risks for petroleum hydrocarbons, it is useful to assess the degradation rate by including it in an analytical model that can calculate the attenuation of the vapour concentration C_a with radial distance r, from the source zone (Hohener et al., 2006).

For a constant concentration on the edge of a spherical source with radius r_0 in a homogenous infinite porous medium, the attenuation of the vapour concentration C_a with radial distance r at steady-state is:

$$C_a(r,\infty) = \frac{C_{a0} r_0}{r}\, e^{-\sqrt{\frac{k_{app}}{D\prime}}\,(r-r_0)} \qquad \textbf{Equation 3-1}$$

For more details about the model parameters and their abbreviations, please refer to chapter 3, part 3.8.

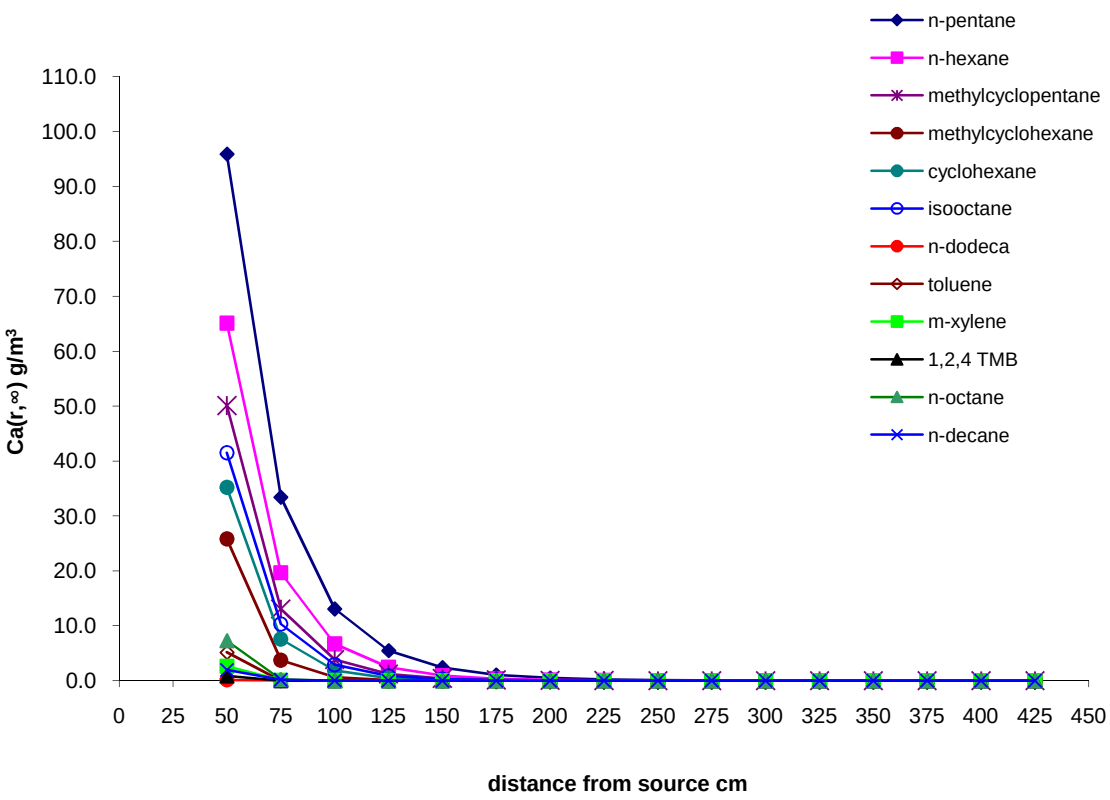

Figure 5.4 Attenuation of VOCs released from a 50 cm source zone

5.4.1 Analytical model results using experimental data

Results of the analytical model based on measured first order apparent biodegradation rates and solid-water distribution coefficients are shown in Figure 5.4. The results show the concentration attenuation of VOCs as they diffuse away from the source zone. Figure 5.5 illustrates the rapid attenuation of the concentration of the VOCs as a result of biodegradation, and eventually the pollutant levels reach near zero concentration within a very short distance. The no biodegradation data in the plot confirms that the VOCs concentrations also decrease with distance solely as a result of the dilution process. The comparison of results with and without biodegradation illustrates that biodegradation is the most active natural attenuation parameter of VOCs rather than the other parameters as reported by Andre et al. (2009), who have investigated the biodegradation of NAPL under unsaturated conditions, and

they have concluded that, biodegradation in porous media can efficiently remove pollutant hydrocarbon compounds.

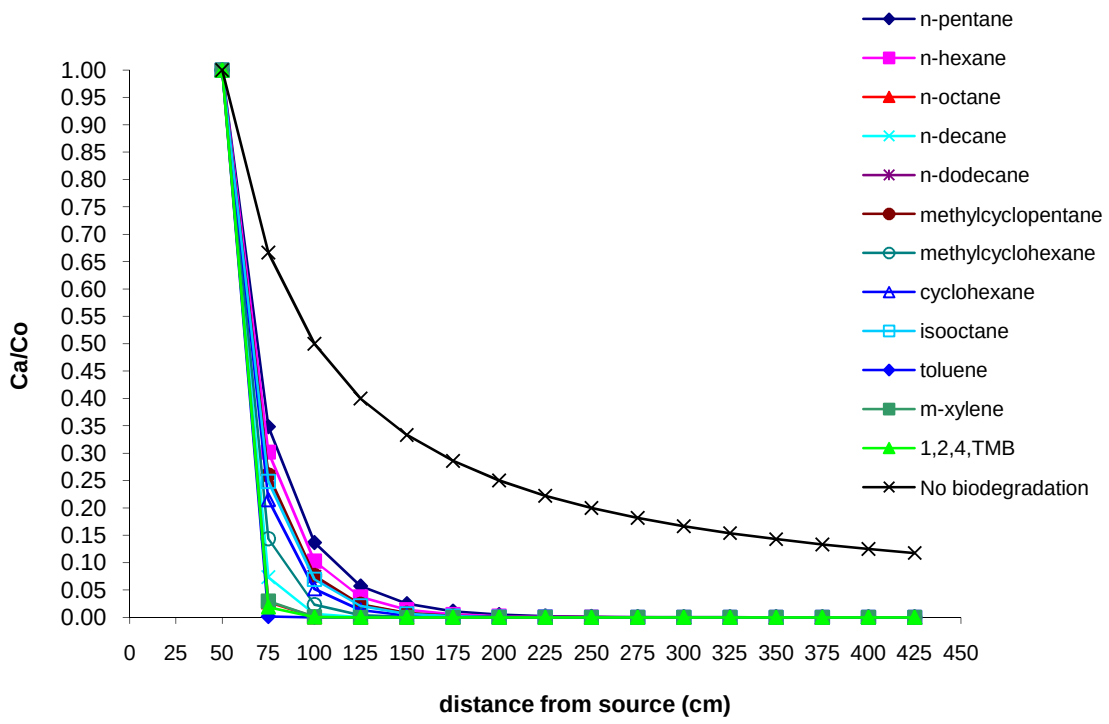

Figure 5.5 Attenuation distance of VOCs from the source zone

The analytical results demonstrating how far a constituent can migrate from a 50 cm source zone before 95% attenuation is reached are shown in Figure 5.6. The distance $(r_{95\%})$ ranged from 75 cm away from the source for the monoaromatics, (toluene, m-xylene and 1,2,4 TMB) as well as n-octane, to 125 cm which corresponds to the high volatiles such as n-pentane and n-hexane, while the attenuation distance of the cycloalkanes ranged from 90 cm for methylcyclohexane to 100 and 115 cm for cyclohexane and methylcyclopentane respectively. These data suggest that the combined effect of sorption and biodegradation attenuates the more soluble monoaromatics constituents faster than the high volatile constituents.

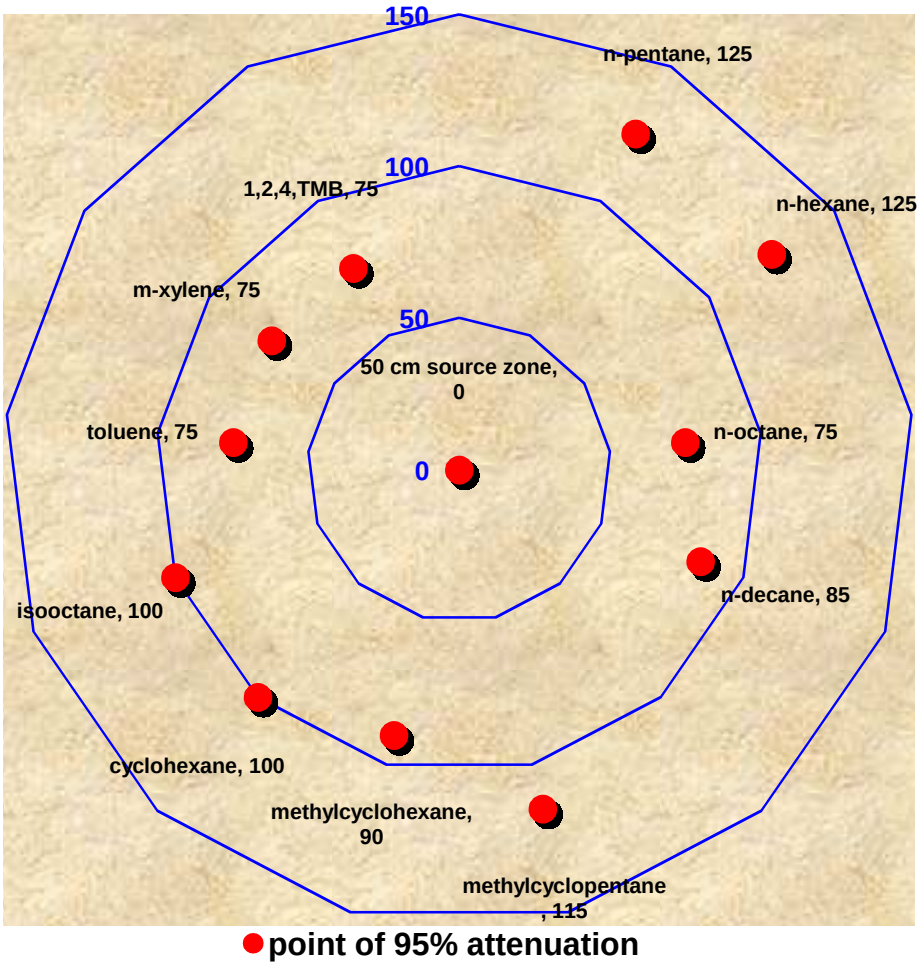

Figure 5.6 VOCs attenuation distance from 50 (cm) source zone

5.4.2 Analytical model results comparison between experimental batches and field lysimeter data

To validate and fine-tune numerical models for comparison reason, comprehensive data sets are required from a field experiment. Here, the data from a lysimeter test performed to quantify biodegradation of VOCs of an artificial fuel mixture are used for a comprehensive understanding of the attenuation distance from a source zone in a real field scenario. Data from the lysimeter experiment include apparent biodegradation rates and solid-water distribution coefficient (Pasteris et al., 2002). Data have been applied to the analytical model in order to compare the batches results and the field data model results.

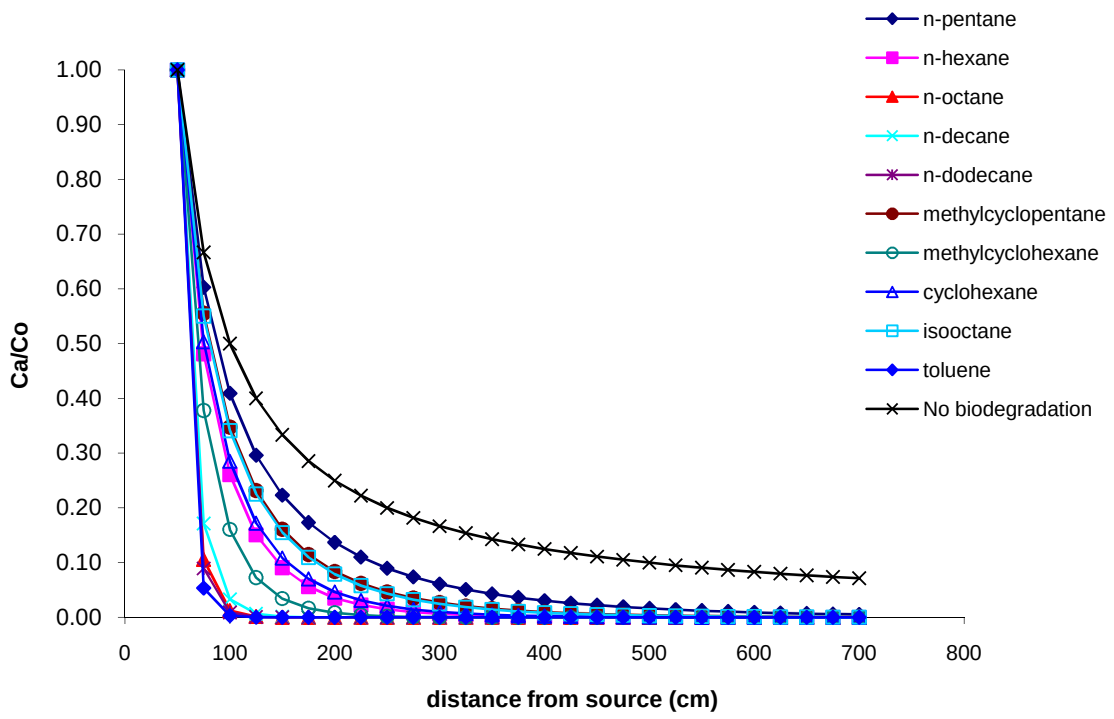

Figure 5.7 Attenuation distance of VOCs released from a 50 cm source zone (Lysimeter data) (Pasteris et al., 2002).

The analytical results of how far a constituent can migrate from a 50 cm source zone before its attenuation, based on the field lysimeter data are shown in Figure 5.7. Figure 5.8 illustrates the distance $(r_{95\%})$, ranged from 75 cm to 350 cm away from the source. 75-100 cm distance from the source zone illustrates the 95% attenuation of toluene and n-octane respectively. While the attenuation distance of cyclohexane and methylcyclopentane was 200 and 250 cm respectively, n-pentane and n-hexane and iso-octane have 95% attenuation distances of 350, 200 and 225 cm respectively. These data suggest that the significant differences in the attenuation distance from the source zone between the laboratory data and field data was related to the difference in the apparent biodegradation rates, which were faster for the soil investigated in the laboratory in this study.

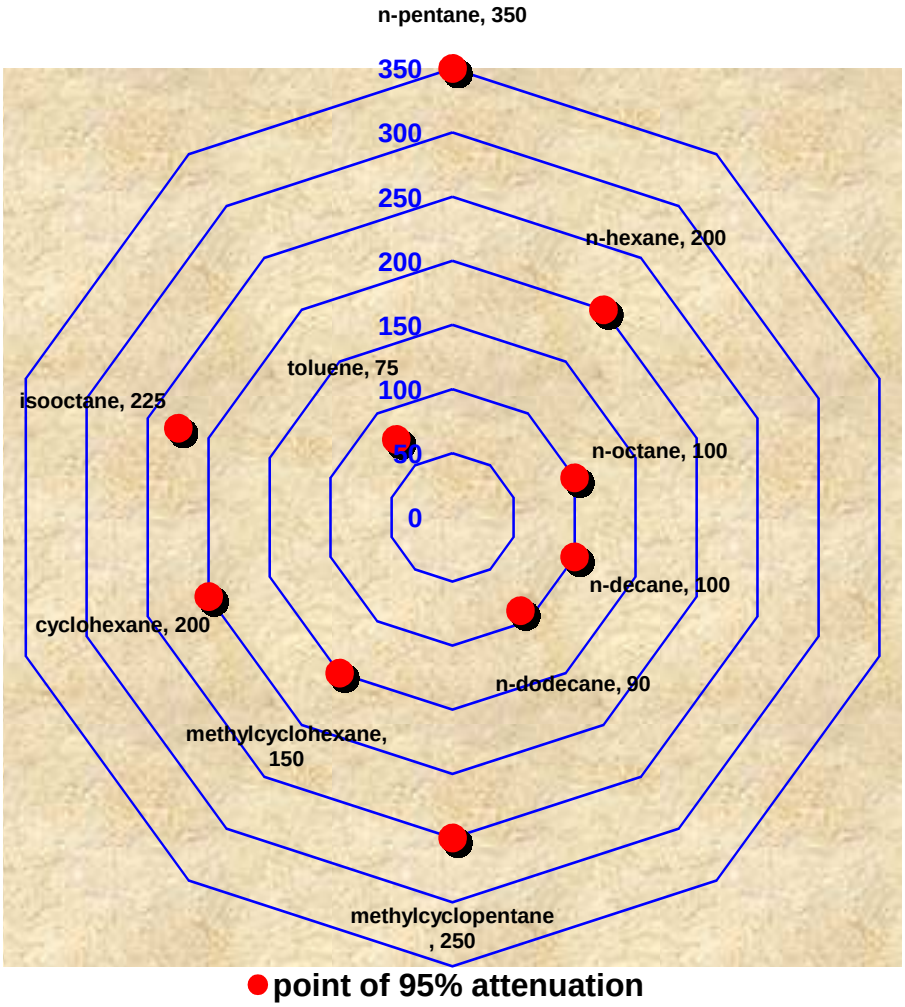

Figure 5.8 VOCs attenuation from a 50 (cm) source zone (Lysimeter data). (Pasteris et al., 2002)

It is noticeably that when simulating the actual lysimeter radius value, 60 cm rather than 50 cm, no dramatic increase in the extent of migration of the VOCs from the 60 cm source zone is predicted except for iso-octane, decane, dodecane and cyclohexane, for which their attenuation distance have increased to 22, 10, 11 and 10% further away from the source zone. Data from the lysimeter simulation with two different radius values 50 and 60 cm for the source zone, confirm findings from the batches data, which show that in addition to the biodegradation the source zone radius is the main parameter affecting the natural attenuation in reducing contaminant concentration rather than other processes (Song et al., 2010). However, the no biodegradation plot in all cases demonstrates that in the absence of the indigenous microorganisms

or the electron acceptors or the availability of inorganic nutrients, natural attenuation may still take place in particular due to sorption into soil and/or soil-water (Chiou et al., 1983) and dilution. These processes are capable of reducing the contaminant concentration while it is migrating away from the source zone. However, it should be noted that based on k_{app} and K_d batches measurements, data clearly illustrate that most of the VOCs in the live sand have completely disappeared under the analytical detection limit during the time between 48 and 72 hours, while for the same constituents in the abiotic sand they persisted at fairly high levels during sorption equilibrium for more than 7 days, which clearly demonstrated that within the experiment conditions biodegradation is a more active mechanism of VOCs degradation than any other natural attenuation process such as sorption (Seagren and Becker, 2002).

5.4.3 Analytical risk assessment of VOCs source in the subsurface

Based on the ability of VOCs and their extent of migration to different distances, potential receptors will be experiencing different exposure (Fan et al., 2009).

Based on the lysimeter data for the 50 cm source zone, Figure 5.8 one could assume as a scenario that a groundwater table is just 100 cm in the vertical direction (r_1) and a residential or industrial property basement just 200 cm (r_2) away from the source zone. In this case (r_1) is shorter than (r_2). As a result the receptor at (r_1), which is the groundwater table, will be significantly affected, because it is within the reach of most VOCs, except toluene which has been attenuated at 80 cm. The contaminants when they reach the groundwater table are reduced to less harmful concentrations of approximately 5% of their initial concentration. Similarily, n-octane, n-decane, n-dodecane, methylcyclopentane, toluene and 1,2,4 TMB will not reach the (r_2) receptors.

These data illustrate just the risk of theses contaminants when their initial concentration reduced to 95%. If 99% attenuation is required, the assessment of the scenario might be completely changed as contaminants will migrate further from the source zone before they are reduced to that level (Waldner,

2008). It should be noted that the presence of a groundwater table would of course violate the "infinite medium with constant properties" assumption underpinning the radial diffusion model, and natural processes like infiltration of groundwater could cause contamination at distance further than the calculated distance of 95% attenuation (Durmusoglu et al., 2010; Fan et al., 2009; Provoost et al., 2009). Nevertheless the radial diffusion model allows for an initial assessment of natural attenuation and environmental risks.

5.5 Conclusion

In summary the data presented in this part illustrate the phenomenon of biodegradation and sorption of VOCs in the unsaturated zone and the analytical model analyses data results demonstrate the VOCs extent of migration from source zone under different scenarios (source zone radius, biodegradation rate and sorption distribution coefficients). All data show that biodegradation by indigenous microorganisms is the key parameter controlling the fate and transport of contaminants in the subsurface, and in the absence of effective biodegradation another parameter may become most important in particular sorption and partitioning (Schwarzenbach and Westall, 1981).

6 Fate and Transport of Pure Petroleum, Ethanol-Blended Fuel (E10) and Biodiesel-Blended Fuel (B20) in Mini-Lysimeters

6.1 Introduction

Demand for renewable fuels is increasing worldwide because of new legislation. The EU directive 2009/28/EC, also known as Renewable Energy Directive, obliges a 10% share of renewable energy in the transport fuel mix by 2020, subject to the sustainability of production. Biofuel usage also increases because of environmental concerns about the fuel oxygenate MTBE which has been eliminated in the U.S. from 2005 onwards (2001b; 2001a) with ethanol being the only economically feasible alternative. Brazil has replaced a large amount of its fossil fuel usage by renewable ethanol produced from sugar cane. In the UK the Renewable Transport Fuels Obligation will require 5% of all fuel sold in the UK to come from renewable sources by 2013/4. Ethanol and biodiesel are the main renewable fuels for petroleum and diesel engines respectively. Because of current fuel standards and car manufacturer warranty limitations, the most likely scenario of the near-future fuel composition in Europe and the US is the blending of a low proportion of bioethanol (5-10%) with petroleum or the blending of a relatively small proportion of biodiesel (up to 20%) with diesel. According to the Governments water strategy document for England, 75% of England's groundwater bodies are at risk of failing to meet good status by 2015, mainly because of diffuse pollution by nutrients and/or hazardous chemicals (Defra, 2008). Oil and fuels are the most frequently reported type of pollutant of inland waters in England and Wales. Every year there are more than 5,000 pollution incidents involving oil and fuel (EA, 2010). In this context it is imperative to properly assess the environmental impact of changes in fuel policies.

The ability of environmental microorganisms to degrade a wide range of fuel components is the most relevant intrinsic defense against pollution where fuels are spilled or leaked into the environment. The impact of a biofuel component on the microbial degradation of harmful petroleum compounds such as the BTEX compounds is controversially discussed (Dakhel et al., 2003) . While the biofuel component of blended fuel is typically less toxic and more readily biodegraded than the petroleum hydrocarbons, there are concerns about an

inhibition of the microbial petroleum hydrocarbon degradation in the presence of ethanol (Da Silva and Alvarez, 2002) or biodiesel (Lapinskiene et al., 2006). Most studies so far have been focused on the complex impact of ethanol on the microbial petroleum hydrocarbon degradation for large spills reaching groundwater (Da Silva and Alvarez, 2002), and evidence for prolonged BTEX plumes at ethanol impacted sites has been reported (Ruiz-Aguilar et al., 2002). Depletion of electron acceptors in groundwater because of rapid ethanol degradation may inhibit BTEX degradation in groundwater (Da Silva and Alvarez, 2002).

In aquifers, ethanol degradation appears to result in microbial community structure changes which decrease the relative abundance of BTEX degraders (Da Silva and Alvarez, 2002). The presence of ethanol may also reduce the rate of BTEX degradation per cell of known BTEX degraders because BTEX compounds are degraded by inducible enzymes that can be repressed when a more easily degradable substrate such as ethanol is available (Lovanh et al., 2002).

Very little is known about the microbiology of blended fuel degradation in soils (Osterreicher-Cunha et al., 2009). The degradation of petroleum hydrocarbons by intrinsic soil microorganisms may effectively protect groundwater resources from diffuse pollution via the vapour phase or leachate in the case of smaller fuel spills retained in the unsaturated zone. These smaller spills often go unnoticed. For such scenarios, the availability of electron acceptors may be less of an issue, since oxygen can be resupplied as an electron acceptor from the atmosphere via the air-filled soil pore space. However, the petroleum hydrocarbon degradation in aerobic soil is often limited by nutrient, especially nitrogen, availability.

6.2 Experimental

The experimental part of this phase which includes the preparation of the three fuel mixtures PP, E10 and B20, characterization of the sand, mini-lysimeters set-up, soil gas sampling and analysis, non-aqueous phase liquid (NAPL) residuals quantification, and the microbiological methods have been discussed in the materials and methods chapter, for more details please refer to chapter four.

6.3 Results and discussion

6.3.1 Vapour phase concentrations of PP, E10 and B20 Fuel compounds

Profiles of vapour concentrations of the fuel compounds in the headspace of the mini-lysimeter are shown in Figure 6.1 for the PP mixture for the first seven compounds, while the concentrations profiles of the three monoaromatic compounds of the same mixture are shown in Figure 6.2. Decane and dodecane gas phase concentrations were difficult to measure because of their low volatility as discussed in chapter 4 and for this reason they have been excluded from the vapour-phase plots. The maximum vapour concentrations of most PP constituents were recorded in day 2, and then most of the PP constituents decreased continuously until day 92. The vapour concentrations of these compounds decreased because of volatilization during the purging of the headspace on day 11, 21, 24, 30, 38, 46, 58, 67, 75 and/or biodegradation (Lahvis et al., 1999).

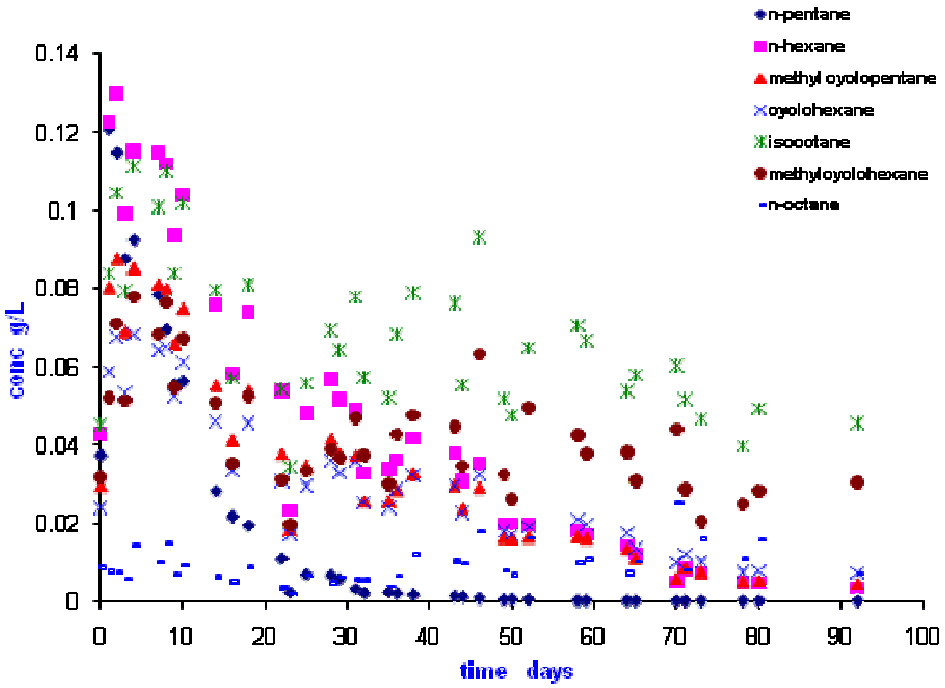

Figure 6.1 Headspace vapour phase concentration profile of the non-blended fuel alkanes in the unsaturated zone during the attenuation period (92 days).

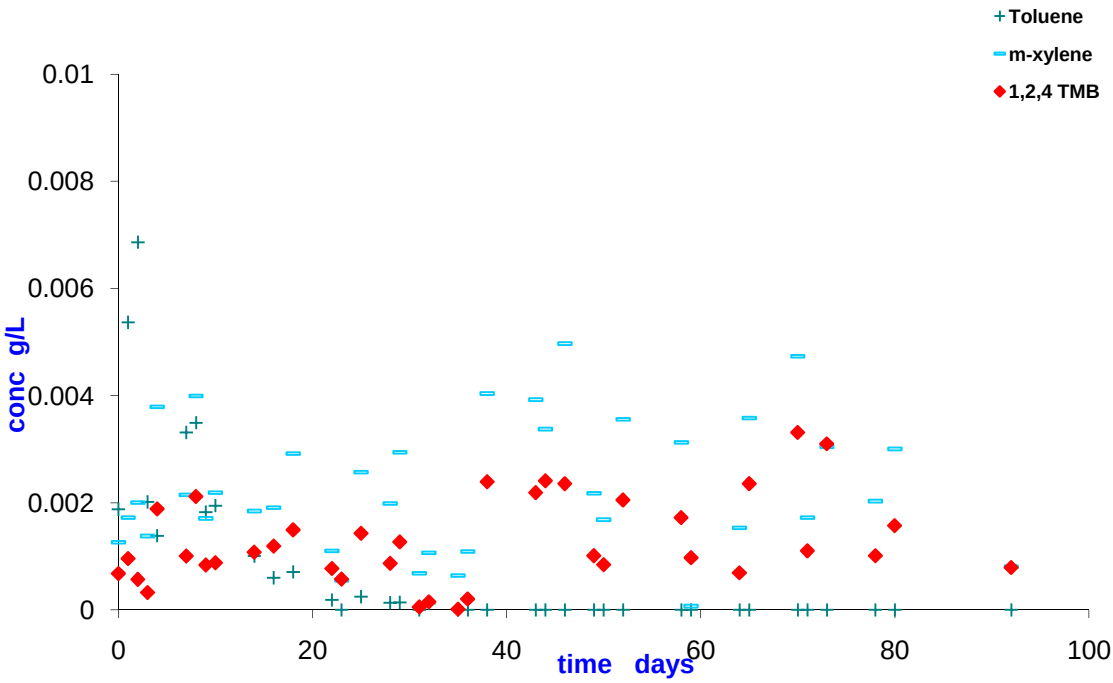

Figure 6.2 Headspace vapour phase concentration profile of the non-blended fuel aromatics in the unsaturated zone during the attenuation period (92 days).

The profiles of headspace vapour concentrations of the E10 fuel compounds are shown in two separate figures. Figure 6.3 for the E10 alkanes and Figure 6.4 for the E10 monoaromatic compounds.

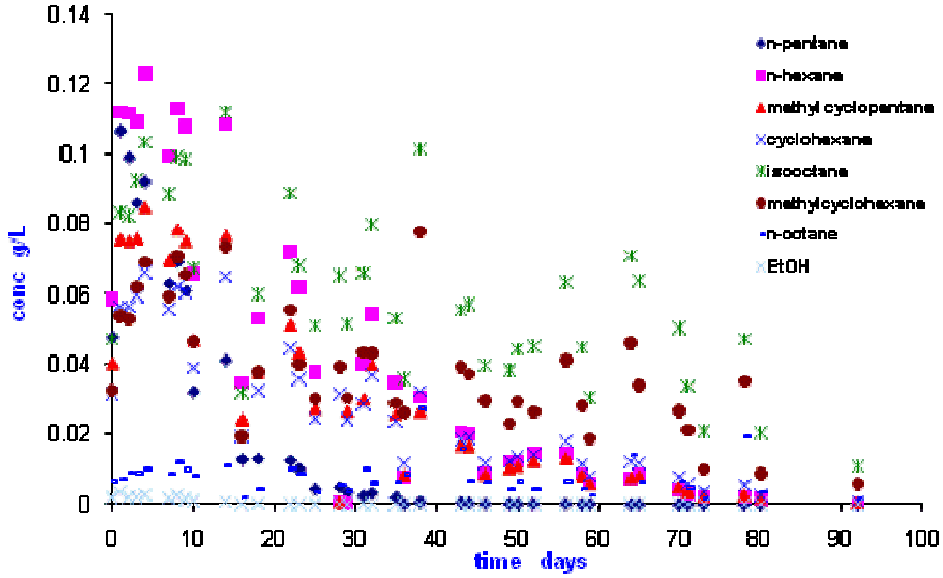

Figure 6.3 Headspace vapour phase concentration profile of ethanol-blended fuel alkanes in the unsaturated zone during the attenuation period (92 days).

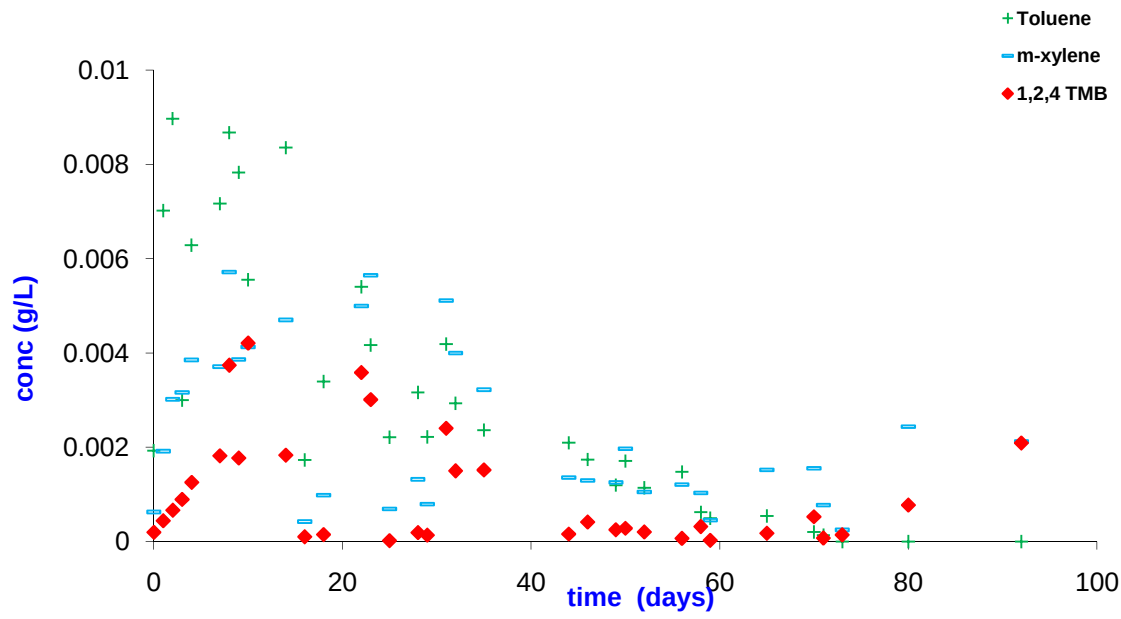

Figure 6.4 Headspace vapour phase concentration profile of ethanol-blended fuel aromatics in the unsaturated zone during the attenuation period (92 days).

The profiles of headspace vapour concentrations of the B20 fuel constituents are shown in Figure 6.5 and Figure 6.6.

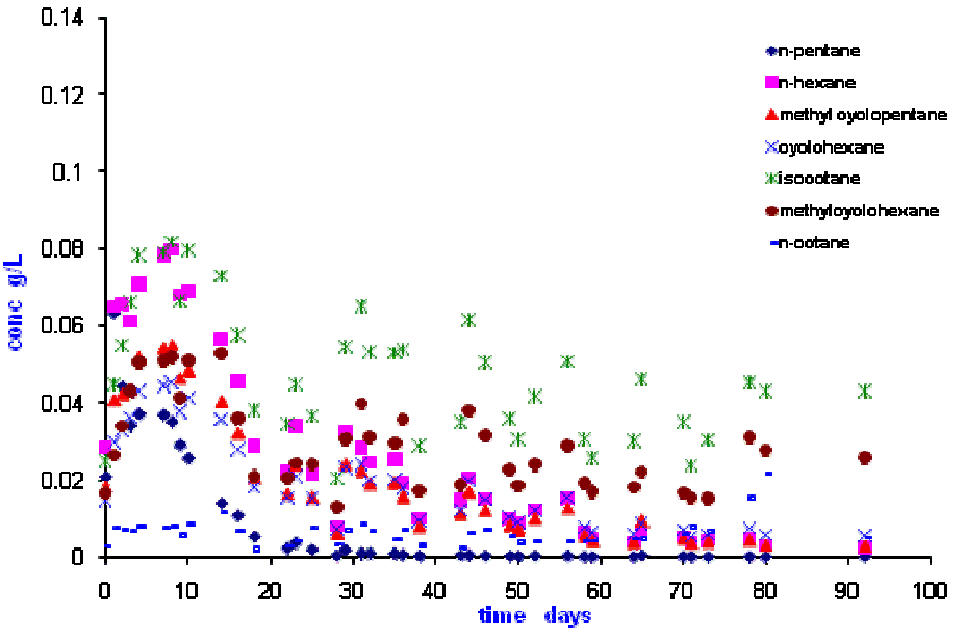

Figure 6.5 Headspace vapour phase concentration profile of biodiesel-blended fuel alkanes in the unsaturated zone during the attenuation period (92 days).

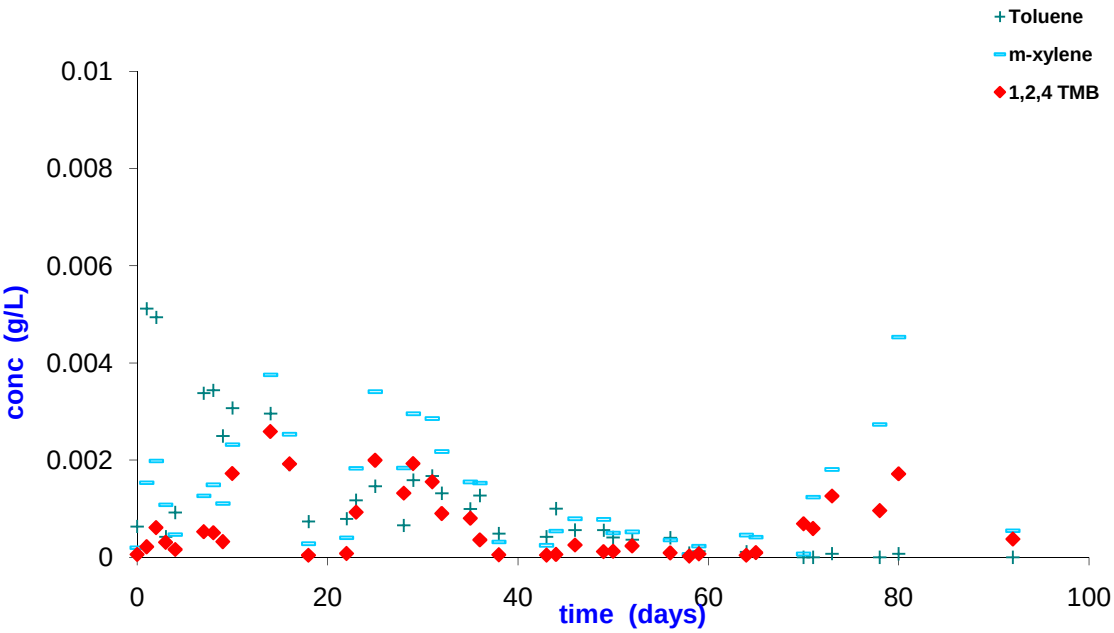

Figure 6.6 Headspace vapour phase concentration profile of biodiesel-blended fuel aromatics in the unsaturated zone during the attenuation period (92 days).

On the basis of the experimental design, absence of advection, leaching, and transience implies that the analysis is a straight forward balance of gaseous

diffusion and biological degradation within the mini-lysimeter in between the headspace purging periods coupled stoichiometrically in the constituents (Ostendorf and Kampbell, 1991).

The rate and extent of vapour concentration decline was influenced by molecular structure. Straight chain and branched alkanes headspace concentrations rapidly decreased in the first 20 days in the approximate order n-pentane >n-hexane > methylcyclopentane > cyclohexane. No significant differences in the vapour reduction of alkanes of PP and E10 were observed except for some monoaromatic compounds. This could be explained by the rapid degradation and volatilisation of ethanol (see below) resulting in a comparable composition of the residual NAPL and hence mole fraction of the petroleum hydrocarbon compounds in the source zone. On the other hand, a significant difference in the vapour-phase concentrations profiles can be seen between PP and B20 from the concentration scales, probably reflecting the fact that the mole fraction of the petroleum hydrocarbons was significantly lower for the B20 mixture since biodiesel was more slowly degraded or volatilized than ethanol (see below), thus "diluting" the petroleum.
The partition of non-aqueous phase liquids (NAPLs) to the vapour phase can be quantified by using Raoult's Law:

$$\boldsymbol{C = \frac{X_i \ P^o}{RT}} \qquad \textbf{Equation 6-1}$$

Where,

X_i is the mole fraction of the pure compound in NAPL mixture [-]
P_o is the pure compound vapour pressure, atm
R is the universal gas constant, $\frac{m^3 \ atm}{mol \ k}$
T is the temperature, K
C constituent concentration mol m^{-3}

According to this equation, the presence of a significant portion of biodiesel in the B20 mixture should result in lower gas phase concentrations.

6.3.2 Vapour phase transport

In general, gas transport in natural porous media occurs via several flux mechanisms including; viscous flow, free-molecule or Knudsen flow, continuum or ordinary diffusion (molecular and nonequimolar fluxes), surface flow or diffusion, and thermal flow. The relative importance of these mechanisms depends on factors related to permeate gases (molecular weight, and viscosity) and the porous media (the type of porous media, porosity, moisture content, and bulk density). Three models are currently used to quantify the diffusive transport of gases in natural porous media, namely, Fick's first law, the Stefan-Maxwell equations, and the dusty gas model (DGM). The application of these models requires the quantification of many transport parameters, such as gas permeability coefficients, the effective binary diffusion coefficient, and Knudsen diffusion coefficients (Abu-El-Sha'r Wa'il, 2006).

Diffusive transport of fuel compound vapours in this experiment occurred over a distance of 15 cm in one direction upward from the source zone and breakthrough of vapours was observed within 1 hour.

It can be seen from the vapour phase concentration profiles in the mini-lysimeters that the volatilization of most of fuel compounds towards the mini-lysimeters surface started 1h after contamination. The volatilization to the headspace at the mini-lysimeters surfaces was estimated through measuring the diffusive fluxes F (g min^{-1} cm^{-2}) for each hydrocarbon profile after the purging of the headspace with fresh air.

The headspace of the three mini-lysimeters was simultaneously flushed on day 11, 21, 24, 30, 38, 46, 58, 67, and 75 with air at a flow rate of about 100 ml per minute for 12 hours to keep the mini-lysimeters aerobic. The linear increase in the headspace concentration of petroleum hydrocarbons following the pumping period was used to estimate diffusive fluxes. Volatilization fluxes could

only be measured for one out of every three purging events, since all mini-lysimeters were purged simultaneously and only one mini-lysimeter could be closely monitored at any one time.

VOC mass flux per surface area F (g min^{-1} cm^{-2}) was estimated from the initial linear increase in concentration as:

$$F = \frac{\Delta C * V_{HS}}{\frac{\Delta t}{S_a}}$$

Equation 6-2

Where:

ΔC is the difference in headspace concentrations (g L^{-1})

Δt is the time difference (min)

V_{HS} is the mini-lysimeter headspace volume (L)

S_a in the mini-lysimeter surface area (cm^2)

Data of the average hydrocarbon volatilisation flux for each constituent in PP, E10 and B20, can be seen in Table 6.1. The data of the measured and estimated diffusive flux of each constituent in PP, E10 and B20 mixtures during 92 days, obtained from the interpolation of the measurements, can be seen in Table 9.1 to Table 9.3 in the appendix.

As seen from the volatilization data Table 9.1 to Table 9.3 in the appendix that, the individual compounds in the PP mixture volatilized more rapidly in comparison with E10 and B20 compounds. For PP compounds, the volatilization of the normal and cyclo alkanes decreased as a function of time, while within the same mixture the mono-aromatics (except toluene) and octane isomers their fluxes increased as a function of time. However, the diffusive volatilization fluxes of the E10 and B20 compounds decreased as a function of time for all compounds.

The maximum diffusive flux of all compounds except toluene was observed in the PP mixture, this could be correlated to the absence of biofuel components that may affect the volatilization of the hydrocarbons, according to Raoult's Law

equation 6.1, the presence of a significant portion of biodiesel in the B20 mixture should result in lower gas phase concentrations in the source zone.

The maximum diffusive flux of the normal and cyclo alkanes was observed on day 11 (first day of flux measurement). The maximum flux of n-pentane, n-hexane, methylcyclopentane and cyclohexane was $4.8x10^{-07}$, $9.8x10^{-07}$, $6.5x10^{-07}$ and $5.0x10^{-07}$ g min^{-1} cm^{-2} respectively. High initial fluxes of these compounds are due to their high volatility and little retardation (Dakhel et al., 2003; Pasteris et al., 2002). The flux decreased later to 0.0, $4.0x10^{-08}$, 0.0 and $8.0x10^{-08}$ g min^{-1} cm^{-2} on day 64 respectively, probably due to a depletion of these compounds in the source. Conversely, the maximum diffusive flux of n-octane, isooctane, m-xylene, and 1,2,4TMB was observed on days 64 of $1.5x10^{-06}$, $1.2x10^{-06}$, $2.8x10^{-07}$, $3.6x10^{-07}$, $1.6x10^{-06}$ and $5.6x10^{-07}$ g min^{-1} cm^{-2} respectively, see Table 9.1 in the appendix. Because of their lower volatility, the mole fraction of these compounds increased in the source zone leading to higher gas-phase concentrations.

Comparison between toluene diffusive fluxes in three different mixtures indicates that its diffusive flux from the PP mixture was much lower than its diffusive flux from the other two mixtures. These data indicate that the flux of toluene within E10 and B20 mixtures are strongly influenced by the addition of ethanol and biodiesel, most likely because of the impact of the biofuels on toluene biodegradation (Jóice et al., 2009).

Toluene diffusive fluxes in the PP mixture and ethanol diffusive fluxes in the E10 mixtures were mostly zero (day 11 of the experiment period was the first day of diffusive flux measurement), this is due to the rapid degradation of toluene at the mini-lysimeter subsurface in the absence of ethanol or biodiesel (Pasteris et al., 2002), see Figure 6.15.

Constituent	PP flux (g min^{-1} cm^{-2})	E10 flux (g min^{-1} cm^{-2})	B20 flux (g min^{-1} cm^{-2})
n-pentane	$1.08x10^{-07}$	$4.47x10^{-08}$	$2.94x10^{-08}$
n-hexane	$6.62x10^{-07}$	$3.42x10^{-07}$	$3.01x10^{-07}$
Methylcyclopentane	$5.15x10^{-07}$	$2.44x10^{-07}$	$2.43X10^{-07}$
Cyclohexane	$4.73\ x10^{-07}$	$2.94\ x10^{-07}$	$2.\ 61x10^{-07}$
Isooctane	$1.17\ x10^{-06}$	$3.85\ x10^{-07}$	$6.21\ x10^{-07}$
Methylcyclohexane	$7.37\ x10^{-07}$	$1.78\ x10^{-07}$	$3.63\ x10^{-07}$
Toluene	$1.36\ x10^{-09}$	$2.89\ x10^{-08}$	$1.66\ x10^{-08}$
n-octane	$4.62\ x10^{-07}$	$4.56\ x10^{-08}$	$9.92\ x10^{-08}$
m-xylene	$8.81\ x10^{-08}$	$2.34x10^{-08}$	$1.47\ x10^{-08}$
1,2,4 TMB	$1.14\ x10^{-07}$	$2.33\ x10^{-08}$	$1.31x10^{-08}$

Table 6-1 Average volatilization flux (g min^{-1} cm^{-2}) of individual compounds in PP, E10 and B20

6.3.3 Oxygen and Carbon dioxide

Profiles of the concentrations of CO_2 and O_2 in the mini-lysimeters are shown in Figure 6.7 and Figure 6.9 respectively.

The CO_2 concentration in the mini-lysimeters before contamination was in the range of 0.001 g/L. Shortly after the sand was contaminated by fuel constituents, it rose to a maximum of 0.25 g/L for E10 on day 8, 0.30 g/L for B20 on day 57 and 0.2 g/L for PP on day 74. The control values for the unpolluted soil during these measurements were 0.002 g/L, 0.008 g/L and 0.009 g/L respectively. From the concentrations of O_2 it can be seen that O_2 consumptions values mirror the CO_2 production. The O_2 concentrations during the maximum CO_2 production were 0.125 g/L, 0.074 g/L and 0.214 g/l for PP, E10 and B20 respectively, while the control value during the three measurements were 0.27 g/L, 0.23 g/L and 0.30 g/L respectively. It can be

noticed that the O_2 concentration for the control system during the three measurements remains very close to the atmospheric O_2 concentration 0.301 g/L (Figure 6.9), which confirms the reduction of the O_2 concentrations during the highest three CO_2 measurements mainly related to the mineralization of the VOCs by the indigenous microorganisms in the three different fuel polluted systems (Zhou and Crawford, 1995). Through regular purging of the headspace the mini-lysimeters were maintained aerobic, although the existence of pockets of anaerobic soil for instance within the source zone cannot be excluded.

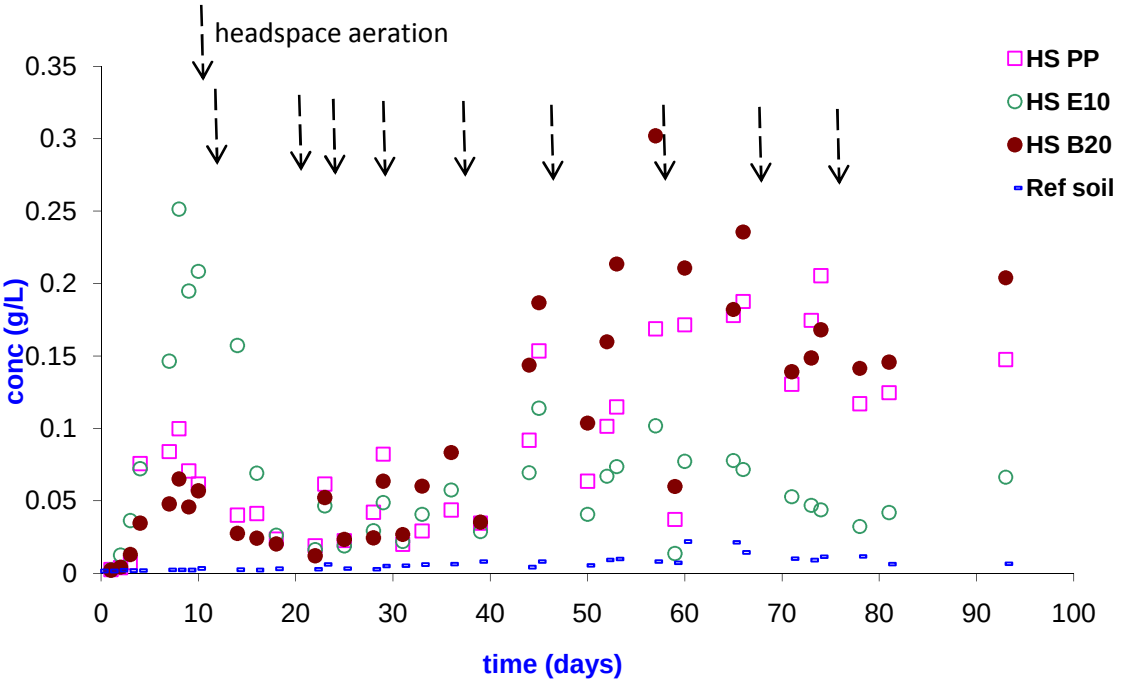

Figure 6.7 CO_2 concentration profiles in PP, E10 and B20 mixtures in the mini-lysimeter headspace, during the study period (92 days).

The CO_2 plot allows best to illustrate when biodegradation was active at the three different mini-lysimeter systems. From day 2 to 92, elevated CO_2 levels were clearly indicating active biodegradation processes. From the plot it can be clearly seen that the CO_2 production started immediately after source burial, see Figure 6.7. The CO_2 increases were correlated to O_2 decreases, and the value of the CO_2 control system reflects closely the atmospheric CO_2 concentration which confirms the hydrocarbon degradation rather than that of soil organic matter.

For the E10 system, the highest CO_2 value was observed at day 8 much higher than the initial CO_2 concentration in the B20 mixture system and the PP mixture system. The increase in CO_2 concentration indicated that some degree of biodegradation did indeed take place. The degradation was however not immediately noticeable in the vapour-phase hydrocarbon concentrations because it was negligible in relation to the amount of contaminant introduced into the system. Ethanol on the other hand was completely degraded in the E10 mixture with 100% disappearance on day 18 (Dakhel et al., 2003).

It is interesting to note from Figure 6.8 that the initial high CO_2 production in the E10 system was in good agreement with EtOH depletion, suggesting that the initial CO_2 production in E10 mixture was mainly from EtOH mineralization, rather than VOCs mineralization in comparison with the CO_2 plots of the control, PP and B20 which can be seen in Figure 6.7.

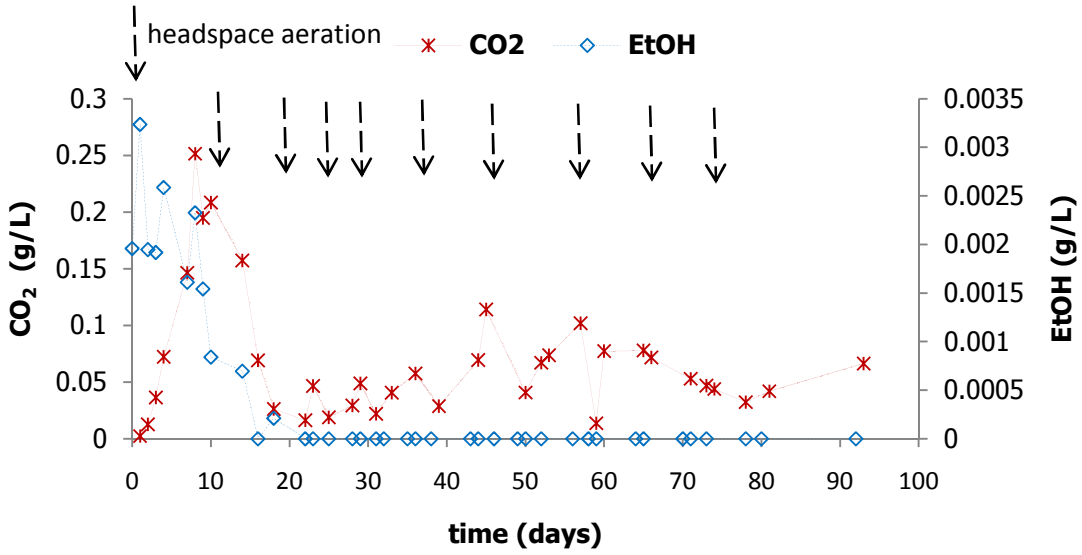

Figure 6.8 Relation between the CO_2 concentration increase 1st axis and EtOH concentration decrease in the E10 mixture 2nd axis

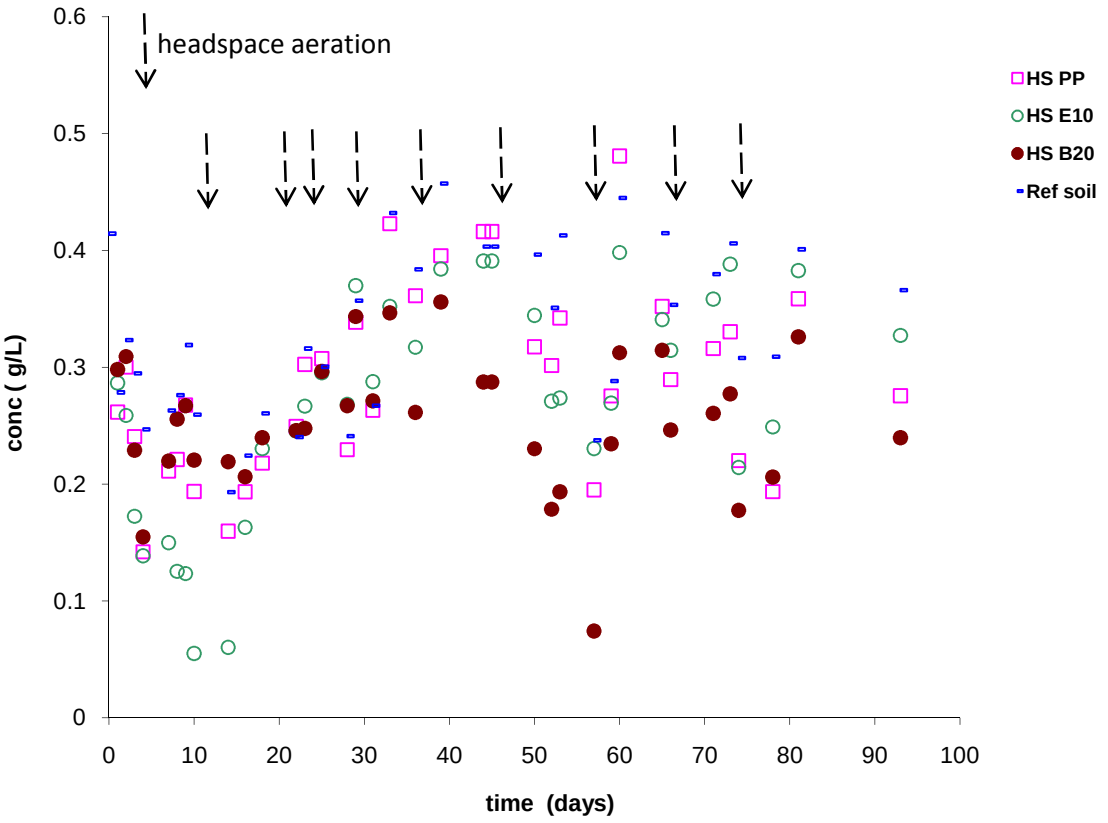

Figure 6.9 Oxygen concentration profiles in PP, E10 and B20 mixtures in the mini-lysimeter headspace, during the study period (92 days).

6.3.4 NAPLs in the sand

The chemical composition and percentage of the added mass remaining as NAPLs residual in the contaminated soil collected at day 92 from the PP, E10 and B20 mini-lysimeters are shown in Figure 6.10.

The initial PP, E10 and B20 constituents mass was 0.0158, 0.0160 and 0.0158 g/g soil, respectively. After 92 days of bioremediation it was reduced to 0.0072, 0.0055 and 0.0041 g g^{-1} soil for PP, E10 and B20 respectively. The biodegradation and volatilisation during headspace purging was able to remove about 55%, 62% and 68% for PP, E10 and B20 respectively, from the initial emplaced NAPLs at day = 0. The results showed that different constituents of

the hydrocarbons had different degrees of degradability (Ostendorf and Kampbell, 1991); for example, the aliphatic hydrocarbons may have been readily removed by volatilisation and biodegradation but the aromatics except toluene were more slowly removed and n-octane, decane, and dodecane were the most recalcitrant.

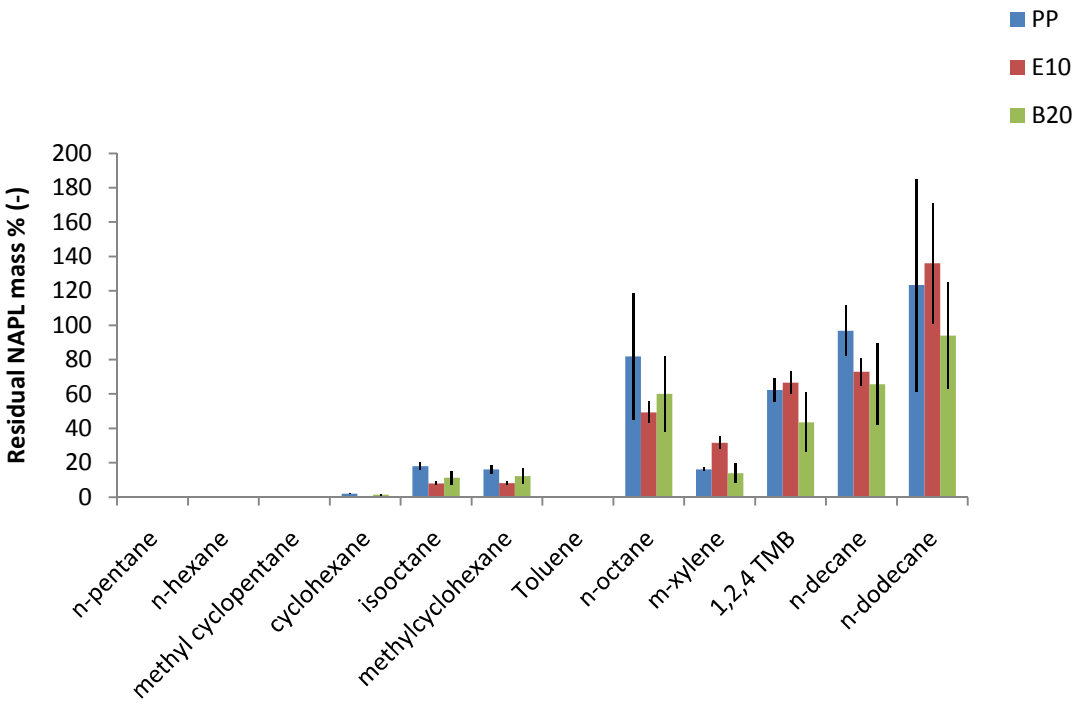

Figure 6.10 Residual NAPLs mass % (-) of PP, E10 and B20 in the unsaturated zone after 92 days. Error bars: ± 1 standard deviation (SD, n=3)

6.3.5 Biodiesel in the sand

For the mini-lysimeter with B20 mixture a biodiesel residual of 18.3 ± 8.5% of the amount added remained after 92 days, consisting of 24.9 ± 10.9%, 11.6 ± 7.7%, 26.6 ± 10.3% and 34.7 ± 13.7% of the added mass of palmitic (acid methyl ester AME), linoleic AME, oleic AME and stearic AME remaining respectively, see Figure 6.11. These data suggest that the more gradual increase in CO_2 headspace concentrations shown in Figure 6.7, as compared with the E10 mixture indicates that biodiesel is more slowly degraded than ethanol.

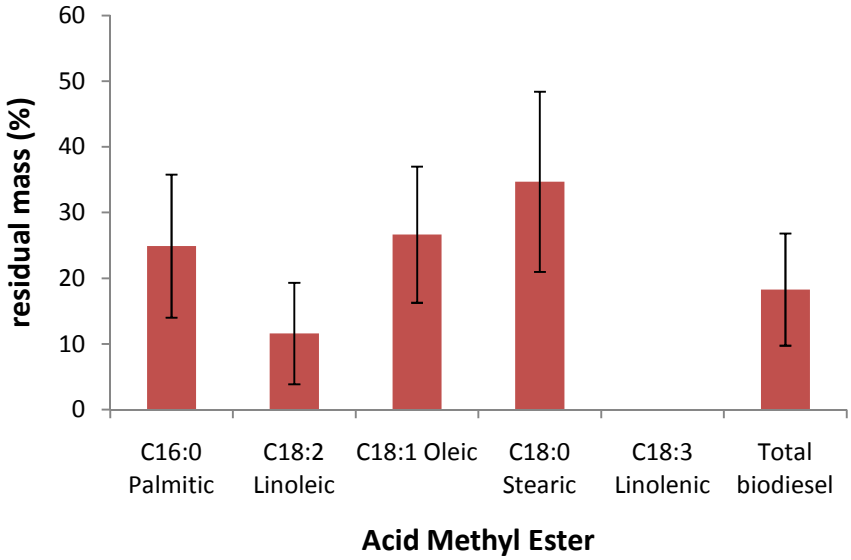

Figure 6.11 Residual biodiesel mass % (-) of B20 mixture in the unsaturated zone after 92 days. Error bars: ± 1 standard deviation (SD, n=3)

6.3.6 Total cell numbers

On day 0 the sand contained an indigenous microbial flora of $6x10^7$ cells g^{-1} of dry soil. On day 92 the control sand contained about $7.5x10^7$ cells g^{-1} of dry soil, which confirms no significant biomass growth occurred in the control soil. Indigenous microorganisms from the PP, E10 and B20 fuels contaminated unsaturated zone were able to grow on VOCs under the aerobic conditions. The oxidation of the VOCs to CO_2 was strongly coupled to the reduction of O_2. Through occasional purging of the headspace the mini-lysimeters remained aerobic.

A significant difference in the total cell numbers can be noticed between the control and all the other three fuel mixtures (non-parametric test K-W $P<0.005$). It was reported that when the population of indigenous microorganisms capable of degrading the target contaminant is less than 10^5 (cfu) g^{-1} of soil, bioremediation will not occur at a significant rate (Hinchee et al., 1995a).

Total microbial cell carbon per g of soil on day 92 in the mini-lysimeters is shown in Figure 6.12. It was significantly higher in the mini-lysimeter with the E10 mixture as compared to the lysimeter with the PP mixture (non-parametric test K-W P<0.005) probably reflecting the fact that a substantial portion of the more volatile petroleum hydrocarbon mass, but an insignificant amount of ethanol volatilized from the mini-lysimeters during pumping instead of being transformed into biomass. When the headspace of the mini-lysimeters was flushed for the first time on day 11 ethanol headspace concentrations had already decreased to 0.0007 g/L. For the PP mixture, cell counts in the source zone (bottom third of the mini-lysimeter) were a factor 1.9 higher than in the soil without NAPL (middle and top third of the mini-lysimeter), for the E10 mixture they were a factor 0.65 lower, and for the B20 mixture they were a factor 2.9 higher in the source zone. This indicates that ethanol biodegradation occurred throughout the soil-filled mini-lysimeter volume, whereas petroleum hydrocarbon and biodiesel biodegradation occurred mainly in the source zone.

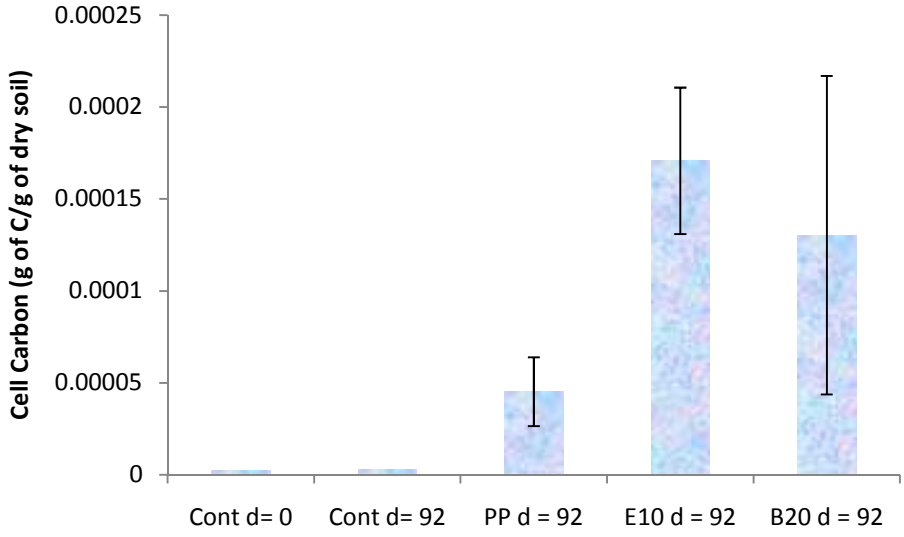

Figure 6.12 Cell Carbon (g of C/g of dry soil) for the control, PP, E10 and B20 mixtures. Error bars: ± 1 standard deviation (SD, n=3)

6.3.7 Denaturing gradient gel electrophoresis

To study the microbial community structures of the control and the other three fuel mixtures a denaturing gradient gel electrophoresis (DGGE) method was performed for soil sampled from the mini-lysimeters on day 92.

A DGGE gel comparison of microbial community structures in the mini-lysimeters is presented in Figure 6.13. DGGE analysis showed a richer bacterial community present in all samples in comparison with the control samples. It is interesting to note in Figure 6.13 that bacterial community richness was higher within E10 bands in comparison with PP and B20 bands.

Non metric Multi Dimensional Scaling (NMDS) was used to analyse DGGEs. This was conducted using the Primer V6 multivariate statistical software package (Primer-E Ltd, Plymouth, UK). This tested the significance of spatial trends based on a Bray Curtis rank similarity matrix and Analysis of similarity (ANOSIM), to determine the significance of any clustering of replicates or treatments in soil samples.

The similarity express as dice coefficients was only > 40 % and there was a statistically significant difference between the microbial communities from the different mini-lysimeters in terms of presence and absence of bands (ANOSIM $p \leq 0.001$). Figure 6.14 illustrates the Bray-Curtis similarities in a plot which groups similar communities in close proximities. It is evident that replicates from different locations in each mini-lysimeter are fairly similar to each other, but addition of a biofuel component appears to have resulting in a significant long-term shift in the structures of the microbial communities.

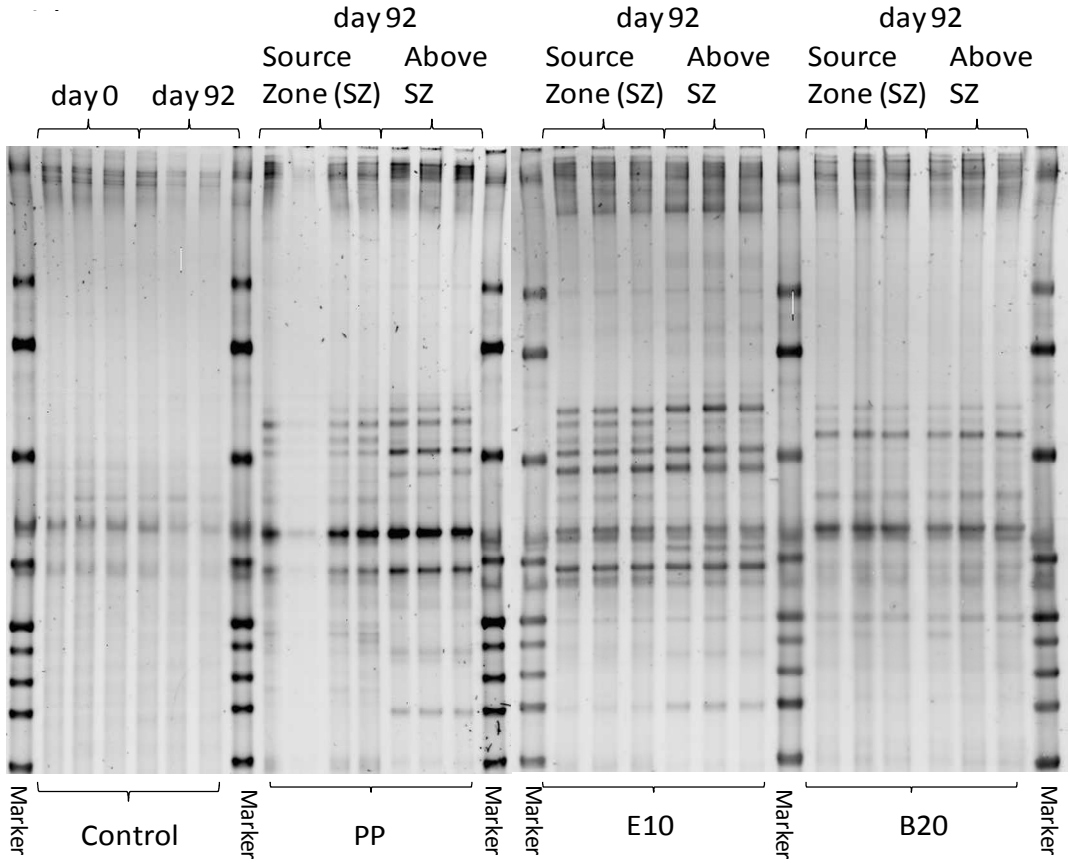

Figure 6.13 Lysimeter DGGE samples.

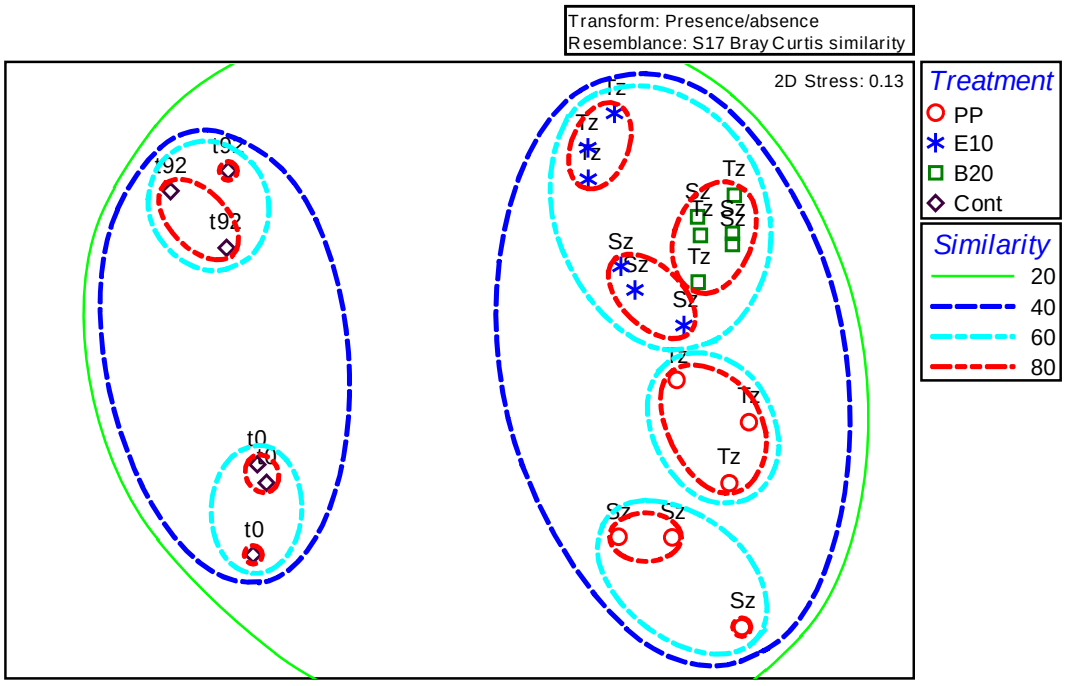

Figure 6.14 Bray-Curtis Similarity Matrix of mini-lysimeters samples for Cont, PP, E10 and B20 at top zone (Tz) and source zone (Sz).

ANOSIM analysis presented in Table -6-2 indicated a significant difference in bacterial community structures between treatments (cont, PP, E10 and B20) rather than within triplicates ($P \leq 0.001$) confirming similar species composition in samples from the same mini-lysimeter. On the basis of the assumption that all communities at day t= 0 were the same, the different fuel mixtures have a significant effect on shifts in microbial community structure. On the basis of the R-value Table -6-2 it can be concluded that the strongest differences in community structure were between Cont vs all treatments and between the pure and the blended treatments, PP vs E10 and PP vs B20 since their R-value was 0.95 ± 0.01 , 0.85 and 0.96 respectively.

6.3.7.1 NMDS for (Petroleum Fuel mixtures)

Figure 6.14 shows clustering of different fuel contaminated soil (PP, E10, and B20) and the control samples at 0 and 92 days. Samples indicate high similarity of replicate microbial communities. Blended-petroleum samples E10 and B20 have shown the highest community structure similarity > 60% which shows that fuel additives had a stronger effect on the microbial community structure. The community structure similarity between PP vs E10 and B20 was > 40% which was greater than the similarity between Cont and any fuel treated community which was < 40%.

Table -6-2 and Table 6-3 shows the ANOSIM and diversity indices results respectively, of the control, PP, E10 and B20 mixtures. On the basis of the richness values (S) the most diverse are the E10 samples which include a significant number of microorganisms. E10 has the highest richness value in comparison with PP and B20, and that is probably due to the different kind of VOCs and ethanol making up the ethanol-blended fuel. A greater diversity of taxa, some with the ability to degrade ethanol, resulted in additional bands to those found in the pure fuel treated system. It is remarkable that this signature should remain after 92 days, when most of the ethanol has long been degraded.

The PP mixture has a richness value of about 18.67 ± 0.47. In comparison the richness value for the B20 mixture was the lowest at 16.17 ± 0.24 which may represent the dominance of microorganisms able to degrade biodiesel only.

Global Test

Sample statistic (GlobalR):0.892

Significance level of sample statistic: 0.1%

Number of permutations: 999 (Random sample from a large number)

Number of permuted statistics greater than or equal to Global R: 0

Pairwise Tests

Groups	R Statistic	Significance Level %	Possible Permutations	Actual Permutations	Number >= Observed
PP, E10	0.85	0.2	462	462	1
PP, B20	0.96	0.2	462	462	1
PP, Cont	0.96	0.2	462	462	1
E10, B20	0.91	0.2	462	462	1
E10, Cont	0.94	0.2	462	462	1
B20, Cont	0.96	0.2	462	462	1

Table -6-2 Analysis of Similarity of the mini-lysimeter soil samples Cont, PP, E10 and B20.

From Table 6-3 it can be concluded that, on the basis of the lambda value for which the greater value is correlated to the high diversity, it has been found that, lambda values decreased in the approximate order E10>PP>B20>Cont. Lambda values have been found to be in a good agreement with richness values.

Treatment	Band richness (S)	Pielou's equitability (E)	Shannon diversity index (H')	1-Lambda
E10	21.83 ± 3.06	0.91 ± 0.01	2.81 ± 0.11	0.93 ± 0.01
B20	16.17 ± 0.24	0.87 ± 0.01	2.42 ± 0.04	0.89 ± 0.01
PP	18.67 ± 0.47	0.88 ± 0.0	2.57 ± 0.03	0.90 ± 0.01
Cont0d	11.00 ± 2.00	0.88 ± 0.03	2.11 ± 0.15	0.86 ± 0.02
Cont92d	10.33 ± 1.15	0.91 ± 0.0	2.31 ± 0.10	0.87 ± 0.01

Table 6-3 Diversity and evenness values for the soil biodegradation mini-lysimeters

6.3.8 Importance of biofuel addition

Figure 6.15 illustrates the effect of biofuel addition on the headspace vapour-phase concentration of toluene in the mini-lysimeters with PP, E10 and B20 mixtures.

Toluene was chosen as an example to demonstrate the effect of ethanol and biodiesel addition on the movement and biodegradation of the most readily biodegradable aromatic VOC in the unsaturated zone. Toluene is a key member within the BTEX group and it is one of the compounds that is known to readily biodegrade (Pasteris et al., 2002).

The toluene profiles in PP, E10 and B20 mixtures which can be seen in Figure 6.15 suggest that toluene vapour phase concentration in PP mixture was completely removed to under the analytical detection limit by day 31, while it remains measurable in the other two mixtures E10 and B20 until the end of the experiment. These headspace concentrations indicate that toluene biodegradation was fastest for the PP mixture and slowest for the E10 mixture. These findings were in a good agreement with the CO_2 production and O_2

consumption in the E10 mixture. During the initial 15 days in which rapid ethanol biodegradation occurred (Figure 6.8) toluene headspace concentrations remained constant for the E10 mixture indicating slow toluene biodegradation.

For other petroleum hydrocarbon compounds both additives have not shown any significant effect. From the vapour concentration profiles for the all constituents it can be speculated that limited nutrient availability may have caused the observed difference between toluene degradation in the three fuel mixtures. Therefore, the impact of nutrient availability on the biodegradation of petroleum hydrocarbons in the presence of biofuel components will be further investigated in the next chapter.

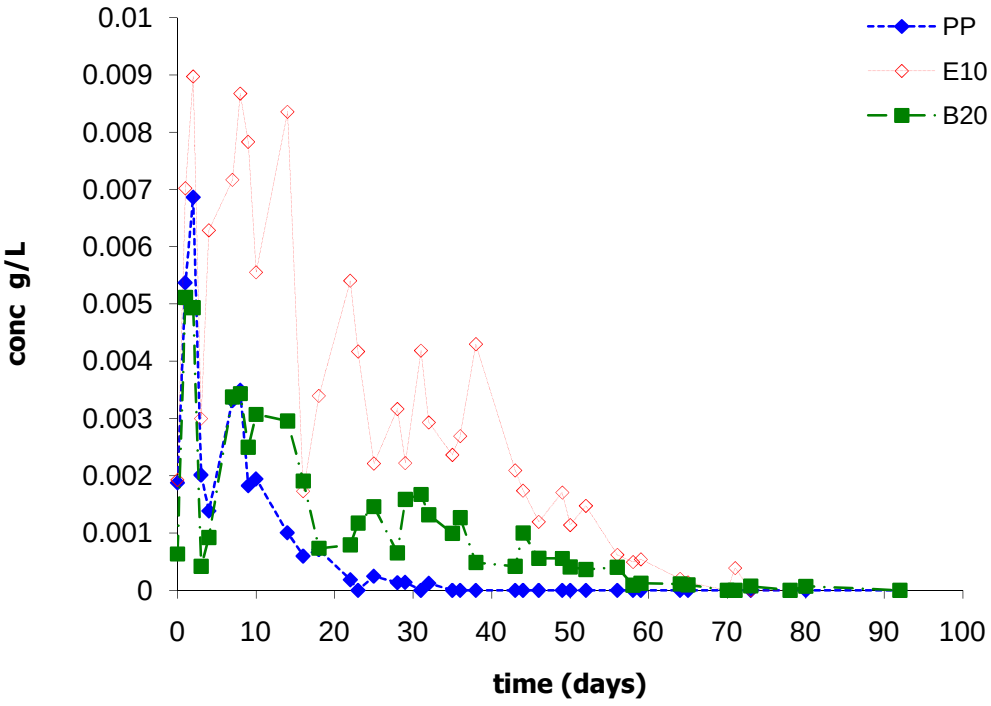

Figure 6.15 Toluene concentration profiles in PP, E10 and B20 mixtures

6.3.9 Mass balance

Mass balance for the mini-lysimeter studies are shown in Table 6-4. The estimation of the volatilization flux required frequent sampling and could only be performed on one mini-lysimeter at a time, but the headspace of all three mini-lysimeters was purged simultaneously. Consequently, volatilization fluxes could only be measured for one out of every three purging events and had to be interpolated for the other two. The resulting uncertainty may explain the relative high percentage of uncounted carbon mass for the E10 and B20.

	Residual NAPL and Volatilization C (%)	Biomass C (%)	CO_2 C (%)	Uncounted C[a] (%)
PP	96.4	0.8	1.4	1.3
E10	55.0	3.6	1.0	40.2
B20	64.3	3.1	2.6	29.9

Table 6-4: Mass balance as % of the carbon added for the mini-lysimeters studies
[a]Unaccounted C may be explained by experimental error or poor recovery of ethanol and potentially more polar metabolites such fatty acids formed from biodiesel in the extraction and clean-up procedure. Some biodiesel residuals (esters) were found in the extracts of the mini-lysimeter studies.

7 Effect of Nutrients Addition on the Transport and Biodegradation of Pure and Blended Fuel in the Subsurface (In Situ Biostimulation)

7.1 Introduction

Microbial biodegradation of Petroleum VOCs during the process of bioremediation can be constrained by lack of nutrients, low bioavailability of the contaminants, availability of electron acceptors, or scarcity of VOC-biodegrading microorganisms.

Soil contaminated with organic pollutants such as oils and fuels is likely to contain an excess of carbon compared to nitrogen and phosphorus. Even if the pollutant is highly biodegradable and a high source of calories, the indigenous microorganisms (bacteria) may be unable to biodegrade the pollutant, due to a nutrient limitation (Atlas and Philp, 2005).

Nitrogen is the most commonly used biostimulant in oil bioremediation studies. It is used primarily to support biosynthesis (NH_4^+ and NO_3^-) or as an alternative electron acceptor to oxygen (NO_3^-). It is commonly applied in the form of urea (ammonium salts). Bacteria readily assimilate all of these, Phosphorus is routinely seen as the next most important nutrient. Phosphorus is used for cell growth and is added as a phosphate salt.

Conflicting effectiveness of nutrient amendments has been demonstrated, including those added as synthetic inorganic and organic compounds such as urea and oleophilic fertilizers (Fallgren and Jin, 2008). Other studies have demonstrated that other nutrients, including crop residues, biosolids, and fish bones, are effective in bioremediation studies. We indentified the direct addition of inorganic nitrogen; NH_4Cl, and phosphorus; KH_2PO_4, as an effective nutrient amendment (Xu and Obbard, 2003). These nutrients were added at a ratio which has been calculated on the basis of the pure carbon mass, as previously described by Atlas and Philip (Atlas and Philp, 2005).

7.2 Experimental section

The experimental part of this phase which includes the preparation of the three fuel mixtures PP, E10 and B20, characterization of the sand, preparation of the nutrients solution and preparation and incubation of the microcosms, soil gas

sampling and analysis, non-aqueous phase liquid (NAPL) residuals quantification, and the microbiological methods which include the total cell numbers and DGGE have been discussed in the materials and methods chapter, for more details please refer to chapter four.

7.2.1 Preparation and incubation of in situ microcosms

In brief, two sets of 65 mL batches were prepared one with added nutrients and the other set without added nutrients, each set includes triplicate 65 mL batches with 15.0 g of soil, for the control, PP, E10 and B20 mixtures to make a total of 24 batches, twelve with and twelve without nutrient addition. Then, 30uL of PP, E10 or B20 as pure and blended fuel mixture was injected to the PP, E10 and B20 batches respectively in the two sets. Sampling and measuring headspace gases were carried out each 48 hours for each set, the soil was not sterilized in order to allow biodegradation to occur.

The rate of CO_2 produced by microbial degradation of organic carbon was used as an indicator to evaluate microbial degradation activity. Carbon dioxide was measured by injecting 40uL from the microcosm headspace to a GC-MS, and the microbial respired CO_2 from degradation of hydrocarbon compounds was measured every 48 hrs during the experimental period. The treatments include ammonium chloride and potassium dihydrogen phosphate as nutrients amendments. Microcosms containing no nutrients amendments served as controls.

7.3 Results and discussion

7.3.1 Vapour phase concentrations of PP, E10 and B20 Fuel compounds

Profiles of vapour-phase concentrations of the PP alkanes in nutrient unamended and nutrient amended batches are shown in Figure 7.1 (A) and (B) respectively. The mentioned figure shows only the first seven compounds for each mixture, while the concentration profiles of the three monoaromatics of the two mixtures are shown in another separate graph Figure 7.2 for better

visibility and comparison. Again because of measurement difficulties caused by their low volatility, decane and dodecane vapour-phase concentrations were not reliably measured with the employed methods, for these reasons they have been excluded from the vapour-phase plots. The maximum vapour concentrations of most PP constituents of the nutrients unamended batches were recorded up until day 9, while for the nutrients amended batches the maximum vapour-phase concentrations were recorded up until day 4, then most of the PP constituents' mixture decreased continuously until day 24 in particular for nutrients amended mixture. It can be shown that the vapour concentrations of these compounds decreased because of biodegradation.

For PP aromatics a significant difference can be shown for the vapour-phase concentration between the nutrient unamended and amended batches for each constituent, see Figure 7.2. The vapour-phase concentration at day 22 for toluene, m-xylene and 1,2,4 TMB was 0.0 ± 0.0, 0.0 ± 0.0 and 4.67×10^{-5} ± 4.0×10^{-6} respectively, for the nutrient amended batches while the vapour-phase concentration for the same constituents on the same day for the nutrient unamended system was 0.0004 ± 0.00006, 0.009 ± 0.005 and 0.008 ± 0.004 g/L respectively.

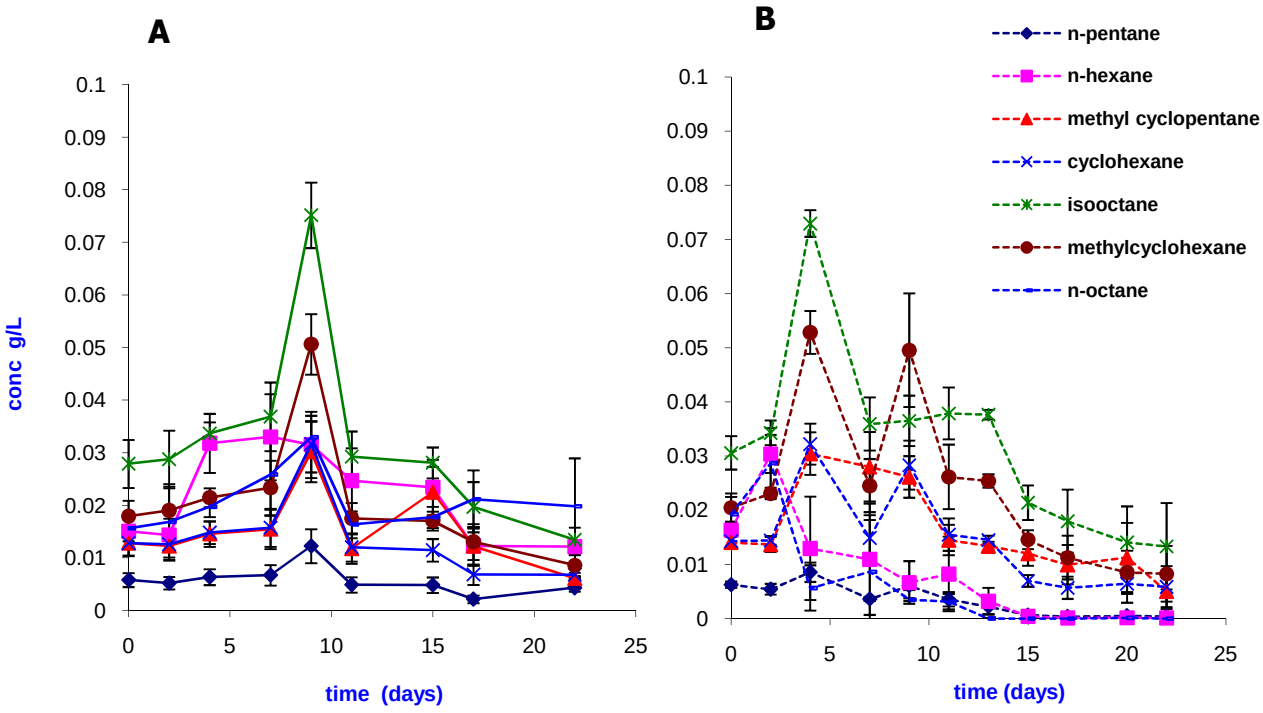

Figure 7.1 Comparison of PP alkanes biodegradation in contaminated soil, as a function of the time of treatment by: (A) indigenous microorganisms only, (B) indigenous microorganisms and nutrients. Error bars: ±1 standard deviation (SD, n=3)

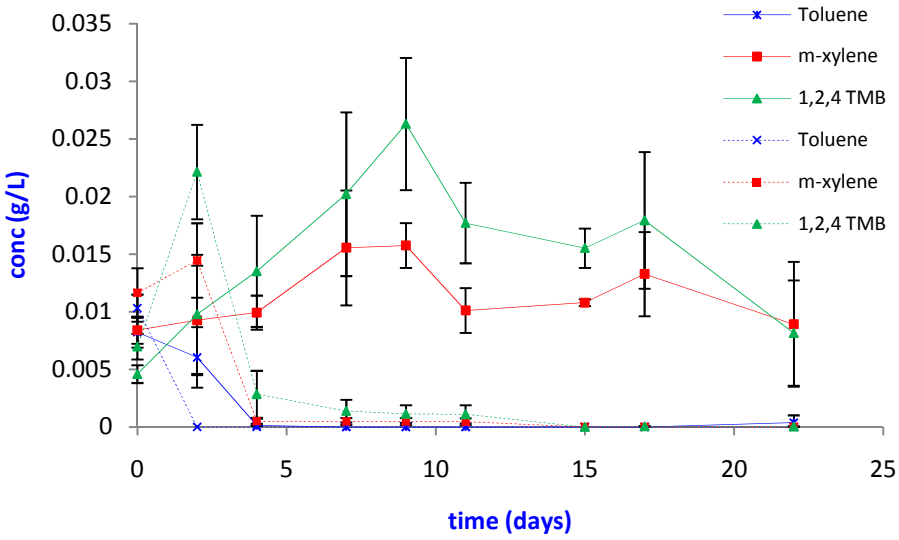

Figure 7.2 Changes in average vapour-phase concentrations for PP monoaromatics during incubation, nutrient unamended (continuous line) and nutrient amended (dashed line). Error bars: ±1 standard deviation (SD, n=3)

Vapour-phase concentration plots of E10 VOCs were divided into three graphs

Figure 7.3 (A) and (B) shows the vapour-phase concentration of E10 alkanes

nutrient unamended and amended respectively, and Figure 7.4 shows the vapour-phase concentration of E10 aromatics for both nutrient unamended and amended batches, for better visibility and comparison.

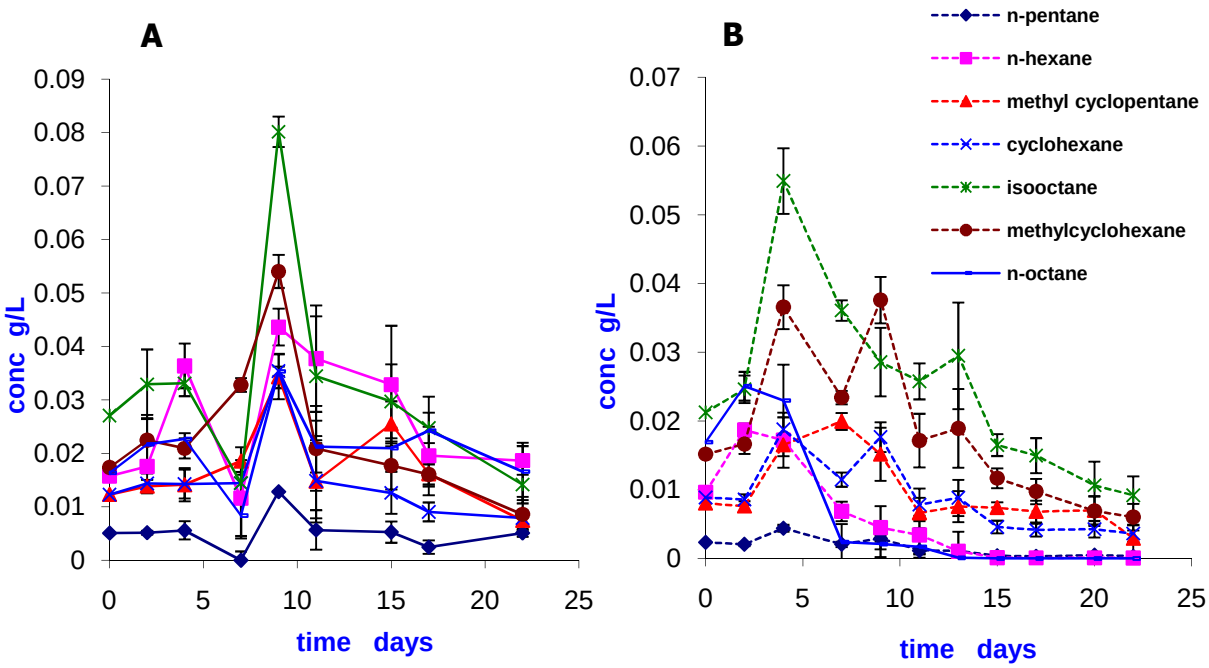

Figure 7.3 Comparison of E10 alkanes biodegradation in contaminated soil, as a function of the time of treatment by: (A) indigenous microorganisms only, (B) indigenous microorganisms and nutrients. Error bars: ±1 standard deviation (SD, n=3)

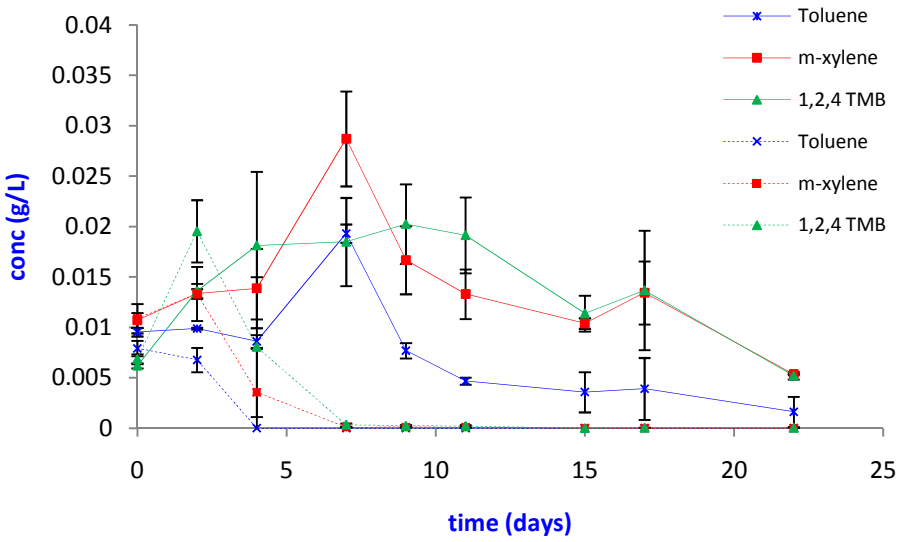

Figure 7.4 Changes in average vapour-phase concentrations for E10 monoaromatics during incubation, nutrient unamended (continuous line) and nutrient amended (dashed line). Error bars: ±1 standard deviation (SD, n=3)

Comparison of E10 alkanes vapour-phase concentrations shows slight differences observed between the nutrients unamended and amended constituents. Except for isooctane no significant difference can be observed between the two systems, until day 15 onwards, when a significant difference can be observed.

Ethanol was completely degraded in the E10 mixtures with 100% disappearance from the vapour phase on days 2 and 9 for the nutrients amended and unamended batches respectively, see Figure 9.5 in the appendix. This is in accordance with (CANNON, 1999) who reported that only large amounts of alcohols are not biodegradable due to their toxicity to most microorganisms at high concentration. In our study simulating a new proposed fuel, a blend of 10% ethanol should therefore be very readily degraded. Toxicity of ethanol or any of its intermediates is not likely to be a cause of the absence of significant biodegradation in particular for the nutrients unamended system. According to Cannon and Rice (1999), none of the intermediates in the common aerobic metabolic pathway of ethanol is toxic. Lack of significant degradation for the unameneded constituents, is more likely to have been due to the limited nutrients available for the experiment, or toxicity of some of the hydrocarbon due to their concentration in the mixture (Haritash and Kaushik, 2009).

Since degradation was faster in the nutrient amended batches for the three mixtures, which had sufficient O_2 levels throughout the experiment, it is suggested that nutrient availability may have a significant effect on the degradation of the VOCs in the subsurface, which can be seen most clearly through the plots of the monoaromatics for the three mixtures when comparing the nutrient amended and unamended plots.

It can be seen form Figure 7.4, that the vapour-phase concentration at day 22 for toluene, m-xylene and 1,2,4 TMB was 0.0 ± 0.0, 0.0 ± 0.0 and $1.7x10^{-5}$ ± $1.5x10^{-5}$ respectively for the nutrient amended batches while the vapour-phase

concentrations for the same constituents at the same day for the nutrients unamended system was 0.0018 ± 0.001, 0.0065 ± 0.002 and 0.0061 ± 0.001 g/L respectively.

Profiles of vapour-phase concentrations of the B20 alkanes nutrient unamended and nutrient amended batches is shown in Figure 7.5 (A) and (B) respectively, the mentioned figure shows only the first seven compounds for each mixture, while the concentration profiles of the three monoaromatics of the two mixtures are shown in another separate graph Figure 7.6, again for better visibility and comparison. The maximum vapour-phase concentration for the nutrient unamended batches was recorded up until day 9, while for the nutrient amended batches it was recorded up until day 4.

For B20 monoaromatics, again the biodegradation was similar to the previous two mixtures PP and E10, toluene, m-xylene and 1,2,4 TMB were completely disappearing from the nutrients amended mixture by day 4, 13 and 22 respectively, while their concentrations in the unamended mixture were 0.0012 ±0.0011 , 0.0067 ± 0.0010 and 0.0068 ± 0.0010 g/L respectively at day 22.

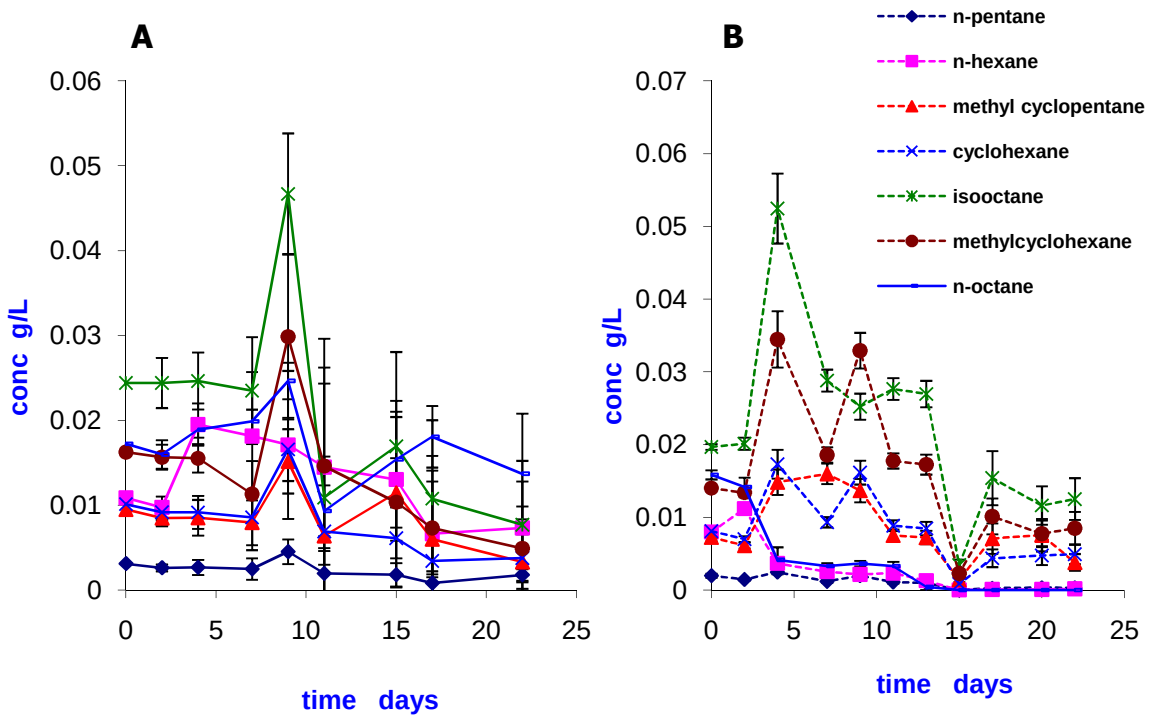

Figure 7.5 Comparison of B20 alkanes biodegradation in contaminated soil, as a function of the time of treatment by: (A) indigenous microorganisms only, (B) indigenous microorganisms and nutrients. Error bars: ±1 standard deviation (SD, n=3)

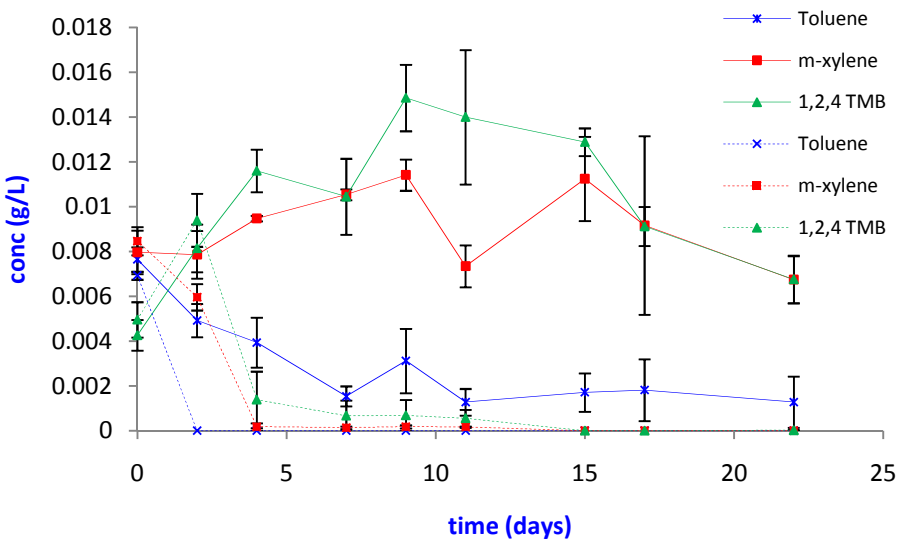

Figure 7.6 Changes in average vapour-phase concentrations for B20 monoaromatics during incubation, nutrient unamended (continuous line) and nutrient amended (dashed line). Error bars: ±1 standard deviation (SD, n=3).

7.3.2 Oxygen and carbon dioxide

Profiles of the concentrations of CO_2 and O_2 in the batches are shown in Figure 7.7 and Figure 7.8 respectively. The concentration of O_2 in the nutrients amended batches reached its lowest rate at day 11 and day 20. On day 0 the O_2 concentration was 0.305 ± 0.00047 , 0.302 ± 0.0034, 0.303 ± 0.0017 and 0.319 ± 0.0048 g/L for PP, E10, B20 and the control respectively, close to the atmospheric O_2 concentration of 0.303 g/L, then there is a steady drop of the O_2 concentrations until day 4, after that it reduces slightly less on day 7, but falls quickly to its lowest level at day 11 to reach 0.0064 ± 0.0022, 0.0086 ± 0.0020 and 0.0070 ± 0.0030 g/L for PP, E10 and B20 respectively. On day 14 aeration was supplied to the nutrient amended microcosms, 40 mL from the headspace was removed and replaced by the same amount of pure air using gas-tight syringes to ensure oxygen supply was not limiting hydrocarbon mineralisation. The VOC and CO_2 concentration in the gas removed was analyzed for the mass balance.

After the aeration, it is noticeably that, the O_2 concentration rises sharply reaching a peak of atmospheric oxygen concentration 0.303 g/L at day 15, but as a biodegradation process continues, again a drop in the O_2 concentration can be seen to just 0.1930 ± 0.1126, 0.1197 ± 0.0736 and 0.0537 ± 0.0344 for PP, E10 and B20 respectively. In the batches without nutrient amendment O_2 concentrations remain generally close to the atmospheric concentration, see Figure 7.8.

Inversely a CO_2 production increase was clearly seen in the headspace, Figure 7.7. From the plots it can be clearly seen that CO_2 production started immediately after source addition without any significant lag phase period, see Figure 7.7, and the CO_2 production was correlated to the O_2 consumption. On day 0 the CO_2 concentrations in the nutrient amended batches were 0.00054 ± $1.4x10^{-05}$, 0.00065 ± $3.2x10^{-05}$, 0.000624 ± $3.67x10^{-05}$ and 0.00055 ± 2.02 x^{-05} g/L for PP, E10, B20 and the control respectively, close to the CO_2 atmospheric concentration which is 0.0006 g/L. Before the aeration process CO_2 rises sharply to reach a peak of 0.0791 ± 0.0017, 0.0840 ± 0.0036, 0.0836 ± 0.0015 g/L for PP, E10 and B20 respectively. In the batches without nutrient amendment, CO_2 levels remain closely to the atmospheric concentration for just 0.0007 ± 0.0001. After the aeration process on day 15 CO_2 falls quickly to reach 0.0327 ± 0.0122, 0.0425 ± 0.0041, 0.0497 ± 0.0104 for PP, E10 and B20 respectively, and the control remains close to the atmospheric value 0.0005 ± 0.0003. Between days 15 and 20 CO_2 concentration in the nutrient amended batches again rises sharply to reach a peak of 0.0725 ± 0.0421, 0.0958 ± 0.0201 and 0.1185 ± 0.0154 for PP, E10 and B20 respectively at day 20, while CO_2 levels in batches without nutrient addition remain fairly constant. The tracer SF_6 in the nutrient amended batches remained reasonably constant until day 15, when some headspace gas was replaced, suggesting that there were no significant losses due to volatilization.

The increase in CO_2 concentration indicated that a significant degree of biodegradation did indeed take place for the nutrients amended batches. The

degradation was however not noticeable in the hydrocarbon profile for the nutrients unamended batches, except for toluene and ethanol and the amount of CO_2 produced was negligible in comparison with the amount of CO_2 produced in the nutrient amended batches, see Figure 7.7. There is a statistically significant difference between the amount of CO_2 produced in the nutrient amended and unamended batches $P < 0.05$ (M-W test).

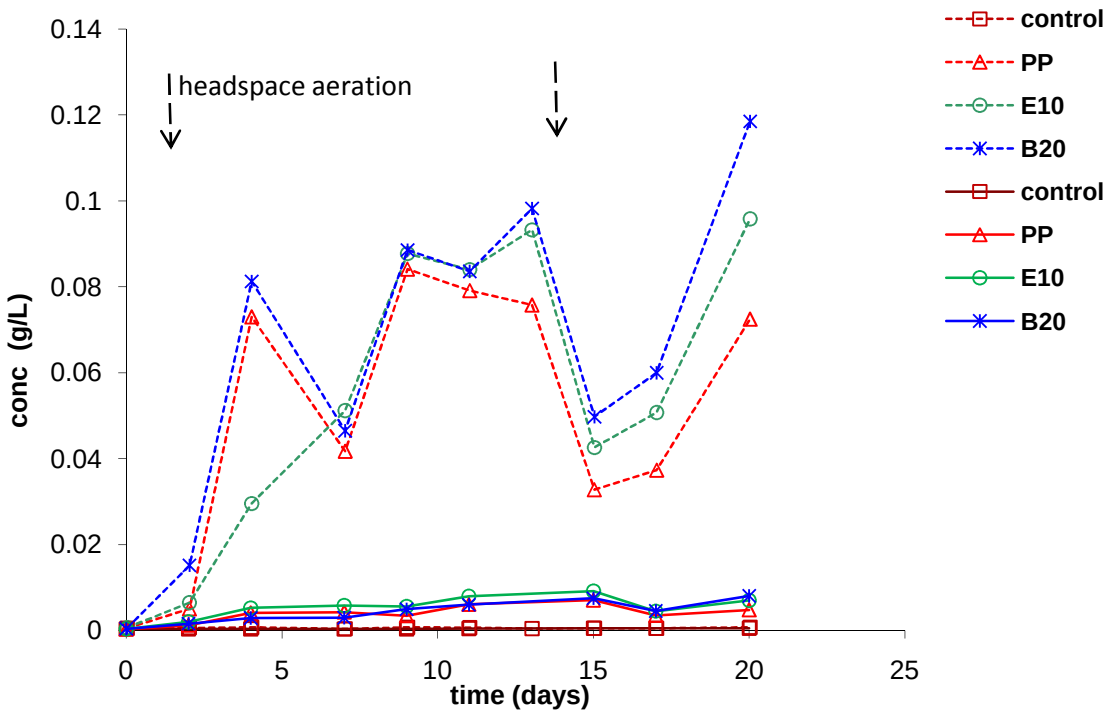

Figure 7.7 CO_2 headspace concentration profile for the PP, E10 and B20 mixtures in the two sets of batches, no added nutrients (continuous line) and nutrient amended (dashed line).

The O_2 and CO_2 plots allow best to illustrate when biodegradation was active at the three nutrients amended different fuel systems, from the plots it can be clearly seen that for E10 and B20 the CO_2 production reaches its highest level on day 20, and a clear difference can be seen for the CO_2 production and O_2 consumption between the nutrients amended and unamended systems Figure 7.7 and Figure 7.8. Linear regression analysis was carried out to measure the degree of correlation between O_2 consumption and CO_2 production in this phase. An average coefficient of determination of (R^2) value $\geqslant 0.6$ was

obtained. R^2 values were 0.68, 0.71 and 0.60 for PP, E10 and B20, Figure 9.2, Figure 9.3 and Figure 9.4 in the appendix. This indicated a high correlation, taking into account the nature of the experiment suggesting that CO_2 production was a good indicator of biodegradation in the nutrients amended batches (Sharabi and Bartha, 1993).

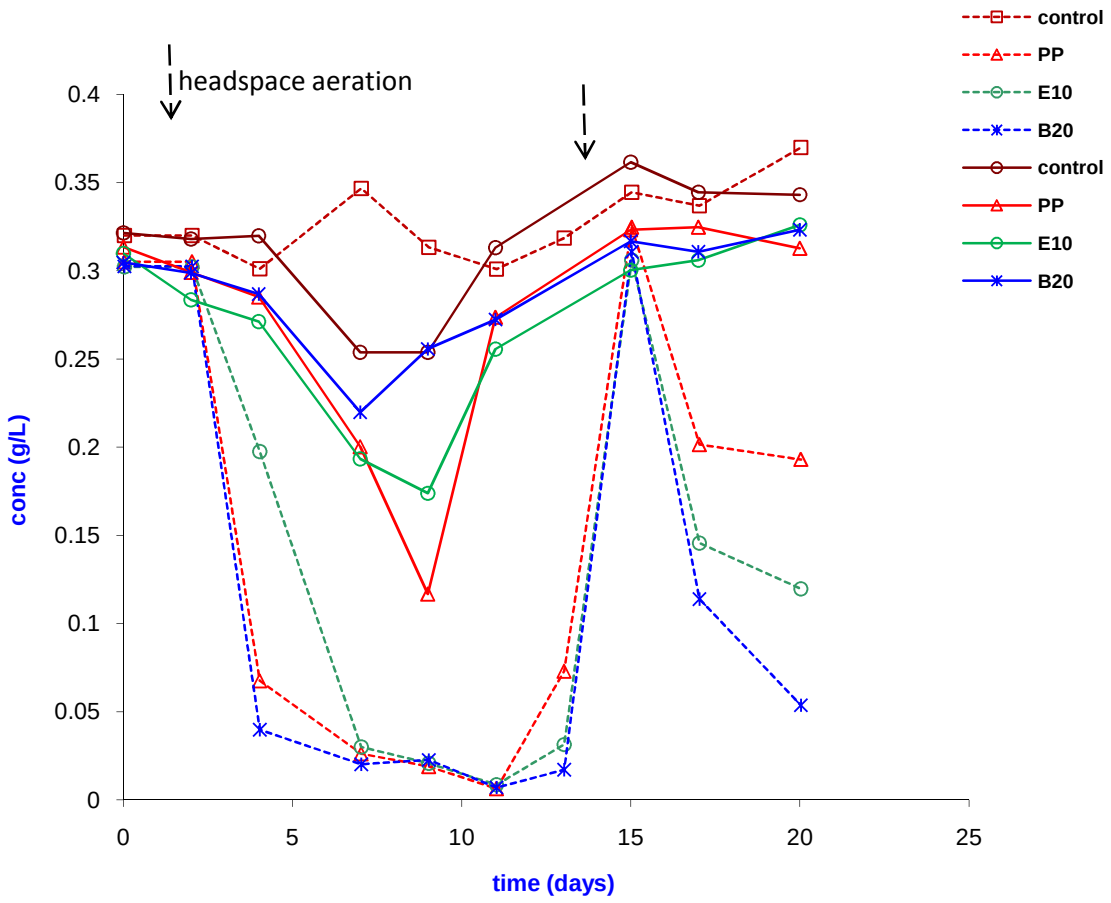

Figure 7.8 Oxygen concentration profiles in PP, E10 and B20 mixtures in the two sets batches headspace no added nutrients (continuous line) and nutrients amended (dashed line).

7.3.3 NAPLs in the sand

The initial total petroleum hydrocarbons TPH content of soil was $1.48x10^{-03}$, $1.34x10^{-03}$ and $1.18x10^{-03}$ g g^{-1} soil for PP, E10 and B20 respectively before incubation for both the nutrients amended and unamended batches.
Basic treatment (without nutrients), showed only a small reduction of TPH concentration during the incubation period. However, microcosms that involved

nutrients addition led to a large decrease in TPH measured at the end of the experiment.

The total reduction of total petroleum hydrocarbons was similar ($3.32x10^{-04}$ ± $4.43x10^{-05}$, $5.25x10^{-04}$ ± $2.71x10^{-04}$ and $3.38x10^{-04}$ ± $1.11x10^{-04}$ g g^{-1} soil for PP, E10 and B20 respectively) for the three fuel types in treatments with no addition of nutrients during 24 days of incubation, and in those with addition of nutrients ($6.09x10^{-05}$ ± $3.02x10^{-05}$, $5.79x10^{-05}$ ± $4.5x10^{-05}$ and $5.02x10^{-05}$ ± $2.45x10^{-05}$) g g^{-1} for PP, E10 and B20 respectively, for the same period of incubation.

Accordingly, the microbial populations of microorganisms without nutrients had to use part of total nitrogen as a nitrogen source, probably through slow transformation to available forms and its immediate incorporation to their biomass, and in nutrients amended microcosms, the immediate availability of available forms of nutrients was translated into a rapid use of hydrocarbons as growth substrate (Sabate et al., 2004).

The treatments containing nutrients were the most efficient and TPH gradually decreased significantly at the end of the incubation time, see Figure 7.10. After 24 days, TPH content showed an average NAPLs attenuation of 95.78 ± 2.04, 95.64 ± 3.43 and 95.75 ± 2.07 % due to volatilisation into the headspace and biodegradation for PP, E10 and B20 respectively, while in microcosms without nutrient addition it was just 77.56 ± 2.99, 60.53 ± 20.42 and 71.40 ± 10.02 % for PP, E10 and B20. No ethanol or biodiesel components were detected in both systems, probably due to their ready mineralization during the incubation period.

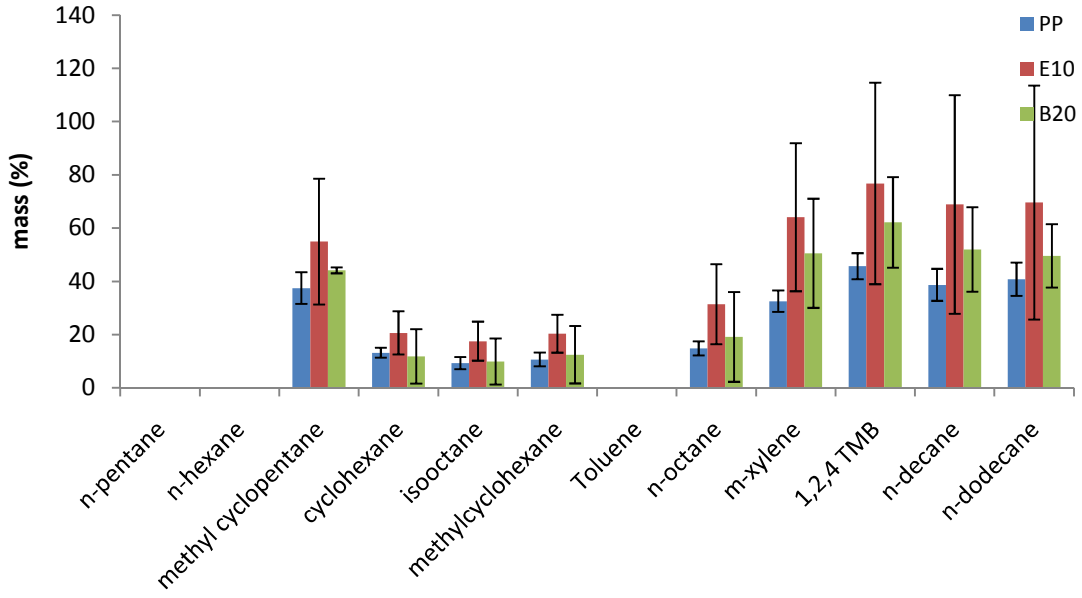

Figure 7.9 NAPLs residual as percent of the mass added in soil without added nutrients for PP, E10 and B20. Error bars: ± 1 standard deviation (SD, n=3)

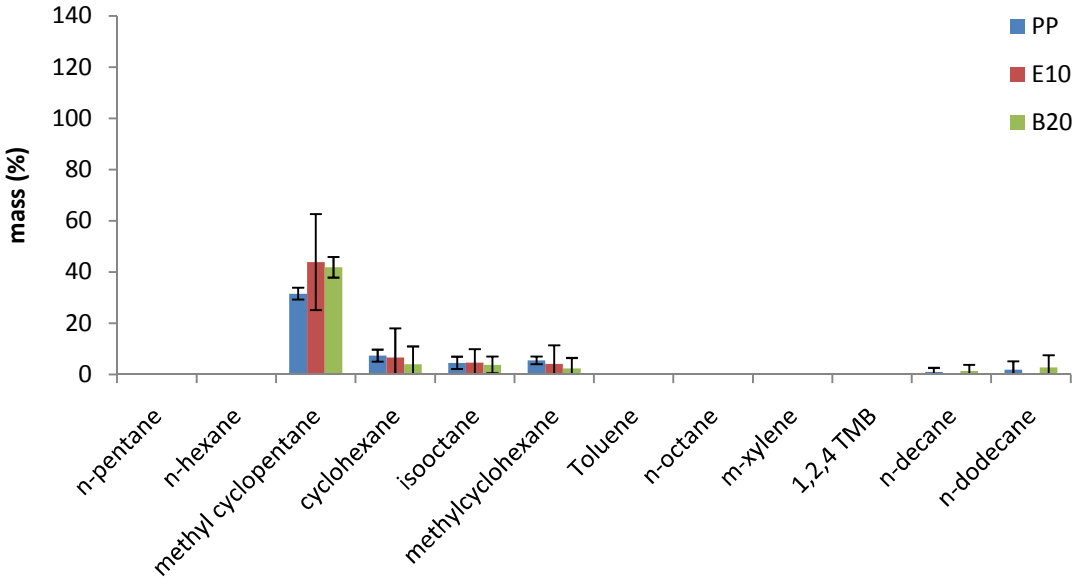

Figure 7.10 NAPLs residual as percent of the mass added in nutrient amended soil for PP, E10 and B20. Error bars: ± 1 standard deviation (SD, n=3)

7.3.4 Microorganisms in the sand

As mentioned previously epifluorescence microscopy is a reliable quantitative tool for direct cell counting of microbiological populations in a specific environment.

7.3.4.1 Total cell numbers

Total microbial cell carbon per g of soil in the batches is shown in Figure 7.11. On day 0, the sand contained an indigenous microbial flora of (4.48± 0.98) × 10^7cells g^{-1} of dry soil. On day 24, the control batches contained about 2.5× 10^7 and (6.49± 0.85) × 10^7 cells g^{-1} of dry soil for the unamended and nutrient-amended control respectively, see Table 7-1. The nutrient addition alone therefore resulted in an increase in microbial biomass of 54.83 ± 19 % in comparison with the unamended control at day 24.

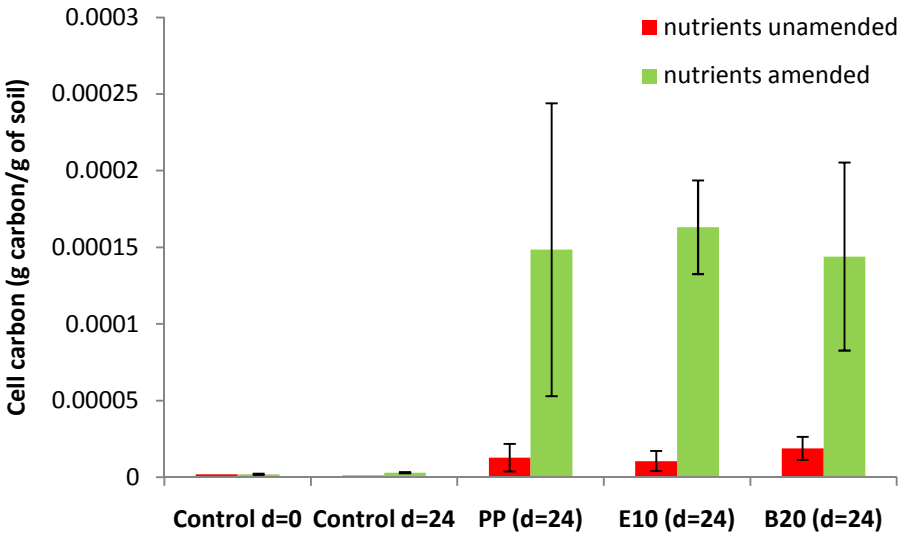

Figure 7.11 Cell carbon (g of C/g of dry soil) for the control, PP, E10 and B20 mixtures. Error bars: ± 1 standard deviation (SD, n=3)

Control d=0	Control d=24	PP d=24	E10 d=24	B20 d=24
Nutrients Unamended				
$4.48x10^7 \pm 9.86x10^6$	$2.50x10^7$	$8.28x10^7 \pm 2.77x10^7$	$9.88x10^7 \pm 3.43x10^7$	$1.40x10^8 \pm 1.19x10^7$
Nutrients amended				
$4.48x10^7 \pm 9.86x10^6$	$6.94x10^7 \pm 8.49x10^6$	$4.79x10^8 \pm 1.08x10^8$	$5.25x10^8 \pm 4.40x10^7$	$7.50x10^8 \pm 9.80x10^7$

Table 7-1 Total cell numbers g^{-1} dry soil for the control, PP, E10 and B20 treatments in nutrient-unamended and amended batches.

Cell abundance and mean volume in the microcosms increased during incubation, leading to an increase in total bacterial biovolume. These increases were usually more pronounced under nutrient-enriched conditions. However, the degree of the increase was variable, depending on the substrate added, the presence or absence of biofuel components with the main substrate, the chemical composition, and the amount of the biofuel components. The largest increases in mean cell volume after 24 days were found in microcosms enriched with nutrients. The mean cell biovolume values for control, PP, E10 and B20 in the nutrient-unamended batches, were 0.14, 0.35 ± 0.10, 0.35 ± 0.03 and 0.43 ± 0.16 μm^3 respectively, while for the same substrates under nutrient-enriched conditions were 0.96 ± 0.45, 0.99 ± 0.11 and 0.61 ± 0.19 μm^3 for PP, E10 and B20 respectively. It would therefore seem that a lack of nutrients, and not carbon, was responsible for the observed differences in cell size and number (Xu and Obbard, 2003; Kilham et al., 1997).

These increases in cell biovolume are correlated with increases in cell biomass, see Table 7-2 and Figure 7.11, although cell size was also affected by treatments.

Control d=0	Control d=24	PP d=24	E10 d=24	B20 d=24
Nutrient Unamended				
$1.96x10^{-06}$ ± 0.0	$1.10x10^{-06}$ ± 0.0	$1.30x10^{-05}$ ± $8.97x10^{-06}$	$1.06x10^{-05}$ ± $6.58x10^{-06}$	$1.90x10^{-05}$ ± $7.52x10^{-06}$
Nutrient amended				
$1.96x10^{-06}$ ± $4.30x10^{-07}$	$3.04x10^{-06}$ ± $3.72x10^{-07}$	$1.49x10^{-04}$ ± $9.55x10^{-05}$	$1.36x10^{-04}$ ±$3.050x10^{-05}$	$1.44x10^{-04}$ ± $6.13x10^{-05}$

Table 7-2 Cell biomass g C g^{-1} dry soil for the control, PP, E10 and B20 treatments in nutrient unamended and amended batches.

Microbial growth on the added fuel is evident in all batches by greater cell numbers on day 24 as compared to the control batches $P < 0.05$ (Mann-Whitney nonparametric test) between each fuel treatment and the control, with no statistically significant differences between fuel treatments $P > 0.05$ (Mann-Whitney test), for the nutrient unamended and amended batches. However, there was a statistically significant difference between nutrient amended and unamended batches within each fuel treatment, $P < 0.05$. The corresponding cell doubling times were calculated based on an assumed exponential growth as 27.11 ± 6.8, 21.06 ± 7.29 and 14.56 ± 1.03 days for PP, E10 and B20 respectively, for nutrient-unamended, while the corresponding doubling times for nutrient-amended was 7.02 ± 0.57, 6.76 ± 0.27 and 5.90 ± 0.29 days for PP, E10 and B20 respectively.

Only 0.6 % of the total added petroleum carbon in PP, 1.2 % of the total added petroleum carbon and ethanol carbon in E10 and 1.7 % of the total added petroleum and biodiesel carbon in B20 was transformed to CO_2 in nutrient unamended batches. The microbial biomass carbon was also only a small percentage of the amount of carbon added. The average yield calculated from these numbers were comparable for all three fuel mixtures; 0.51 ± 0.22, 0.40 ±

0.16, and 0.47 ± 0.12 g cell C per g petroleum or biofuel C degraded for batches with the PP, E10 and B20 respectively.
The microbial populations without nutrients had to use part of total nitrogen in the soil and fuel mixtures as a nitrogen source, probably through slow transformation to available forms for incorporation into their biomass. In nutrient amended microcosms, the immediately available forms of nutrients enabled the rapid use of hydrocarbons, which resulted in significant growth.

The significant differences for the total cell numbers, cell biovolume and cell biomass between the nutrient unamended and amended batches, suggest that the availability of inorganic nutrients plays an important role in the biodegradation of specific fuel components.

7.3.4.2 *Denaturing gradient gel electrophoresis*

A DGGE gel comparison of the bacterial community structures in the nutrient amended and unamended batches is presented in Figure 7.12. DGGE analysis showed that there was greater bacterial taxa (i.e. band) richness in all treatments compared to the control samples. It is interesting to note in Figure 7.12 that bacterial taxa richness was higher within B20 than PP and E10, in agreement with the mini-lysimeter study.

Each DGGE band theoretically represents a different taxon ("species"), and the intensity of each band can be used to measure the relative abundance of that taxon in a given sample. Bands appearing in different samples at the same position suggest that the same taxon is present in those samples.

Based on DGGE results, all treatments at day0 were dominated by a few bacterial community members.

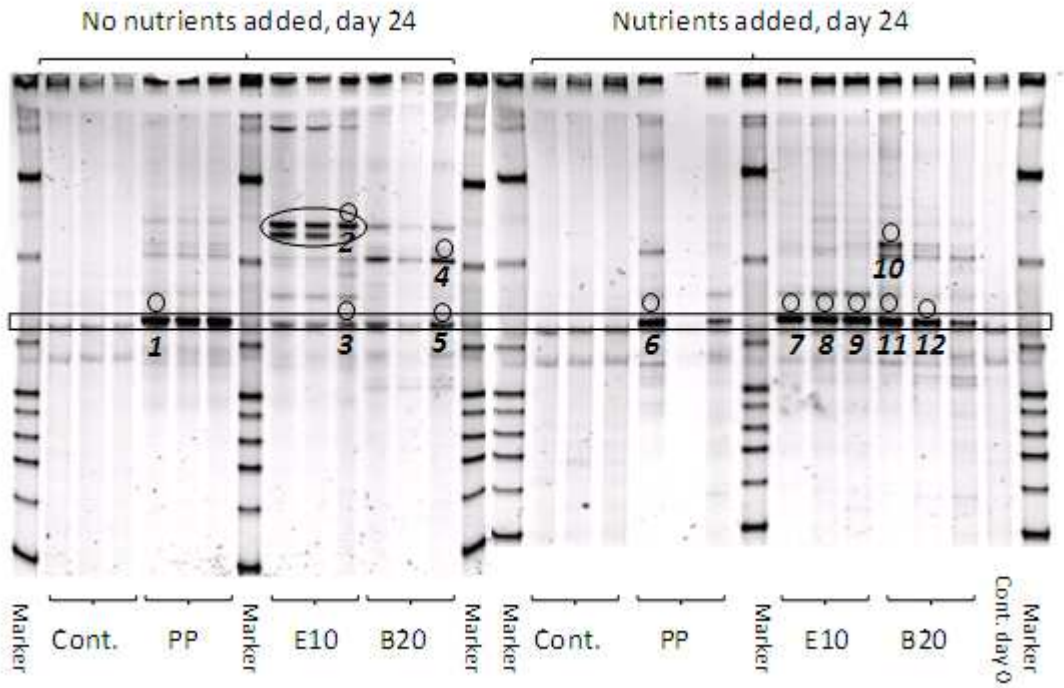

Figure 7.12 DGGE profiles of the bacterial community composition over time in nutrient amended and unamended batches. Separate gels were used for the two systems. Each excised, cloned, and sequenced band is numbered on the bottom and labelled by a circle on the top. The relationships of excised band sequences to other sequences in the GenBank database are indicated in Table 9.4 in the appendix.

The dominant species diversity changed and increased substantially over 24 days in all treatments plots. The nature of this change was altered by nutrient-addition and the addition of the biofuel components. By day 24, the microbial community was highly diverse and the original species in the control plots were not abundant enough to be detected. There were no obvious differences between the original bands in days 0 and 24 control samples. This suggests that, the community structure of the control plots were unchangeable through 24 days, but more additional species of bacteria were detectable by day 24 for the treated plots.

7.3.4.3 *Effect of biofuel addition on microbial community structures*

The bacterial population from different treatments showed distinctly different profiles based on the number and position of migration of the PCR products or bands (Figure 7.12). The intensity of the PCR product is suggested to be proportional to the abundance of the template and therefore the abundance of

each population (ØVREÅS et al., 1997). Hence, the appearance and disappearance of bands, and changes in the intensity of the bands, in the DGGE profiles approximate shifts in the microbial community structure. Comparison of DGGE profiles shows that the structure of microbial communities in different treatments and amendments differ from one another (Figure 7.12). In general, there are a greater number of bands (i.e. taxa) in pure and blended fuel treatments in comparison to the control. This is known as the band or taxa richness and is one measure of the diversity of bacterial communities, which is quantified in more detail below.

One putative "taxon" of particular interest, is highlighted by the boxed area in Figure 7.12, as the intensity (i.e. abundance) and predominance of this band changed dramatically depending on treatment and nutrient addition.

Visual examination of the DGGE gel indicates that the highlighted band, which appears to be absent from the natural sand bacterial community, was enriched by the addition of fuel, and becomes particularly more predominant in those treatments receiving nutrient addition.

Biological diversity has been defined by Kennedy and Smith, as the variety of species in ecosystems as well as the genetic variability within each species and the biodiversity is the richness of life as indicated by the variety of biota and interrelationship of biochemical processes in the soil (Kennedy and Smith, 1995). Band richness in DGGE analysis is a measure of taxa richness among the most abundant members of the community analysed.

The diversity indices used to characterize species richness and evenness are the Shannon diversity index and Pielou's equitability (Pielou, 1969), for more details please refer to the methods chapter, part 4.5.3.

The Shannon index of diversity, H', was higher in all treatments, which ranged between 1.78 ± 0.21 to 2.10 ± 0.19, compared with the control values 1.33 and 1.43 ± 0.19 at days 0 and 24 respectively. The Shannon index of diversity, H', was also higher in nutrient amended batches which ranged between 1.78 ±

0.21 to 2.10 ± 0.19 compared with nutrient unamended batches which ranged between 1.80 ± 0.04 to 1.96 ± 0.19 and control values, 1.33 and 1.43 ± 0.19 at days 0 and 24 respectively.

Within nutrient amended batches H' was highest for B20 2.10 ± 0.19 compared with E10, 1.78 ± 0.21, and PP, 1.97 ± 0.18, and the same observation was found for the nutrient unamended batches. However, these differences were not significantly different $P > 0.05$ (Mann-Whitney test). The only significant differences in H' were found between each set of treatments and its control for both nutrient amended and unamended batches.

Diversity indices for bacterial communities from nutrient amended and unameded treatments are listed in Table 7-3. The band richness index S, decreased in the order B20>PP>E10>Control, the same observation was found for Shannon's index H', Pielou's equitability E, and Simpson's diversity index.

The average evenness for communities in the B20 nutrient amended batches was 11.33 ± 2.52, which was higher than all other treatments, see Table 7-3. There was no significant difference in the ranking of the number of treatments among three treatments ($P > 0.05$, Kruskal-Wallis test).

Non metric Multi Dimensional Scaling (NMDS) with cluster analysis, followed by analysis of similarity (ANOSIM) were used to statistically compare the similarity of bacterial communities between replicate and treatment batches, with and without nutrient amendment. ANOSIM is a non-parametric test equivalent to ANOVA. It compares the rank similarity between pairs of replicates within a group (treatments) to the rank similarity of all pairs of replicates between groups (treatments) giving an R value. An $R = 1$ when all replicates within a group are more similar to each other than any replicates from different groups. $R = 0$ if the similarities between and within groups (treatments) are on average the same. In ANOSIM the group (treatment) labels are randomly shuffled (permutated) and the similarity comparisons are made. This procedure is repeated to give a normal distribution of R values for randomly non-replicated communities.

Microcosm amendment	Time (days)	Band richness (S)	Shannon diversity index (H)	Pielou's equitability (E)	Lambda response diversity index (1-λ)
Cont unamended	0	4.00	1.33	0.96	0.73
Cont amended	0	4.00	1.33	0.96	0.73
Cont amended	24	4.67 ± 1.15	1.43 ± 0.19	0.94 ± 0.02	0.74 ± 0.04
Cont unamended	24	5.67 ± 0.58	1.54 ± 0.09	0.89 ± 0.03	0.75 ± 0.03
PP unamended	24	10.00 ± 0.0	1.80 ± 0.04	0.78 ± 0.02	0.77 ± 0.01
PP amended	24	10.50 ± 3.54	1.97 ± 0.18	0.85 ± 0.05	0.82 ± 0.02
E10 unamended	24	10.00 ± 0.0	1.80 ± 0.04	0.78 ± 0.02	0.77 ± 0.01
E10 amended	24	8.33 ± 2.08	1.78 ± 0.21	0.85 ± 0.02	0.79 ± 0.04
B20 unamended	24	10.33 ± 2.52	1.96 ± 0.19	0.85 ± 0.01	0.82 ± 0.03
B20 amended	24	11.33 ± 2.52	2.10 ± 0.19	0.87 ± 0.02	0.84 ± 0.04

Table 7-3 Average diversity indices values for the soil biodegradation microcosms of the microbial community in different plots ±1 standard deviation (SD, n=3)

The ANOSIM attributes a significance level by comparing the R value for real data to the normal distribution of the R value for the non-replicated communities (Clarke K.R, 2001). This was conducted using the Primer V6 multivariate statistical software package (Primer-E Ltd, Plymouth, UK). Bray Curtis rank similarity coefficient was used on presence/absence data to derive similarity values between samples:

$$S_{jk} = 100\left\{1 - \frac{\sum_{i=1}^{p}\left|y_{ij} - y_{ik}\right|}{\sum_{i=1}^{p}\left(y_{ij} + y_{ik}\right)}\right\}$$

Equation 7-1

$$= 100\left\{\frac{\sum_{i=1}^{p} 2min\left(y_{ij}, y_{ik}\right)}{\sum_{i=1}^{p}\left(y_{ij} + y_{ik}\right)}\right\}$$

Equation 7-2

Here y_{ij} represents the entry in the ith row and jth column of the data matrix, i.e. the abundance (or biomass, or cover) for the *i* th species in the *j*th sample (*i*= 1,2 ….*P*; *j* = 1,2 ….n). Similarity y_{ik} is the count for the *i*th species in the *k*th sample.

| … | represents the absolute value of the difference (the sign is ignored) and min (.,.) the minimum of the two counts; the separate sum in the numerator and denominator are both over all rows (species) in the matrix.

With the presence/absence data, this is equivalent to:

$$S_{jk} = 100\,[2a/(2a + b + c)]$$

Equation 7-3

Where:

a = the number of species which are present in both samples;

b = the number of species present in sample j but absent from sample k;

c = the number of species present in sample k but absent from sample j

When presence/absence data are used this is identical to the Sorensen or Dice coefficient (Clarke and Warwick, 2001).

The NMDS plot Figure -7.13 shows large differences in the similarity of bacterial communities between nutrient amended and unamended treatments.

These data suggest that addition of inorganic nutrient in the presence or absence of biofuel have resulted in a significant shift in the bacterial community structure.

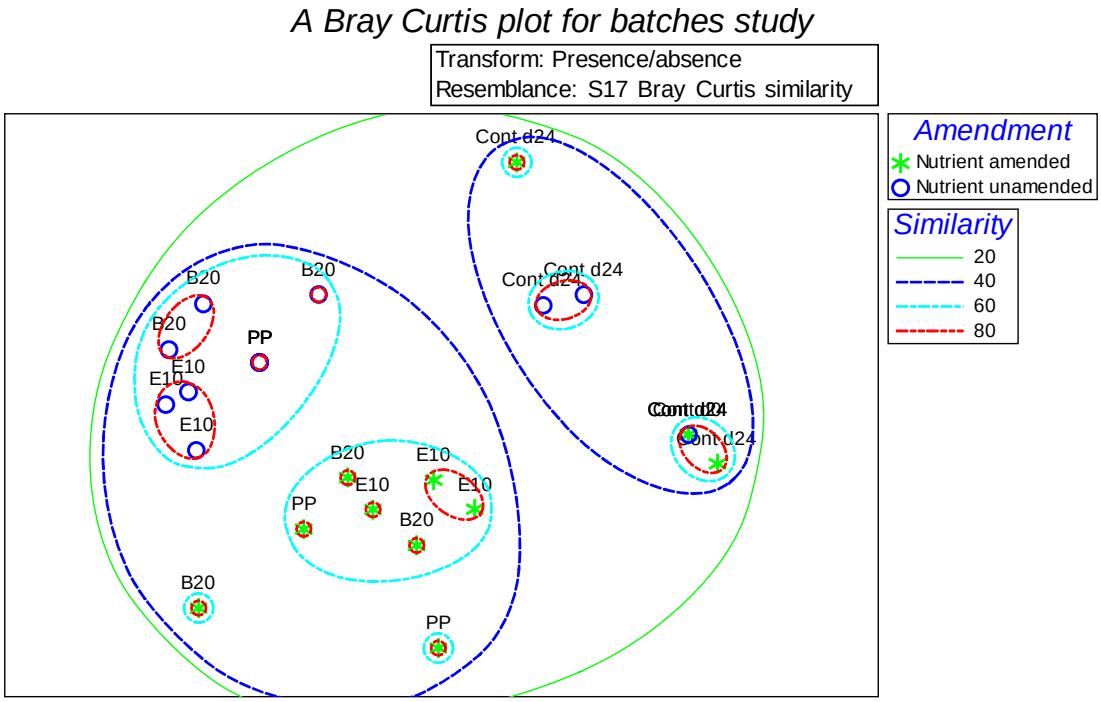

Figure -7.13 NMDS plot of batches soil samples, the triplicate data points for PP nutrient-unamended have the same value showing only one point.

The NMDS and cluster analysis demonstrate that replicate similarities were generally high. ANOSIM analysis in Table -7-4 indicated that similarities in bacterial community structures among different treatments were greater than within treatments (i.e. between replicates; generally > 60% similarity) ($P < 0.001$).

Overall, there was a statistically significant difference in the similarity between the bacterial communities from the different treatments/batches (ANOSIM $P < 0.001$).

Figure -7.13, illustrates the Bray-Curtis similarities between bacterial communities in a plot where the proximity of the data points reflects the degree of similarity between samples.

In this analysis, it was not possible to get a significant value less of than 10% for pairwise comparisons between individual batches (treatment plus nutrient amendment) because of the low number of replicates. Therefore, under these

conditions the difference level 10% may be represent a significant level, especially when the R-value is high (close to 1), which indicates high similarity between replicates within a batch. For example, if comparing only two treatments with a one-Way ANOSIM test, based on 3 replicates for each treatment, there are only 10 distinct permutations and a significant level better than 10% could never be attained. A test demanding a significance level of 5% would then have no power to detect a difference between the treatments, however large that difference is (Clarke K.R, 2001). According to the above assumption to consider the value 10% as a significant level, it can be showed that there is a significant difference between the community structures within most of the treatments with a p-value 10% and a high R-value in Table -7-4.

The results of the study revealed a significant shift in bacterial community structure upon fuel treatment and nutrient-amendment ($R \leqslant 1$, $P < 0.1$). Data in Table -7-4 shows that for bacterial communities, all nutrient-amended and unamended fuel treatments were significantly different to the control ($R = 1$, $P < 0.1$), while a significant difference was also observed between each nutrient-amended fuel treatment and the other two nutrient-unamended fuel treatments ($R = 0.75\text{-}1$, $P < 0.1$).

The same observation was also found for the same pair of treatments within the nutrient-amended and unamended batches ($R = 1$ except for B20 treatments $R = 0.72$ and $P < 0.1$). For the nutrient-amended batches no significant difference was observed between each fuel treatment ($R \leqslant 0.5$, $P \geqslant 0.1$), while for the nutrient-unamended batches there was a significant difference in most cases ($R = 0.4$, 0.63 and 1 for (PP, B20), (E10, B20) and (PP, E10) respectively, $P < 0.1$).

These experiments show that the additive treatment (ethanol, biodiesel, and pure petroleum) resulted in bacterial communities that were significantly different to those in control samples (Table -7-4). In addition, the data suggest that nutrient addition also leads to significant differences between bacterial community structures.

Global Test
Sample statistic (Global R): 0.799
Significance level of sample statistic: 0.1%
Number of permutations: 999 (Random sample from a large number)
Number of permuted statistics greater than or equal to Global R: 0
Pairwise Tests

Groups	R Statistic	Significance Level %	Possible Permutations	Actual Permutations	Number >= Observed
PP+N, B20+N	0.25	40	10	10	4
PP+N, E10+N	0.5	10	10	10	1
PP+N, PP	1	10	10	10	1
PP+N, B20	0.75	10	10	10	1
PP+N, E10	0.792	10	10	10	1
PP+N, Ct d24	1	10	10	10	1
PP+N, Ct d24+N	1	10	10	10	1
PP+N, Ct d0	1	33.3	3	3	1
B20+N, E10+N	0.185	30	10	10	3
B20+N, PP	0.444	10	10	10	1
B20+N, B20	0.722	10	10	10	1
B20+N, E10	0.759	10	10	10	1
B20+N, Ct d24	1	10	10	10	1
B20+N, Ct d24+N	1	10	10	10	1
B20+N, Ct d0	1	25	4	4	1
E10+N, PP	1	10	10	10	1
E10+N, B20	0.944	10	10	10	1
E10+N, E10	1	10	10	10	1
E10+N, Ct d24	1	10	10	10	1
E10+N, Ct d24+N	1	10	10	10	1
E10+N, Ct d0	1	25	4	4	1
PP, B20	0.389	10	10	10	1
PP, E10	1	10	10	10	1
PP, Ct d24	1	10	10	10	1
PP, Ct d24+N	1	10	10	10	1
PP, Ct d0	1	25	4	4	1
B20, E10	0.63	10	10	10	1
B20, Ct d24	1	10	10	10	1
B20, Ct d24+N	1	10	10	10	1
B20, Ct d0	1	25	4	4	1
E10, Ct d24	1	10	10	10	1
E10, Ct d24+N	1	10	10	10	1
E10, Ct d0	1	25	4	4	1
Ct d24, Ct d24+N	0.704	10	10	10	1
Ct d24, Ct d0	0.111	50	4	4	2
Ct d24+N, Ct d0	-0.333	100	4	4	4

Table -7-4 ANOSIM results of batches samples (treatments), Nutrient amended and unamended.

7.3.4.4 Closest matching relatives and classification of the selected sequences

Searches in the Genbank with the BLAST program (Altschul et al., 1997) were performed to determine the closest known relatives of the sequences from the DGGE bands of 16S rRNA gene fragments.
The closest matching sequences to determine the identity of nearest neighbours of DGGE band sequences, and their classification using the RDP classifier, are shown in Appendix Table 9.4 together with their GenBank accession numbers.

All the recovered sequences had more than 98% identity with previously identified bacterial 16S rRNA gene sequences from uncultured organisms or cultured strain isolates. A similarity cut-off of 97% is often used for 16S rRNA genes/gene fragments to identify taxa belonging to the same species (Quince et al., 2009). All sequences were also classified using the RDP Classifier (Cole et al., 2005) as belonging to the either the family *Pseudomonadaceae* (> 95% confidence) or the genus *Pseudomonas* (>80% confidence), which are a common and ubiquitous environmental bacteria, but many of which also possess oxygenase enzymes for the degradation of aromatic compounds (Tancsics et al., 2010).

After multiple alignment, sequences from bands 1, 3, 5-9, and 11-12, which migrated to the position on the gel framed by the box in Figure 7.12, were shown to share 100% homology in regions of shared sequence (116 bp), but varied slightly in terms of the number of bases; 122 – 169 bp. These differences in sequence length led to the identification of different closest matching sequences in the BLAST search (Table 9.4 in the appendix). Interestingly, the most common identity of the closest relative of these sequences was an uncultured cloned partial sequence from the clone library of a petroleum hydrocarbon (BTEX) contaminated groundwater dominated by *Pseudomonas spp.* (Tancsics et al., 2010).

Analysis using the RDP Classifier (Wang et al., 2007), identified this sequence as belonging to the genus *Pseudomonas* (mean confidence level of 52%).

7.3.5 Importance of nutrients addition

Toluene was chosen as an example to demonstrate the effect of inorganic nutrient addition on the movement and biodegradation of aromatic VOCs in the unsaturated zone in the presence of biofuel components. Toluene is a key member within the BTEX group and it is one of the compounds that is known to be fairly soluble in water and therefore poses a potential groundwater pollution risk, although rapid biodegradation may effectively attenuate toluene in the unsaturated zone before it reaches groundwater (Pasteris et al., 2002). The toluene profiles in PP, E10 and B20 treatments suggest that the vapour phase concentration in nutrient amended batches Figure 7.14 (b) was completely removed to under the analytical detection limit by day 5 for the three mixtures, while it remained measurable in the nutrient unamended batches Figure 7.14 (a) until the end of the experiment. The headspace concentrations indicated that toluene biodegradation was fastest for the PP and B20 treatments followed by E10 treatment, and slowest for the nutrient unamended mixtures as is illustrated in Figure 7.14. These findings were in a good agreement with the CO_2 production and O_2 consumption and the biomass in nutrient unamended and amended batches.

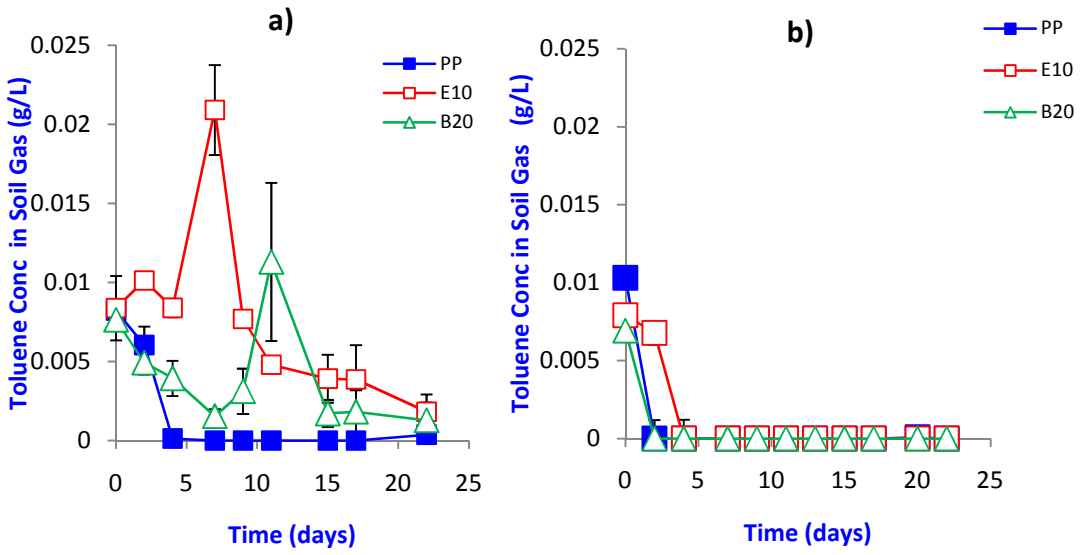

Figure 7.14 Toluene concentration profiles in PP, E10 and B20 mixtures for nutrient unamended batches (a) and nutrient amended batches (b).

Bacteria were the entities responsible for the removal of carbon in the two systems. Bacteria carried out at least 90% of the total carbon removal to carbon biomass and carbon CO_2, according to the carbon mass balance Table 7-5. It is likely that the predominant *Pseudomonas sp.* highlighted in the DGGE gel (Figure 7.12), played an important role in degradation as its mean proportional abundance increased in the treatment batches from 0% to 29.7%. A number of other taxa were also present in treatment batches but not the controls, although each treatment had a distinct bacterial population. Hence, the extent and the pathways of carbon removal were affected by the composition and kinetics of the bacterial communities present and by the factors affecting these bacterial communities.

Without nutrient addition, microbial communities from batches containing a biofuel component are characterized by appearance of additional and/or stronger bands in the DGGE gels compared to the control and PP batches. The strength of these bands (some of which were identified as different *Pseudomonas sp.*) was most intense in microbial communities from the batches

with E10 (highlighted by the oval in Figure 7.12). The additional strong bands would likely be linked to species growing on the biofuel. These changes in microbial community structure are associated with the slower degradation of toluene and m-xylene in the presence of ethanol, consistent with the observations of DaSilva et al. (Da Silva and Alvarez, 2002), and also biodiesel. These data suggest that the presence of the biofuels result in the growth of biofuel-degraders and reduced degradation of BTEX rather than a reduced rate of BTEX degradation per cell of BTEX degrader per se (Lovanh et al., 2002) which would not have resulted in the observed differences in the presence and intensities of different bands in the DGGE gel.

Addition of inorganic nutrients allowed more petroleum hydrocarbon biodegradation to occur, and the most intense band in the community analysis of nutrient amended batches is therefore the same for the PP, E10 and B20 mixtures (framed by the box in Figure 7.12), although some additional strong bands remain notable for the B20 mixture, likely because biodiesel is not degraded as rapidly as ethanol.

The addition of inorganic nutrients also has an additive affect on mineralization. Ethanol will be taken as an example. The vapour phase concentration of ethanol in E10 mixture, nutrient unamended and amended batches can be seen in Figure 9.5 in the appendix. Ethanol was completely degraded in the E10 mixtures with 100% disappearance from the headspace of batches on days 2 and 9, for the nutrient amended and unamended batches respectively.

Analysis of microbial cell numbers and carbon content indicated that there was a significant growth of biomass, but which was not associated with significant biodegradation of the VOCs in the nutrient unamended batches, probably due to the lack of nutrients. After addition of inorganic nutrients it was noticeable that there was significant growth of biomass in the three treatments in comparison with nutrient unamended batches. For E10 and B20 batches bacterial growth probably correlated to ethanol and biodiesel biodegradation respectively, again in agreement with the NAPLs residual findings. The effect of

inorganic nutrients addition on the abundance, size and biovolume of bacterial cells can be clearly seen in Figure 7.15.

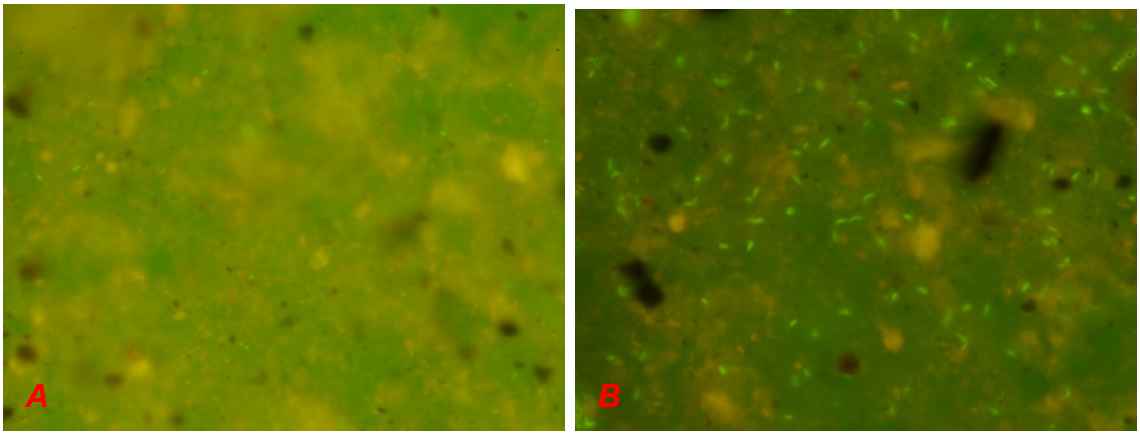

Figure 7.15 Bacterial cells for nutrient unamended batches (a) and nutrient amended batches (b).

7.3.6 Mass balance

A mass balance for the batches shown in Table 7-5 demonstrates that most of the carbon added remained after 24 days either as vapour or as NAPL or adsorbed residual, especially in the unamended batches.

In nutrient amended batches between 31 and 44% of the added carbon were transformed into CO_2 and biomass.

	Residual NAPL and Vapour C (%)	Biomass C (%)	CO_2 C (%)	Uncounted C[a] (%)
		No nutrients added		
PP	95.0 ± 5.6	0.87 ± 0.10	0.6 ± 0.12	3.5
E10	127.4 ± 10.1	0.90 ± 0.37	1.2 ± 0.18	-29.5
B20	82.6 ± 10.3	1.6 ± 0.64	1.7 ± 0.49	14.1
		Nutrients added		
PP	72.1 ± 3.6	12.2 ± 2.7	18.6 ± 8.6	-2.9
E10	52.7 ± 3.8	13.83 ± 2.5	25.7 ± 7.8	7.7
B20	59.4 ± 1.1	11.92 ± 2.2	32.2 ± 2.9	-3.5

Table 7-5 Mass balance as % of the carbon added for the batches study

[a]Unaccounted C may be explained by volatile losses, experimental error or poor recovery of ethanol and potentially more polar metabolites such fatty acids formed from biodiesel in the extraction and clean-up procedure. No biodiesel residuals (esters) were found in the extracts of the batch studies.

7.4 Conclusion

The completed study of the effect of nutrient addition on the biodegradation of VOCs in the presence of biofuel components has shown that nitrogen and phosphorus are important parameters in biodegradation reactions. VOC mineralisation was greatest in the nutrient amended soils, suggesting that in these treatments, the viable biomass was either large in size or metabolically active. Considered together, these results suggest that nutrient probably has led to differences in bacterial communities in soils.

To our knowledge this is the first study to investigate the effect of two different biofuel components, ethanol and biodiesel addition on the fate and transport of petroleum hydrocarbons in the subsurface by multidisciplinary methods including soil analysis, chemical and geochemical analysis, and molecular analysis (including total cell count and DGGE), throughout an experiment.

Changes in CO_2 evolution can be indicative of TPH reduction, here it suggested that little degradation is occurring in nutrient unamended soils and vapour phase concentrations are maintaining approximately at a steady state. Whereas higher CO_2 levels in nutrient amended soils and subsequent reductions suggest more degradation initially that is subsequently decreasing as microbial food sources are consumed over time. However, NAPLs analysis shows that whilst this holds true for nutrient unamended soils Figure 7.9, it does represent the degradation seen in nutrient amended soils (Figure 7.10).

As described in other studies, the addition of nutrients can improve the degradation of contaminants. Although the literature contains a wide variety range of responses to the addition of nutrients, our findings coincide with those described by other authors (Vyas and Dave, 2010; Singh and Lin, 2009; Jean et al., 2008).

It can be concluded that there were significant differences in the vapour phase concentrations, CO_2 plots, O_2 plots, NAPL plots and biomass between nutrient unamended and amended batches, and our findings are in a good agreement

with other studies (Coulon et al., 2005; Xu and Obbard, 2003; Brook et al., 2001).

These data indicate that under nutrient limitation, indigenous source zone soil bacterial assemblages were incapable of utilizing the accumulated NAPLs as a substrate to support rapid bacterial production.

Petroleum hydrocarbon degradation appeared to be associated with the presence and appearance of a predominant strong band in PP, E10 and B20 batches, which was less prominent in control batches (framed by the rectangle in Figure 7.12). This band was identified as belonging to the genus of Pseudomonas.

8 Overall Results, Discussion and Conclusion

8.1 Introduction

Natural attenuation is an important process for contamination mass reduction and plume containment. To increase the ability to understand and predict the contaminant fate and transport, techniques for natural attenuation rate calculation are required (Kao and Prosser, 2001). The techniques applied in this study such as, microcosms test, mini-lysimeter study, fate and transport model application, mass flux and first-order biodegradation calculations are relevant for natural attenuation and biodegradation rate and efficiency evaluations.

8.2 Overall results and discussion

8.2.1 Modelling biodegradation and transport of VOCs in the unsaturated zone

The analytical model results showed that the migration distance of the VOCs was predicted to be short in the soil investigated, and biodegradation was found to be the most relevant attenuation process. The predicted 95% attenuation distance from the source zone was less than 1.5 meters.

8.2.2 Mini-lysimeter experiments

Observations in the mini-lysimeter experiments are consistent with the main findings of the batch studies (see below). In comparison with the batch studies, the amount of fuel added per g of soil was much higher in the mini-lysimeters at 0.0158, 0.0160 and 0.0158 g/g of soil for the PP, E10 and B20 mixtures in the source zone of these experiments. Occasional purging of the headspace kept the soil in the mini-lysimeters aerobic and allowed for some volatilization. Consequently, the more volatile petroleum hydrocarbons were found to be more depleted than less volatile petroleum hydrocarbons in the solvent extracted residuals as is illustrated in Figure 6.10. The percentage of the added amount of m-xylene remaining after 92 days was statistically significantly higher for the E10 mixture as compared to the PP and B20 mixtures ($P < 0.05$, Mann-Whitney test). Toluene was absent from the solvent extracts of all three mini-lysimeters, but headspace concentrations indicated that toluene biodegradation

was fastest for the PP mixture and slowest for the E10 mixture as is illustrated in Figure 6.15. Ethanol headspace concentrations in the mini-lysimeter with the E10 mixture fell below the detection limit after 18 days, as is illustrated in Figure 6.8. Ethanol degradation coincided with high CO_2 production. A more gradual increase in CO_2 headspace concentrations was observed for the PP and B20 mixture as is shown in Figure 6.7. This indicates that biodiesel is more slowly degraded than ethanol. For the lysimeter with the B20 mixture a biodiesel residual of 18.3 ± 9.6 % of the amount added remained after 92 days as measured in the solvent extracts.

Total microbial cell carbon per g of soil in the mini-lysimeters is shown in Figure 6.12. It was significantly higher in the mini-lysimeter with the E10 mixture as compared to the lysimeter with the PP mixture (t-test, $p < 0.05$) probably reflecting the fact that a substantial portion of the more volatile petroleum hydrocarbon mass, but an insignificant amount of ethanol volatilized from the mini-lysimeters during pumping instead of being transformed into biomass. When the headspace of the mini-lysimeters was flushed for the first time on day 11, ethanol headspace concentrations had already decreased to 0.0007 g/L. For the PP mixture, cell counts in the source zone (bottom third of the mini-lysimeter) were a factor 1.9 higher than in the soil without NAPL (middle and top third of the mini-lysimeter), for the E10 mixture they were a factor 0.65 lower, and for the B20 mixture they were a factor 2.9 higher in the source zone. This indicates that ethanol biodegradation occurred throughout the soil-filled mini-lysimeter volume, whereas petroleum hydrocarbon and biodiesel biodegradation occurred mainly in the source zone.

Calculated biomass doubling times were 22, 15 and 16 days for PP, E10 and B20 respectively, which is 2.5, 1.6, and 2.2 times slower than in the batch study without inorganic nutrient addition for PP, E10 and B20 respectively.

From a DGGE gel comparison of microbial community structures in the mini-lysimeters, presented in Figure 6.13, it is evident that replicates from different locations in each mini-lysimeter are fairly similar to each other, but addition of a

biofuel component appears to have resulting in a significant long-term shift in the structures of the microbial communities.

8.2.3 Batch experiments

Toluene was the only hydrocarbon no longer present after 24 days in solvent extracts of batches containing 15 g of soil and initially spiked with 22.2 mg of each fuel type (PP, E10, B20) as is shown in Figure 7.9. Monitoring of headspace concentrations indicated that toluene was most rapidly degraded in batches with the PP mixture and least rapidly in batches with the E10 mixture as is shown in Figure 7.14. Ethanol headspace concentrations in batches with the E10 mixture decreased below the detection limit within 9 days. The residual amounts of each petroleum hydrocarbon compound as a percentage of the amount added was statistically indistinguishable between treatments, except for m-xylene which was presented in higher residual amounts in batches spiked with E10 as compared to batches spiked with PP, $P < 0.05$ (Mann-Whitney test), see Figure 7.9. Residual biodiesel was undetected in the solvent extracts of batches polluted with the B20 mixture. Residual of potential metabolites of both ethanol and biodiesel could not be quantified with the method employed in this study due to the polarity of these compounds.

A mass balance for the batches without added nutrients shown in Table 7-5 demonstrates that most of the carbon added remained after 24 days either as vapour or as NAPL or adsorbed residual. Microbial growth on the added fuel is evident in all batches by greater cell numbers on day 24 as compared to the control batches with no significant difference between PP, E10 and B20 mixtures as shown in Figure 7.11. The corresponding cell doubling times were calculated based on an assumed exponential growth as 9, 10 and 7 days for PP, E10 and B20 respectively. Only 0.6 % of the total added petroleum carbon in PP, 1.2 % of the total added petroleum carbon and ethanol carbon in E10 and 1.7 % of the total added petroleum and biodiesel carbon in B20 was transformed to CO_2, and biomass carbon was similar to the amount of CO_2 carbon produced. The average yield calculated from these numbers (g cell C per g petroleum or biofuel C degraded) would be 0.51 ± 0.22 for batches with

the PP mixture, 0.40 ± 0.16 for batches with E10 mixture and 0.47 ± 0.12 for batches with B20 mixture, which is comparable for all three mixtures.

Fuel biodegradation in the batch experiments was limited by inorganic nutrient availability. Addition of 0.12 mg nitrogen and 0.012 mg phosphorus per g of soil allowed faster biodegradation to occur as is evident from the lower residual amounts found in solvent extracts after 24 days (Figure 7.10), more rapid decline of vapour concentrations (Figures 7.1, 7.3 and 7.5b), greater microbial cell numbers after 24 days (Figure 7.11) and greater CO_2 production (Figure 7.7). Similar to the previous observation it appears that toluene degradation is delayed in batches with the E10 mixture, although by a much shorter period of about 2 days as shown in Figure 7.14. Calculated biomass doubling times were 3.8, 3.8 and 3.9 days for PP, E10 and B20 respectively, which is 2.4, 2.6 and 1.8 times faster than without inorganic nutrient addition for PP, E10 and B20 respectively.

Assuming complete degradation to CO_2, the average calculated yield (g cell C per g petroleum or biofuel C degraded) was 0.37 ± 0.18 for batches with the PP mixture, 0.35 ± 0.04 for batches with E10 mixture and 0.27 ± 0.08 for batches with B20 mixture, which is comparable for all three mixtures and somewhat lower than without nutrient addition.

A DGGE analysis for the batch experiments is presented in Figure 7.12. The similarity express as dice coefficients was > 40 % and the NMDS plot Figure -7.13 shows large differences in the similarity of bacterial communities between nutrient amended and unamended treatments.

These data suggest that addition of inorganic nutrient in the presence or absence of biofuel have resulted in a significant shift in the bacterial community structure. The NMDS and cluster analysis demonstrate that replicate similarities were generally high. ANOSIM analysis in Table -7-4 indicated that similarities in bacterial community structures among different treatments were greater than within treatments (i.e. between replicates; generally > 60% similarity) ($P < 0.001$).

Overall, there was a statistically significant difference in the similarity between the bacterial communities from the different treatments/batches (ANOSIM $p < 0.001$). Figure -7.13, illustrates the Bray-Curtis similarities between bacterial communities in a plot where the proximity of the data points reflects the degree of similarity between samples.

The results of the study revealed a significant shift in bacterial community structure up on fuel treatment and nutrient-amendment ($r_s \leqslant 1$, $P < 0.1$) Table -7-4.

Petroleum hydrocarbon degradation appeared to be associated with the presence and appearance of a predominant strong band in PP, E10 and B20 batches, which was less prominent in control batches (framed by the rectangle in Figure 7.12).

This band was identified by sequencing as belonging to the genus of *Pseudomonas*. Without nutrient addition, microbial communities from batches containing a biofuel component are characterized by additional and/or stronger bands in the DGGE gels compared to the control and PP batches. The strength of these bands was most intense in microbial communities from batches with E10 (highlighted by the oval in Figure 7.12). The additional strong bands would likely be linked to species growing on the biofuels. These changes in microbial community structure are associated with the slower degradation of toluene and m-xylene in the presence of ethanol, consistent with the observations of DaSilva et al. (Da Silva and Alvarez, 2002), and also biodiesel. These data suggest that the presence of the biofuels result in the growth of biofuel-degraders and reduced degradation of BTEX rather than a reduced rate of BTEX degradation per cell of BTEX degrader per se (Lovanh et al., 2002) which would not have resulted in the observed differences in the presence and intensities of different bands in the DGGE gel.

Addition of inorganic nutrients allowed more petroleum hydrocarbon biodegradation to occur, and the most intense band in the community analysis of nutrient amended batches is therefore the same for the PP, E10 and B20

mixtures (framed by the rectangle Figure 7.12, although some additional strong bands remain notable for the B20 mixture, likely because biodiesel is not degraded as rapidly as ethanol.

8.3 Answering the specific research questions

1 What is the impact of ethanol and biodiesel on the biodegradation rate of the petroleum hydrocarbons in aerobic soil?

From the headspace concentration plots of the mini-lysimeter experiments, toluene data clearly demonstrate that addition of either ethanol or biodiesel may delay the biodegradation of this compound. Furthermore, a significant difference in the vapour-phase concentrations profiles in Figure 6.1 and Figure 6.5 can be seen between PP and B20 from the concentration scales, probably reflecting the fact that the mole fraction of the petroleum hydrocarbons was lower for the B20 mixture and biodiesel was more slowly degraded or volatilized than ethanol.

It should be noted that the increasing of the vapour-phase concentration of the VOCs in E10 mixture could possibly also be due to a change in the volatilization. Joice and coworkers (Jóice et al., 2009) who evaluated the (BTX) volatilization have reported that ethanol may decrease the volatilization of benzene in a gasoline-ethanol column, but concentrations of toluene and xylenes in the vapour-phase of the gasoline-ethanol column increase drastically. Cataluna and Silva (Cataluña and Silva, 2006) determined the vapour pressure and vaporization enthalpy of formulations containing of 5, 15, and 25% of ethanol in four phase gasolines. Their results demonstrated that the addition of ethanol to the gasoline hydrocarbons generates a mixture with a boiling point lower than that of the original mixture (Cataluña and Silva, 2006).

2 What are the biodegradation rates of aerobic micro-organisms degrading VOCs in the presence of ethanol and biodiesel?

Biodegradation of fuel compounds to CO_2 started without a significant lag phase. For the E10 system with highest value observed in E10 mixture at day 8 much higher than the initial CO_2 concentration in the B20 mixture system and the PP mixture system. CO_2 and O_2 data clearly indicate active biodegradation and these findings agree with the finding of Hohener et al. (2006) in a field experiment where CO_2 increase and O_2 depletion was clearly indicating the active biodegradation process around the source zone. The initial spike in CO_2 produced in the E10 mixture above the levels observed for the B20 and PP fuel mixtures suggested that the amount of initial CO_2 was mainly generated from ethanol, whereas biodiesel and VOC mineralization was slower. Moreover, ethanol was completely degraded in the E10 mixture with 100% disappearance on day 18. It is interesting to note from Figure 6.8 that the initial CO_2 production was in good agreement with EtOH depletion, confirming that the initial CO_2 production in E10 mixture was mainly from EtOH mineralization, rather than VOCs mineralization in comparison with the CO_2 plots of the control, PP and B20 which can be seen in Figure 6.7. Toluene data suggests that in the presence of readily biodegradable compounds such as ethanol and biodiesel biodegradation of VOCs is slower. It has been reported by Osterreicher-Cunha and coworkers that natural attenuation of gasoline compounds in undisturbed soil took longer when gasoline was introduced with ethanol, and more BTEX were retained in unsaturated soil (Osterreicher-Cunha et al., 2009). The vapour-phase concentration of toluene in PP, E10 and B20 mixtures in the mini-lysimeter experiment Figure 6.15 suggest that the addition of ethanol and biodiesel inhibit the biodegradation of toluene.

3 How strongly are the VOCs absorbed by soil?

From the measured sorption-coefficient values (K_d) in Table 5-1, it can be seen that the aliphatic alkanes have a higher K_d values in comparison with the monoaromatics values. However, within the same aliphatic VOCs family, it could be noted that the K_d values of the normal alkanes are somewhat higher than

the cyclo alkanes. From the K_d values, it could be noted that the aliphatic VOCs are more hydrophobic than the monoaromatics. In general it can be concluded that the sorption of the VOCs are in the order of n-alkanes > cyclo-alkanes > monoaromatics, as a result the monoaromatics will least strongly adsorbed by soil, then the cylco-alkanes and finally the n-alkanes.

4 How easily are the VOCs to evaporate from the soil?

From the vapour-phase concentration of the PP, E10 and B20 for the mini-lysimeter experiments Figure 6.1, Figure 6.3 and Figure 6.5 respectively, it can be shown that the rate of most of the aliphatic VOCs volatilization was similar for both PP and E10, however due to the higher volume percentage and slower degradation of biodiesel constituents VOCs volatilization in B20 was more strongly affected by the presence of biodiesel, Figure 6.5, and the volatilization of the monoaromatics in the three mixtures where somewhat different between each other, Figure 6.2, Figure 6.4 and Figure 6.6.

5 How strongly does the addition of ethanol and biodiesel affect the natural attenuation of small petroleum hydrocarbon spills in the unsaturated zone?

The whole data suggests that when fuel was introduced blended with either ethanol or biodiesel, monoaromatics may persist longer in aerobic, unsaturated soil as also suggested by Osterreicher-Cunha (2009), and natural attenuation of fuel compounds may take longer, as shown by the mentioned chemical analyses of vapours and residues. However, towards the end of both mini-lysimeter and batch studies, NAPL residuals were generally comparable for PP, E10 and B20 mixtures when comparing the percentage of the added petroleum hydrocarbon mass remaining in the soil, and lower when comparing the absolute residual petroleum hydrocarbon mass. These findings are in a satisfactory agreement with Capiro et al. (2008) who have studied the microbial community response to net ethanol release and their overall observation was that growth of hydrocarbon degraders led to an enhancement in aerobic natural

attenuation in shallow aquifers after ethanol and its degradation by-products are degraded or flushed from sites impacted by ethanol-blended fuels (Capiro et al., 2008).

6 Are microorganisms degrading the biofuel component different species from those degrading petroleum hydrocarbons?

The literature has shown some agreement with our findings about the microbial communities responsible for degrading VOCs. A study has shown that three hydrocarbon-degrading psychrotrophic bacteria were isolated from petroleum-contaminated Arctic soils and characterized, and two strains, identified as *Pseudomonas spp.*, degraded C-5 to C-12 n-alkanes, and toluene (Whyte et al., 1997). Another study has been conducted by Stapleton et al. (2000) and concluded that based on 16S rDNA sequence analysis, of 26 isolates were obtained from vapour-plate enrichment technique with the volatile aromatic hydrocarbons (BTEX) and JP-4 jet fuel, were phylogenetically similar to common soil microorganisms, including members of the genera *Pseudomonas* Ralstonia, Burkholderia, Sphingomonas, Flavobacteria, and Bacillus (Stapleton et al., 2000). Lovanh and Alvarez. (2004) have investigated the effect of ethanol on toluene degradation activity. Their findings have shown that toluene metabolic flux (defined as toluene utilization rate per cell) decreased with increasing influent concentrations of ethanol. Thus increasing concentrations of alternative carbon sources "dilute" the metabolic flux of toluene (Lovanh and Alvarez, 2004). Finally, Capiro et al. (2008) have studied the microbial community response to a neat ethanol (E100) onto residual hydrocarbons in sandy soil, their results illustrate that proliferation of *Azospirillum* and *Brevundimonas spp.*, which are bacteria commonly associated with microaerophilic hydrocarbon degradation.

Our findings and the methods showed satisfactory agreement and revealed *Pseudomonas* to be the most dominant microorganism growing on the VOCs mixture. The banding pattern in DGGE gels suggests that the presence of the biofuels stimulated growth of biofuel-degraders and reduced degradation of

BTEX rather than a reduced rate of BTEX degradation per cell of BTEX degrader per se which would not have resulted in the observed differences in the presence and intensities of different bands in the DGGE gel.

A long-term impact was observed in the microbial community structure, which was distinct for each mixture after 92 days at the end of the mini-lysimeter study, even though ethanol seems to have disappeared from the mini-lysimeter with the E10 mixture by day 18.

7 Is competition for inorganic nutrients a potential explanation for the inhibition of petroleum hydrocarbon degradation in aerobic soil?

The experimental observations in the batch and mini-lysimeter experiments show an initial inhibition of toluene and m-xylene biodegradation during ethanol biodegradation and, to a lesser extent, biodiesel degradation. After addition of inorganic nutrients toluene degradation was still delayed when comparing the E10 with the PP mixture, but for a much shorter period. Furthermore, the band intensities in the DGGE gel of the batch studies indicate that additional strong bands in the E10 samples from batches without nutrient addition were likely linked to species growing on the biofuels. With nutrient addition these bands were less intense and the most intense band in the community analysis of nutrient amended batches on day 24 was the same for the PP, E10 and B20 mixtures. It is concluded that a delay in the degradation of monoaromatic compounds in the presence of biofuel is likely because of competition of distinct microbial communities associated with the biofuel component degradation for scarce inorganic nutrients limiting the growth of petroleum hydrocarbon degrading biomass. Kaufmann et al. (2004) have investigated the influence of petroleum hydrocarbons on a microbial community in the vadose zone in nutrient-poor glacial water sand under field conditions, their findings concluded that, at the nutrient-poor site, the microbial community was dominant by natural heterogeneity and that the influence of petroleum hydrocarbon vapours was weak.

8 Are blended fuels containing a biofuel component a lesser or greater environmental risk than pure petroleum when small spills are retained in the unsaturated zone?

The vapour-phase concentration profile of toluene in PP, E10 and B20 in the mini-lysimeter experiment shown in Figure 6.15, and the vapour-phase concentration profile of toluene in PP, E10 and B20 mixtures for nutrient unamended batches in Figure 7.14 (a) and nutrient amended batches in Figure 7.14 (b) show that there is a significant lag phase for the biodegradation time between toluene in PP and its biodegradation time in the other two mixtures. While this inhibition of BTEX biodegradation in soils polluted with a mixture of petroleum and biofuels may imply an increased groundwater pollution risks for small spill scenarios, the percentage of each petroleum hydrocarbon added which remained at the end of the experiments was comparable for all three mixtures in both the batch and mini-lysimeter experiments with the exception of only m-xylene. For fuel spills retained in the unsaturated zone under aerobic conditions, the impact of the biofuel component will likely depend on the amount of fuel spilled, the distance between the fuel spill and receptors, and the availability of inorganic nutrients in between the source and the receptors.

8.4 Overall conclusions

The work has provided valuable information regarding the effect of biofuel components on the biodegradation of the fuel VOCs in the unsaturated zone. At the same time, significant data related to the biodegradation of the biofuel components have been provided. Using data from the well designed laboratory batch and mini-lysimeter experiments and the use of multi-disciplinary assessments allowed for board comparison of VOCs constituents fate, transport, biodegradation, biomass and microbial diversity. Understandably the selection of a biofuel additive (ethanol or biodiesel) will not based on aerobic biodegradation alone, but the presented work can provide an additional resource for the literature and decision makers.

To our knowledge, the present work is the first reporting measurements of volatilization, NAPLs residual, CO_2 and O_2, attenuation distance from a source zone, total cell counts, and DGGE analysis of the mentioned fuel constituents and the effect of ethanol and biodiesel addition on the fate and transport of these VOCs in the subsurface, in the presence and absence of inorganic nutrients, applying two different experimental systems, laboratory sand mini-lysimeters and batches. Joice et al. (2009) reported similar gas phase concentrations of (BTX), evaluating the (BTX) volatilization. However, beside the presence of ethanol, other aspects concerning the (BTX) volatilization, such as adsorption on the sand grains and biodegradation, have not been addressed.

8.5 Future prospects

Given the wide-spread use of blended fuels containing a biofuel component, the microbiology of their degradation in soils should be further investigated to inform risk assessments and remediation decisions at impacted sites. Still, additional and advanced chemical analyses are necessary to better evaluate contaminants residue in soil.

Expanding the present study one should look at the whole BTEX group including the xylenes isomers, and the study could be repeated under the same conditions, to study the electron acceptors limitation, under anaerobic conditions.

The information obtained in this work will be the starting point for the design of quantitative molecular and chemical tools to further analyse the abundance and dynamics of these fuel hydrocarbon and biofuel-degrading bacterial populations in the soil and groundwater environments, and focusing on the microbial diversity under different conditions.

Literature Cited

(2001a) *Introduced to the U.S. Senate on May 15th.* Harkin, T.: (S.892)

(2001b) *Introduced to U.S. Senate on February 6.* Fitzgerald, P.: (S.265)

Abu-El-Sha'r Wa'il, Y. (2006) 'Gaseous Transport Mechanisms in Unsaturated Systems: Estimation of Transport Parameters', in *Remediation of Hazardous Waste in the Subsurface.* Washington, DC: American Chemical Society, pp. 175-200.

Adam, G., Gamoh, K., Morris, D. G. and Duncan, H. (2002) 'Effect of alcohol addition on the movement of petroleum hydrocarbon fuels in soil', *Science of the Total Environment,* 286, (1-3), pp. 15-25.

Allen-King, R. M., Barker, J. F., Gillham, R. W. and Jensen, B. K. (1994) 'Substrate- and nutrient-limited toluene biotransformation in sandy soil', *Environmental Toxicology and Chemistry,* 13, (5), pp. 693-705.

AllenKing, R. M., Gillham, R. W., Barker, J. F. and Sudicky, E. A. (1996) 'Fate of dissolved toluene during steady infiltration through unsaturated soil .2. Biotransformation under nutrient-limited conditions', *Journal of Environmental Quality,* 25, (2), pp. 287-295.

Altschul, S. F., Madden, T. L., Schaffer, A. A., Zhang, J. H., Zhang, Z., Miller, W. and Lipman, D. J. (1997) 'Gapped BLAST and PSI-BLAST: a new generation of protein database search programs', *Nucleic Acids Research,* 25, (17), pp. 3389-3402.

Alvarez, P. J. J. and Hunt, C. S. (2002) 'The effect of fuel alcohol on monoaromatic hydrocarbon biodegradation and natural attenuation', *Revista Latinoamericana de Microbiologia,* 44, (2), pp. 83-104.

Andre, L., Kedziorek, M. A. M., Bourg, A. C. M., Haeseler, F. and Blanchet, D. (2009) 'A novel experimental procedure to investigate the biodegradation of NAPL under unsaturated conditions', *Journal of Hydrology,* 370, (1-4), pp. 1-8.

Aon, M. A., Sarena, D. E., Burgos, J. L. and Cortassa, S. (2001) 'Interaction between gas exchange rates, physical and microbiological properties in soils recently subjected to agriculture', *Soil and Tillage Research,* 60, (3-4), pp. 163-171.

Atlas, R. M. (1981) 'Microbial degradation of petroleum hydrocarbons: an environmental perspective', *Microbiol. Mol. Biol. Rev.,* 45, (1), pp. 180-209.

Atlas, R. M. (1995) 'Bioremediation of petroleum pollutants', *International Biodeterioration & Biodegradation,* 35, (1-3), pp. 317-327.

Atlas, R. M. and Philp, J. (2005) *Bioremediation : applied microbial solutions for real-world environmental cleanup.* Washington, D.C.: ASM press.

Autry, A. R. and Ellis, G. M. (1992) 'BIOREMEDIATION - AN EFFECTIVE REMEDIAL ALTERNATIVE FOR PETROLEUM HYDROCARBON-CONTAMINATED SOIL', *Environmental Progress,* 11, (4), pp. 318-323.

Baehr, A. L. and Baker, R. J. (1995) 'Use of a Reactive Gas Transport Model to Determine Rates of Hydrocarbon Biodegradation in Unsaturated Porous Media', *Water Resources Research,* 31, (11), pp. 2877-2882.

Baehr, A. L., Stackelberg, P. E. and Baker, R. J. (1999) 'Evaluation of the Atmosphere as a Source of Volatile Organic Compounds in Shallow Groundwater', *Water Resources Research,* 35, (1), pp. 127-136.

Baker, R. J., Baehr, A. L. and Lahvis, M. A. (2000) 'Estimation of hydrocarbon biodegradation rates in gasoline-contaminated sediment from measured respiration rates', *Journal of Contaminant Hydrology,* 41, (1-2), pp. 175-192.

Bay, K., Wanko, H. and Ulrich, J. (2006) 'Absorption of volatile organic compounds in biodiesel: Determination of infinite dilution activity coefficients by headspace gas chromatography', *Chemical Engineering Research & Design,* 84, (A1), pp. 22-28.

Boopathy, R. (2000) 'Factors limiting bioremediation technologies', *Bioresource Technology,* 74, (1), pp. 63-67.

Borresen, M. H. and Rike, A. G. (2007) 'Effects of nutrient content, moisture content and salinity on mineralization of hexadecane in an Arctic soil', *Cold Regions Science and Technology,* 48, (2), pp. 129-138.

Brook, T. R., Stiver, W. H. and Zytner, R. G. (2001) 'Biodegradation of diesel fuel in soil under various nitrogen addition regimes', *Soil & Sediment Contamination,* 10, (5), pp. 539-553.

Brusseau, M. L. (1991) 'TRANSPORT OF ORGANIC-CHEMICALS BY GAS ADVECTION IN STRUCTURED OR HETEROGENEOUS POROUS-MEDIA - DEVELOPMENT OF A MODEL AND APPLICATION TO COLUMN EXPERIMENTS', *Water Resources Research,* 27, (12), pp. 3189-3199.

Cairney, T. and Hobson, D. M. (1998) *Contaminated land : problems and solutions.*2nd ed London ; New York: E & FN Spon.

CANNON, G., RICE, D. (1999) *Potential ground and surface water impacts.* Iowa city, university of Iowa. URCL-AR-135949

Capiro, N. L., Da Silva, M. L. B., Stafford, B. P., Rixey, W. G. and Alvarez, P. J. J. (2008) 'Microbial community response to a release of neat ethanol onto residual hydrocarbons in a pilot-scale aquifer tank', *Environmental Microbiology,* 10, (9), pp. 2236-2244.

Cápiro, N. L., Stafford, B. P., Rixey, W. G., Bedient, P. B. and Alvarez, P. J. J. (2007) 'Fuel-grade ethanol transport and impacts to groundwater in a pilot-scale aquifer tank', *Water Research,* 41, (3), pp. 656-664.

Cataluña, R. and Silva, R. (2006) 'Development of a device to valuate the effect of ethanol on the vapor pressure and vaporization enthalpy of fuel gasolines', *Desenvolvimento de um equipamento para avaliação do efeito do etanol na*

pressão de vapor e entalpia de vaporização em gasolinas automotivas, 29, (3), pp. 580-585.

Chan, W. C. and You, H. Y. (2010) 'The influence of nonionic surfactant Brij 30 on biodegradation of toluene in a biofilter', *African Journal of Biotechnology,* 9, (36), pp. 5914-5921.

Chang, Z. Z., Weaver, R. W. and Rhykerd, R. L. (1996) 'Oil bioremediation in a high and a low phosphorus soil', *Journal of Soil Contamination,* 5, (3), pp. 215-224.

Chen, Y. M., Abriola, L. M., Alvarez, P. J. J., Anid, P. J. and Vogel, T. M. (1992) 'Modeling Transport and Biodegradation of Benzene and Toluene in Sandy Aquifer Material - Comparisons with Experimental Measurements', *Water Resources Research,* 28, (7), pp. 1833-1847.

Chiou, C. T., Porter, P. E. and Schmedding, D. W. (1983) 'Partition equilibriums of nonionic organic compounds between soil organic matter and water', *Environ. Sci. Technol.,* 17, (4), pp. 227-231.

Christophersen, M., Broholm, M. M., Mosbaek, H., Karapanagioti, H. K., Burganos, V. N. and Kjeldsen, P. (2005) 'Transport of hydrocarbons from an emplaced fuel source experiment in the vadose zone at Airbase Vaerlose, Denmark', *Journal of Contaminant Hydrology,* 81, (1-4), pp. 1-33.

Clarke K.R, W. R. M. (2001) *Change in Marine Communities: An Approach to Statistical Analysis and Interpretation, 2nd edition.*

Cocolin, L., Manzano, M., Cantoni, C. and Comi, G. (2001) 'Denaturing gradient gel electrophoresis analysis of the 16S rRNA gene V1 region to monitor dynamic changes in the bacterial population during fermentation of Italian sausages', *Applied and Environmental Microbiology,* 67, (11), pp. 5113-5121.

Cole, J. R., Chai, B., Farris, R. J., Wang, Q., Kulam, S. A., McGarrell, D. M., Garrity, G. M. and Tiedje, J. M. (2005) 'The Ribosomal Database Project (RDP-II): sequences and tools for high-throughput rRNA analysis', *Nucleic Acids Research,* 33, (suppl 1), pp. D294-D296.

Conant, B. H., Gillham, R. W. and Mendoza, C. A. (1996) 'Vapor transport of trichloroethylene in the unsaturated zone: Field and numerical modeling investigations', *Water Resources Research,* 32, (1), pp. 9-22.

Corseuil, H. X., Aires, J. R. and Alvarez, P. J. J. (1996) 'Implications of the presence of ethanol on intrinsic bioremediation of BTX plumes in Brazil', *Hazardous Waste & Hazardous Materials,* 13, (2), pp. 213-221.

Corseuil, H. X. and Alvarez, P. J. J. (1996) 'Natural bioremediation of aquifer material contaminated with gasoline-ethanol mixtures', *Revista De Microbiologia,* 27, (1), pp. 19-26.

Corseuil, H. X., Kaipper, B. I. A. and Fernandes, M. (2004) 'Cosolvency effect in subsurface systems contaminated with petroleum hydrocarbons and ethanol', *Water Research,* 38, (6), pp. 1449-1456.

Coulon, F., Pelletier, E., Gourhant, L. and Delille, D. (2005) 'Effects of nutrient and temperature on degradation of petroleum hydrocarbons in contaminated sub-Antarctic soil', *Chemosphere,* 58, (10), pp. 1439-1448.

Crawford, R. L. and Crawford, D. L. (1996) *Bioremediation : principles and applications.* Cambridge ; New York: Cambridge University Press.

Da Silva, M. and Alvarez, P. J. (2002) 'Effects of ethanol versus MTBE on benzene, toluene, ethylbenzene, and xylene natural attenuation in aquifer columns', *J. Environ. Eng. ASCE,* 128, (9), pp. 862-867.

Dakhel, N., Pasteris, G., Werner, D. and Hohener, P. (2003) 'Small-Volume Releases of Gasoline in the Vadose Zone: Impact of the Additives MTBE and Ethanol on Groundwater Quality', *Environ. Sci. Technol.,* 37, (10), pp. 2127-2133.

Deeb, R. A., Chu, K. H., Shih, T., Linder, S., Suffet, I., Kavanaugh, M. C. and Alvarez-Cohen, L. (2003) 'MTBE and other oxygenates: Environmental sources, analysis, occurrence, and treatment', *Environmental Engineering Science,* 20, (5), pp. 433-447.

Defra. (2008) *Future water: The government's water strategy for England.* Department for Environment Food and Rural Affairs

Demeestere, K., Dewulf, J., De Roo, K., De Wispelaere, P. and Van Langenhove, H. (2008) 'Quality control in quantification of volatile organic compounds analysed by thermal desorption-gas chromatography-mass spectrometry', *Journal of Chromatography A,* 1186, (1-2), pp. 348-357.

DeMello, J. A., Carmichael, C. A., Peacock, E. E., Nelson, R. K., Arey, J. S. and Reddy, C. M. (2007) 'Biodegradation and environmental behavior of biodiesel mixtures in the sea: An initial study', *Marine Pollution Bulletin,* 54, (7), pp. 894-904.

Di Serio, M., Cozzolino, M., Tesser, R., Patrono, P., Pinzari, F., Bonelli, B. and Santacesaria, E. (2007) 'Vanadyl phosphate catalysts in biodiesel production', *Applied Catalysis a-General,* 320, pp. 1-7.

Durmusoglu, E., Taspinar, F. and Karademir, A. (2010) 'Health risk assessment of BTEX emissions in the landfill environment', *Journal of Hazardous Materials,* 176, (1-3), pp. 870-877.

EA (2010) *Oil pollution*. Available at: http://www.environment-agency.gov.uk/research/library/position/41233.aspx (Accessed: 06.05).

English, C. W. and Loehr, R. C. (1991) 'Degradation of organic vapors in unsaturated soils', *Journal of Hazardous Materials,* 28, (1-2), pp. 55-64.

Environmental Agency, U. K. (2003) *Principles for Evaluating the Human Health Risks from Petroleum Hydrocarbons in Soils: A Consultant Paper.*

Environmental Agency, U. K. (2006) 'Environmental Protection Acr 1990: Part IIA Contaminated Land'.

Evelyn, J., Macaulay, R. and National smoke abatement society. (1933) *Fumifugium, or, The inconvenience of the aer and smoake of London dissipated.* Manchester: The National smoke abatement society.

Fallgren, P. H. and Jin, S. (2008) 'Biodegradation of petroleum compounds in soil by a solid-phase circulating bioreactor with poultry manure amendments', *Journal of Environmental Science and Health Part a-Toxic/Hazardous Substances & Environmental Engineering,* 43, (2), pp. 125-131.

Falta, R. W., Javandel, I., Pruess, K. and Witherspoon, P. A. (1989) 'Density-Driven Flow of Gas in the Unsaturated Zone Due to the Evaporation of Volatile Organic-Compounds', *Water Resources Research,* 25, (10), pp. 2159-2169.

Fan, C., Wang, G.-S., Chen, Y.-C. and Ko, C.-H. (2009) 'Risk assessment of exposure to volatile organic compounds in groundwater in Taiwan', *Science of the Total Environment,* 407, (7), pp. 2165-2174.

Felizardo, P., Baptista, P., Uva, M. S., Menezes, J. C. and Correia, M. J. N. (2007) 'Monitoring biodiesel fuel quality by near infrared spectroscopy', *Journal of near Infrared Spectroscopy,* 15, (2), pp. 97-105.

Ferguson, S. H., Franzmann, P. D., Revill, A. T., Snape, I. and Rayner, J. L. (2003) 'The effects of nitrogen and water on mineralisation of hydrocarbons in diesel-contaminated terrestrial Antarctic soils', *Cold Regions Science and Technology,* 37, (2), pp. 197-212.

Ferris, M. J., Muyzer, G. and Ward, D. M. (1996) 'Denaturing gradient gel electrophoresis profiles of 16S rRNA-defined populations inhabiting a hot spring microbial mat community', *Appl. Environ. Microbiol.,* 62, (2), pp. 340-346.

Franzmann, P. D., Robertson, W. J., Zappia, L. R. and Davis, G. B. (2002) 'The role of microbial populations in the containment of aromatichydrocarbons in the subsurface', *Biodegradation,* 13, (1), pp. 65-78.

Franzmann, P. D., Zappia, L. R., Power, T. R., Davis, G. B. and Patterson, B. M. (1999) 'Microbial mineralisation of benzene and characterisation of microbial biomass in soil above hydrocarbon-contaminated groundwater', *Fems Microbiology Ecology,* 30, (1), pp. 67-76.

Freijer, J. I., Jonge, H., Bouten, W. and Verstraten, J. M. (1996) 'Assessing mineralization rates of petroleum hydrocarbons in soils in relation to environmental factors and experimental scale', *Biodegradation,* 7, (6), pp. 487-500.

Frind, E. O., Duynisveld, W. H. M., Strebel, O. and Boettcher, J. (1990) 'MODELING OF MULTICOMPONENT TRANSPORT WITH MICROBIAL TRANSFORMATION IN GROUNDWATER - THE FUHRBERG CASE', *Water Resources Research,* 26, (8), pp. 1707-1719.

Frondel, M. and Peters, J. (2007) 'Biodiesel: A new Oildorado?', *Energy Policy,* 35, (3), pp. 1675-1684.

Fry, J. C. (1990) 'Direct methods and biomass estimation', *Methods in Microbiology,* 22, pp. 41-85.

Gaganis, P. and Burganos, V. N. (2002) 'Modeling transport of VOC mixtures using composite constituents', in Hassanizadeh, S. M., Schotting, R. J., Gray, W. G. and Pinder, G. F.(eds) *Computational Methods in Water Resources, Vols 1 and 2, Proceedings.* Vol. 47 Amsterdam: Elsevier Science Bv, pp. 185-192.

Gaganis, P., Karapanagioti, H. K. and Burganos, V. N. (2002) 'Modeling multicomponent NAPL transport in the unsaturated zone with the constituent averaging technique', *Advances in Water Resources,* 25, (7), pp. 723-732.

Gierke, J. S., Hutzler, N. J. and McKenzie, D. B. (1992) 'VAPOR TRANSPORT IN UNSATURATED SOIL COLUMNS - IMPLICATIONS FOR VAPOR EXTRACTION', *Water Resources Research,* 28, (2), pp. 323-335.

Godon, J. J., Zumstein, E., Dabert, P., Habouzit, F. and Moletta, R. (1997) 'Molecular microbial diversity of an anaerobic digestor as determined by small-subunit rDNA sequence analysis', *Appl. Environ. Microbiol.,* 63, (7), pp. 2802-2813.

Grathwohl, P., Klenk, I. D., Maier, U. and Reckhorn, S. B. F. (2002) 'Natural attenuation of volatile hydrocarbons in the unsaturated zone and shallow groundwater plumes: scenario-specific modelling and laboratory experiments', *Groundwater Quality: Natural and Enhanced Restoration of Groundwater Pollution,* (275), pp. 141-146.

Gray, N., Sherry, A., Larter, S., Erdmann, M., Leyris, J., Liengen, T., Beeder, J. and Head, I. (2009) 'Biogenic methane production in formation waters from a large gas field in the North Sea', *Extremophiles,* 13, (3), pp. 511-519.

Guo, Y. S., Zhong, J., Xing, Y., Li, D. and Lin, R. S. (2007) 'Volatility of blended fuel of biodiesel and ethanol', *Energy & Fuels,* 21, (2), pp. 1188-1192.

Halstead, T. and Ebooks Corporation. (1998) *Contaminated Land : Problems and solutions.*2nd ed London: Spon Press.

Hama, S., Yamaji, H., Fukumizu, T., Numata, T., Tamalampudi, S., Kondo, A., Noda, H. and Fukuda, H. (2007) 'Biodiesel-fuel production in a packed-bed reactor using lipase-producing Rhizopus oryzae cells immobilized within biomass support particles', *Biochemical Engineering Journal,* 34, (3), pp. 273-278.

Hansen, A. C., Zhang, Q. and Lyne, P. W. L. (2005) 'Ethanol-diesel fuel blends - a review', *Bioresource Technology,* 96, (3), pp. 277-285.

Haritash, A. K. and Kaushik, C. P. (2009) 'Biodegradation aspects of Polycyclic Aromatic Hydrocarbons (PAHs): A review', *Journal of Hazardous Materials,* 169, (1-3), pp. 1-15.

Harley, R. A., Coulter-Burke, S. C. and Yeung, T. S. (2000) 'Relating Liquid Fuel and Headspace Vapor Composition for California Reformulated Gasoline Samples Containing Ethanol', *Environ. Sci. Technol.,* 34, (19), pp. 4088-4094.

He, B. Q., Shuai, S. J., Wang, J. X. and He, H. (2003) 'The effect of ethanol blended diesel fuels on emissions from a diesel engine', *Atmospheric Environment,* 37, (35), pp. 4965-4971.

Head, I. M., Saunders, J. R. and Pickup, R. W. (1998) 'Microbial evolution, diversity, and ecology: A decade of ribosomal RNA analysis of uncultivated microorganisms', *Microbial Ecology,* 35, (1), pp. 1-21.

Herbert, R. A., Grigorova, R. and Norris, J. R. (1990) '1 Methods for Enumerating Microorganisms and Determining Biomass in Natural Environments', in *Methods in Microbiology.* Vol. Volume 22 Academic Press, pp. 1-39.

Hestor, R. E. and Harrison, R. M. (1997) 'Contaminated Land and its Reclamation', in Royal Society of Chemistry.

Hill, J., Nelson, E., Tilman, D., Polasky, S. and Tiffany, D. (2006) 'Environmental, economic, and energetic costs and benefits of biodiesel and ethanol biofuels', *Proceedings of the National Academy of Sciences of the United States of America,* 103, (30), pp. 11206-11210.

Hinchee, R. E., Fredrickson, J. and Alleman, B. C. (1995a) *Bioaugmentation for site remediation.* Columbus: Battelle Press.

Hinchee, R. E., Kittel, J. A. and Resinger, H. J. (1995b) *Applied of Bioremediation of Petroleum Hydrocarbns.* Columbus, Ohio: Battelle Memorial Institute.

Hohener, P., Dakhel, N., Christophersen, M., Broholm, M. and Kjeldsen, P. (2006) 'Biodegradation of hydrocarbons vapors: Comparison of laboratory studies and field investigations in the vadose zone at the emplaced fuel source experiment, Airbase Vaerlose, Denmark', *Journal of Contaminant Hydrology,* 88, (3-4), pp. 337-358.

Hohener, P., Duwig, C., Pasteris, G., Kaufmann, K., Dakhel, N. and Harms, H. (2003) 'Biodegradation of petroleum hydrocarbon vapors: laboratory studies on rates and kinetics in unsaturated alluvial sand', *Journal of Contaminant Hydrology,* 66, (1-2), pp. 93-115.

Hunt, C. S., Alvarez, P. J. J., Ferreira, R. D. and Corseuil, H. X. (1997) 'Effect of ethanol on aerobic BTX degradation', *In Situ and on-Site Bioremediation, Vol 1,* 4(1), pp. 49-54.

Hutchins, S. R. (1997) 'Effects of microcosm preparation on rates of toluene biodegradation under denitrifying conditions', *Journal of Industrial Microbiology & Biotechnology,* 18, (2-3), pp. 170-176.

Issariyakul, T., Kulkarni, M. G., Dalai, A. K. and Bakhshi, N. N. (2007) 'Production of biodiesel from waste Eryer grease using mixed methanol/ethanol system', *Fuel Processing Technology,* 88, (5), pp. 429-436.

Jassal, R. S., Black, T. A., Drewitt, G. B., Novak, M. D., Gaumont-Guay, D. and Nesic, Z. (2004) 'A model of the production and transport of CO2 in soil: predicting

soil CO2 concentrations and CO2 efflux from a forest floor', *Agricultural and Forest Meteorology*, 124, (3-4), pp. 219-236.

Jean, J.-S., Lee, M.-K., Wang, S.-M., Chattopadhyay, P. and Maity, J. P. (2008) 'Effects of inorganic nutrient levels on the biodegradation of benzene, toluene, and xylene (BTX) by Pseudomonas spp. in a laboratory porous media sand aquifer model', *Bioresource Technology*, 99, (16), pp. 7807-7815.

Jin, F. M., Kawasaki, K., Kishida, H., Tohji, K., Moriya, T. and Enomoto, H. (2007) 'NMR spectroscopic study on methanolysis reaction of vegetable oil', *Fuel*, 86, (7-8), pp. 1201-1207.

Jin, Y., Streck, T. and Jury, W. A. (1994) 'Transport and biodegradation of toluene in unsaturated soil', *Journal of Contaminant Hydrology*, 17, (2), pp. 111-127.

Jóice, C., Francieli, F., Alexandra Rodrigues, F., Cláudia Echevenguá, T. and Irajá do Nascimento, F. (2009) 'Volatilization of monoaromatic compounds (benzene, toluene, and xylenes; BTX) from gasoline: Effect of the ethanol', *Environmental Toxicology and Chemistry*, 29, (4), pp. 808-812.

Jury, W. A., Russo, D., Streile, G. and Elabd, H. (1990) 'EVALUATION OF VOLATILIZATION BY ORGANIC-CHEMICALS RESIDING BELOW THE SOIL SURFACE', *Water Resources Research*, 26, (1), pp. 13-20.

Jury, W. A., Spencer, W. F. and Farmer, W. J. (1983) 'Behavior Assessment Model for Trace Organics in Soil: I. Model Description', *J Environ Qual*, 12, (4), pp. 558-564.

Kao, C. M. and Prosser, J. (2001) 'Evaluation of natural attenuation rate at a gasoline spill site', *Journal of Hazardous Materials*, 82, (3), pp. 275-289.

Karapanagioti, H. K., Gaganis, P., Burganos, V. N. and Hohener, P. (2004) 'Reactive transport of volatile organic compound mixtures in the unsaturated zone: modeling and tuning with lysimeter data', *Environmental Modelling & Software*, 19, (5), pp. 435-450.

Karapanagioti, H. K., Gossard, C. M., Strevett, K. A., Kolar, R. L. and Sabatini, D. A. (2001) 'Model coupling intraparticle diffusion/sorption, nonlinear sorption, and biodegradation processes', *Journal of Contaminant Hydrology*, 48, (1-2), pp. 1-21.

Karapanagioti, H. K., Sabatini, D. A. and Bowman, R. S. (2005) 'Partitioning of hydrophobic organic chemicals (HOC) into anionic and cationic surfactant-modified sorbents', *Water Research*, 39, (4), pp. 699-709.

Kaufmann, K., Christophersen, M., Buttler, A., Harms, H. and Hohener, P. (2004) 'Microbial community response to petroleum hydrocarbon contamination in the unsaturated zone at the experimental field site Vaerlose, Denmark', *Fems Microbiology Ecology*, 48, (3), pp. 387-399.

Kennedy, A. C. and Smith, K. L. (1995) 'SOIL MICROBIAL DIVERSITY AND THE SUSTAINABILITY OF AGRICULTURAL SOILS', *Plant and Soil,* 170, (1), pp. 75-86.

Kepner, R. L. and Pratt, J. R. (1994) 'Use of Fluorochromes for Direct Enumeration of Total Bacteria in Environmental-Samples - Past and Present', *Microbiological Reviews,* 58, (4), pp. 603-615.

Kilham, S. S., Kreeger, D. A., Goulden, C. E. and Lynn, S. G. (1997) 'Effects of nutrient limitation on biochemical constituents of Ankistrodesmus falcatus', *Freshwater Biology,* 38, (3), pp. 591-596.

Kowalchuk, G. A., Stephen, J. R., De Boer, W., Prosser, J. I., Embley, T. M. and Woldendorp, J. W. (1997) 'Analysis of ammonia-oxidizing bacteria of the Î² subdivision of the class Proteobacteria in coastal sand dunes by denaturing gradient gel electrophoresis and sequencing of PCR-amplified 16S ribosomal DNA fragments', *Applied and Environmental Microbiology,* 63, (4), pp. 1489-1497.

Kozakowski, G. (2006) 'Biofuels on the EU engine fuels market', *Przemysl Chemiczny,* 85, (12), pp. 1620-1623.

Kulczycki, A. (2006) 'The role of scientific research in the development of biofuels', *Przemysl Chemiczny,* 85, (12), pp. 1576-1578.

Kwanchareon, P., Luengnaruemitchai, A. and Jai-In, S. (2007) 'Solubility of a diesel-biodiesel-ethanol blend, its fuel properties, and its emission characteristics from diesel engine', *Fuel,* 86, (7-8), pp. 1053-1061.

LAHVIS, M. A. (2003) 'Evaluation of Small-Volume Releases of Ethanol-Blended Gasoline at UST Sites', *API Soil and Groundwater Research Bulletin,* 19, pp. 8.

Lahvis, M. A. and Baehr, A. L. (1996) 'Estimation of rates of aerobic hydrocarbon biodegradation by simulation of gas transport in the unsaturated zone', *Water Resources Research,* 32, (7), pp. 2231-2249.

Lahvis, M. A., Baehr, A. L. and Baker, R. J. (1999) 'Quantification of aerobic biodegradation and volatilization rates of gasoline hydrocarbons near the water table under natural attenuation conditions', *Water Resources Research,* 35, (3), pp. 753-765.

Lapinskiene, A., Martinkus, P. and Rebzdaite, V. (2006) 'Eco-toxicological studies of diesel and biodiesel fuels in aerated soil', *Environmental Pollution,* 142, pp. 432-437.

Leahy, J. G. and Colwell, R. R. (1990) 'MICROBIAL-DEGRADATION OF HYDROCARBONS IN THE ENVIRONMENT', *Microbiological Reviews,* 54, (3), pp. 305-315.

Leong, S. T., Muttamara, S. and Laortanakul, P. (2002) 'Applicability of gasoline containing ethanol as Thailand's alternative fuel to curb toxic VOC pollutants from automobile emission', *Atmospheric Environment,* 36, (21), pp. 3495-3503.

Lin, G.-H., Sauer, N. E. and Cutright, T. J. (1996) 'Environmental regulations: A brief overview of their applications to bioremediation', *International Biodeterioration & Biodegradation,* 38, (1), pp. 1-8.

Linn, D. M. and Doran, J. W. (1984) 'EFFECT OF WATER-FILLED PORE-SPACE ON CARBON-DIOXIDE AND NITROUS-OXIDE PRODUCTION IN TILLED AND NONTILLED SOILS', *Soil Science Society of America Journal,* 48, (6), pp. 1267-1272.

Lois, E. (2007) 'Definition of biodiesel', *Fuel,* 86, (7-8), pp. 1212-1213.

Lovanh, N. and Alvarez, P. J. J. (2004) 'Effect of ethanol, acetate, and phenol on toluene degradation activity and tod-lux expression in Pseudomonas putida TOD102: Evaluation of the metabolic flux dilution model', *Biotechnology and Bioengineering,* 86, (7), pp. 801-808.

Lovanh, N., Hunt, C. S. and Alvarez, P. J. J. (2002) 'Effect of ethanol on BTEX biodegradation kinetics: aerobic continuous culture experiments', *Water Research,* 36, (15), pp. 3739-3746.

Madrid, R. E. and Felice, C. J. (2005) 'Microbial Biomass Estimation', *Critical Reviews in Biotechnology,* 25, (3), pp. 97 - 112.

Malik, S., Beer, M., Megharaj, M. and Naidu, R. (2008) 'The use of molecular techniques to characterize the microbial communities in contaminated soil and water', *Environment International,* 34, (2), pp. 265-276.

McDowell, C. J. and Powers, S. E. (2003) 'Mechanisms Affecting the Infiltration and Distribution of Ethanol-Blended Gasoline in the Vadose Zone', *Environmental Science & Technology,* 37, (9), pp. 1803-1810.

Meher, L. C., Sagar, D. V. and Naik, S. N. (2006) 'Technical aspects of biodiesel production by transesterification - a review', *Renewable & Sustainable Energy Reviews,* 10, (3), pp. 248-268.

Mendoza, C. A. and Frind, E. O. (1990) 'ADVECTIVE-DISPERSIVE TRANSPORT OF DENSE ORGANIC VAPORS IN THE UNSATURATED ZONE .1. MODEL DEVELOPMENT', *Water Resources Research,* 26, (3), pp. 379-387.

Miles, R. A. and Doucette, W. J. (2001) 'Assessing the aerobic biodegradability of 14 hydrocarbons in two soils using a simple microcosm/respiration method', *Chemosphere,* 45, (6-7), pp. 1085-1090.

Millington, R. J. and Quirk, J. P. (1961) 'Permeability of porous solids ', *Transactions of the Faraday Society* 57, pp. 1200-1207.

Mitchell, R. (1992) *Environmental microbiology.* New York: Wiley-Liss.

Mohammed, N. and Allayla, R. I. (1997) 'Modeling transport and biodegradation of BTX compounds in saturated sandy soil', *Journal of Hazardous Materials,* 54, (3), pp. 155-174.

Moldrup, P., Olesen, T., Komatsu, T., Yoshikawa, S., Schjonning, P. and Rolston, D. E. (2003) 'Modeling diffusion and reaction in soils: X. A unifying model for solute and gas diffusivity in unsaturated soil', *Soil Science,* 168, (5), pp. 321-337.

Molz, F. J., Widdowson, M. A. and Benefield, L. D. (1986) 'Simulation of Microbial Growth Dynamics Coupled to Nutrient and Oxygen Transport in Porous Media', *Water Resources Research,* 22, (8), pp. 1207-1216.

Moyer, E. E., Ostendorf, D. W., Richards, R. J. and Goodwin, S. (1996) 'Petroleum hydrocarbon bioventing kinetics determined in soil core, microcosm and tubing cluster studies', *Ground Water Monitoring and Remediation,* 16, (1), pp. 141-153.

Muyzer, G., de Waal, E. C. and Uitterlinden, A. G. (1993) 'Profiling of complex microbial populations by denaturing gradient gel electrophoresis analysis of polymerase chain reaction-amplified genes coding for 16S rRNA', *Appl. Environ. Microbiol.,* 59, (3), pp. 695-700.

National Research Council (U.S.). Committee on Ground Water Cleanup Alternatives. (1994) *Alternatives for ground water cleanup.* Washington, D.C.: National Academy Press.

National Research Council (U.S.). Water Science and Technology Board. (1993) *In situ bioremediation : when does it work?* Washington, D.C.: National Academy Press.

Oliveira, F. C. C., Brandao, C. R. R., Ramalho, H. F., da Costa, L. A. F., Suarez, P. A. Z. and Rubim, J. C. (2007) 'Adulteration of diesel/biodiesel blends by vegetable oil as determined by Fourier transform (FT) near infrared spectrometry and FT-Raman spectroscopy', *Analytica Chimica Acta,* 587, (2), pp. 194-199.

Ostendorf, D. W., Hinlein, E. S. and Schoenberg, T. H. (2000) 'Aerobic biodegradation kinetics and soil gas transport in the unsaturated zone', in *Bioremediation of Contaminated Soils.* Vol. 22 New York: Marcel Dekker, pp. 607-632.

Ostendorf, D. W. and Kampbell, D. H. (1991) 'Biodegradation of Hydrocarbon Vapors in the Unsaturated Zone', *Water Resources Research,* 27, (4), pp. 453-462.

Osterreicher-Cunha, P., Guimaraes, J. R. D., Vargas, E. D. and da Silva, M. I. P. (2007) 'Study of biodegradation processes of BTEX-ethanol mixture in tropical soil', *Water Air and Soil Pollution,* 181, (1-4), pp. 303-317.

Osterreicher-Cunha, P., Vargas, E. D., Guimaraes, J. R. D., Lago, G. P., Antunes, F. D. and da Silva, M. I. P. (2009) 'Effect of ethanol on the biodegradation of gasoline in an unsaturated tropical soil', *International Biodeterioration & Biodegradation,* 63, (2), pp. 208-216.

Österreicher-Cunha, P., Vargas, E. d. A., Guimarães, J. R. D., de Campos, T. M. P., Nunes, C. M. F., Costa, A., Antunes, F. d. S., da Silva, M. I. P. and Mano, D. M. (2004) 'Evaluation of bioventing on a gasoline-ethanol contaminated

undisturbed residual soil', *Journal of Hazardous Materials,* 110, (1-3), pp. 63-76.

Oudot, J., Ambles, A., Bourgeois, S., Gatellier, C. and Sebyera, N. (1989) 'HYDROCARBON INFILTRATION AND BIODEGRADATION IN A LANDFARMING EXPERIMENT', *Environmental Pollution,* 59, (1), pp. 17-40.

ØVREÅS, L., Forney, L., Daae, F. L. and Torsvik, V. (1997) 'Distribution of bacterioplankton in meromictic lake Saelenvannet, as determined by denaturing gradient gel electrophoresis of PCR-amplified gene fragments coding for 16S rRNA', *Applied and Environmental Microbiology,* 63, (9), pp. 3367-3373.

Owsianiak, M., Chrzanowski, L., Szulc, A., Staniewski, J., Olszanowski, A., Olejnik-Schmidt, A. K. and Heipieper, H. J. (2009) 'Biodegradation of diesel/biodiesel blends by a consortium of hydrocarbon degraders: Effect of the type of blend and the addition of biosurfactants', *Bioresource Technology,* 100, (3), pp. 1497-1500.

Pasqualino, J. C., Montane, D. and Salvado, J. (2006) 'Synergic effects of biodiesel in the biodegradability of fossil-derived fuels', *Biomass & Bioenergy,* 30, (10), pp. 874-879.

Pasteris, G., Werner, D., Kaufmann, K. and Hohener, P. (2002) 'Vapor phase transport and biodegradation of volatile fuel compounds in the unsaturated zone: A large scale lysimeter experiment', *Environmental Science & Technology,* 36, (1), pp. 30-39.

Penet, S., Vendeuvre, C., Bertoncini, F., Marchal, R. and Monot, F. (2006) 'Characterisation of biodegradation capacities of environmental microflorae for diesel oil by comprehensive two-dimensional gas chromatography', *Biodegradation,* 17, (6), pp. 577-585.

Pielou, E. C. (1969) *An introduction to mathematical ecology.* New York,: Wiley-Interscience.

Piwoni, M. D. and Banerjee, P. (1989) 'Sorption of volatile organic solvents from aqueous solution onto subsurface solids', *Journal of Contaminant Hydrology,* 4, (2), pp. 163-179.

Powers, S. E., Hunt, C. S., Heermann, S. E., Corseuil, H. X., Rice, D. and Alvarez, P. J. J. (2001) 'The transport and fate of ethanol and BTEX in groundwater contaminated by gasohol', *Critical Reviews in Environmental Science and Technology,* 31, (1), pp. 79-123.

Prince, R. C., Haitmanek, C. and Lee, C. C. (2008) 'The primary aerobic biodegradation of biodiesel B20', *Chemosphere,* 71, (8), pp. 1446-1451.

Providenti, M. A., Lee, H. and Trevors, J. T. (1993) 'SELECTED FACTORS LIMITING THE MICROBIAL-DEGRADATION OF RECALCITRANT COMPOUNDS', *Journal of Industrial Microbiology,* 12, (6), pp. 379-395.

Provoost, J., Reijnders, L., Swartjes, F., Bronders, J., Seuntjens, P. and Lijzen, J. (2009) 'Accuracy of seven vapour intrusion algorithms for VOC in groundwater', *Journal of Soils and Sediments,* 9, (1), pp. 62-73.

Quince, C., Lanzen, A., Curtis, T. P., Davenport, R. J., Hall, N., Head, I. M., Read, L. F. and Sloan, W. T. (2009) 'Accurate determination of microbial diversity from 454 pyrosequencing data', *Nat Meth,* 6, (9), pp. 639-641.

Ruberto, L., Dias, R., Lo Balbo, A., Vazquez, S. C., Hernandez, E. A. and Mac Cormack, W. P. (2009) 'Influence of nutrients addition and bioaugmentation on the hydrocarbon biodegradation of a chronically contaminated Antarctic soil', *Journal of Applied Microbiology,* 106, (4), pp. 1101-1110.

Ruiz-Aguilar, G. M. L., Fernandez-Sanchez, J. M., Kane, S. R., Kim, D. and Alvarez, P. J. J. (2002) 'Effect of ethanol and methyl-tert-butyl ether on monoaromatic hydrocarbon biodegradation: response variability for different aquifer materials under various electron-accepting conditions', *Environmental Toxicology and Chemistry,* 21, (12), pp. 2631-2639.

Ryan, L., Convery, F. and Ferreira, S. (2006) 'Stimulating the use of biofuels in the European Union: Implications for climate change policy', *Energy Policy,* 34, (17), pp. 3184-3194.

Sabate, J., Vinas, M. and Solanas, A. M. (2004) 'Laboratory-scale bioremediation experiments on hydrocarbon-contaminated soils', *International Biodeterioration & Biodegradation,* 54, (1), pp. 19-25.

Schirmer, M., Molson, J. W., Frind, E. O. and Barker, J. F. (2000) 'Biodegradation modelling of a dissolved gasoline plume applying independent laboratory and field parameters', *Journal of Contaminant Hydrology,* 46, (3-4), pp. 339-374.

Schwarzenbach, R. P., Gschwend, P. M. and Imboden, D. M. (1993) *Environmental organic chemistry.* New York: J. Wiley.

Schwarzenbach, R. P. and Westall, J. (1981) 'Transport of nonpolar organic compounds from surface water to groundwater. Laboratory sorption studies', *Environ. Sci. Technol.,* 15, (11), pp. 1360-1367.

Seagren, E. A. and Becker, J. G. (2002) 'Review of natural attenuation of BTEX and MTBE in groundwater', *Practice Periodical of Hazardous, Toxic, and Radioactive Waste Management,* 6, (3), pp. 156-172.

Selinummi, J., Seppala, J., Yli-Harja, O. and Puhakka, J. A. (2005) 'Software for quantification of labeled bacteria from digital microscope images by automated image analysis', *Biotechniques,* 39, (6), pp. 859-863.

Shannon, C. E. and Weaver, W. (1963) *The mathematical theory of communication.* Urbana: University of Illinois Press.

Sharabi, N. E. and Bartha, R. (1993) 'TESTING OF SOME ASSUMPTIONS ABOUT BIODEGRADABILITY IN SOIL AS MEASURED BY CARBON-DIOXIDE

EVOLUTION', *Applied and Environmental Microbiology,* 59, (4), pp. 1201-1205.

Shumaker, J. L., Crofcheck, C., Tackett, S. A., Santillan-Jimenez, E. and Crocker, M. (2007) 'Biodiesel production from soybean oil using calcined Li-Al layered double hydroxide catalysts', *Catalysis Letters,* 115, (1-2), pp. 56-61.

Silka, L. R. (1988) 'Simulation of Vapor Transport through the Unsaturated Zone - Interpretation of Soil-Gas Surveys', *Ground Water Monitoring and Remediation,* 8, (2), pp. 115-123.

Singh, C. and Lin, J. (2009) 'Evaluation of nutrient addition to diesel biodegradation in contaminated soils', *African Journal of Biotechnology,* 8, (14), pp. 3286-3293.

Sleep, B. E. and Mulcahy, L. J. (1998) 'Estimation of biokinetic parameters for unsaturated soils', *Journal of Environmental Engineering-Asce,* 124, (10), pp. 959-969.

Somsamak, P., Richnow, H. H. and Haggblom, M. M. (2005) 'Carbon isotopic fractionation during anaerobic biotransformation of methyl tert-butyl ether and tert-amyl methyl ether', *Environmental Science & Technology,* 39, (1), pp. 103-109.

Song, D., Kitamura, M. and Katayama, A. (2010) 'Approach for Estimating Microbial Growth and Biodegradation of Hydrocarbon Contaminants in Subsoil Based on Field Measurements: 2. Application in a Field Lysimeter Experiment', *Environmental Science & Technology,* 44, (17), pp. 6795-6801.

Squillace, P. J., Moran, M. J., Lapham, W. W., Price, C. V., Clawges, R. M. and Zogorski, J. S. (1999) 'Volatile Organic Compounds in Untreated Ambient Groundwater of the United States, 1985-1995', *Environ. Sci. Technol.,* 33, (23), pp. 4176-4187.

Stapleton, R. D., Bright, N. G. and Sayler, G. S. (2000) 'Catabolic and genetic diversity of degradative bacteria from fuel-hydrocarbon contaminated aquifers', *Microbial Ecology,* 39, (3), pp. 211-221.

Stauffer, E. and Byron, D. (2007) 'Alternative fuels in fire debris analysis: Biodiesel basics', *Journal of Forensic Sciences,* 52, (2), pp. 371-379.

Stelzer, N., Büning, C., Pfeifer, F., Dohrmann, A. B., Tebbe, C. C., Nijenhuis, I., Kästner, M. and Richnow, H. H. (2006) 'In situ microcosms to evaluate natural attenuation potentials in contaminated aquifers', *Organic Geochemistry,* 37, (10), pp. 1394-1410.

Suarez, M. P. and Rifai, H. S. (1999) 'Biodegradation Rates for Fuel Hydrocarbons and Chlorinated Solvents in Groundwater', *Bioremediation Journal,* 3, (4), pp. 337 - 362.

Tancsics, A., Szabo, I., Baka, E., Szoboszlay, S., Kukolya, J., Kriszt, B. and Marialigeti, K. (2010) 'Investigation of catechol 2,3-dioxygenase and 16S rRNA gene

diversity in hypoxic, petroleum hydrocarbon contaminated groundwater', *Systematic and Applied Microbiology,* 33, (7), pp. 398-406.

Tiemann, J. E. M. a. M. (2006) *MTBE in Gasoline: Clean Air and Drinking Water Issues.* CRS

Trevelyan, G. M. (1952) *Illustrated English social history.* London, New York,: Longmans Green.

Tzeneva, V. A., Heilig, H. G. H. J., van Vliet, W. A., Akkermans, A. D. L., de Vos, W. M. and Smidt, H. (2008) '16S rRNA targeted DGGE fingerprinting of microbial communities', in Martin, C. C.(ed), *Methods in Molecular Biology.* Humana Press Inc, pp. 335-349.

U.S.EPA. (2004) 'Cleaning Up the Nation's Waste Sites: Markets and Technology Trends', *2004 Edition; EPA 542-R-04-015; Office of Solid Waste and Emergency Response, U.S. EPA: Washington, D.C., September 2004.*

USEPA. (1999) 'USE OF MONITORED NATURAL ATTENUATION AT SUPERFUND, RCRA CORRECTIVE ACTION, AND UNDERGROUND STORAGE TANK SITES'.

Van De Steene, J. and Verplancke, H. (2007) 'Estimating diesel degradation rates from N-2, O-2 and CO2 concentration versus depth data in a loamy sand', *European Journal of Soil Science,* 58, (1), pp. 115-124.

Vidali, M. (2001) 'Bioremediation. An overview', *Pure and Applied Chemistry,* 73, (7), pp. 1163-1172.

Vyas, T. K. and Dave, B. P. (2010) 'Effect of addition of nitrogen, phosphorus and potassium fertilizers on biodegradation of crude oil by marine bacteria', *Indian Journal of Marine Sciences,* 39, (1), pp. 143-150.

Waldner, C. L. (2008) 'The Association Between Exposure to the Oil and Gas Industry and Beef Calf Mortality in Western Canada', *Archives of Environmental & Occupational Health,* 63, (4), pp. 220-240.

Walworth, J. L. and Reynolds, C. M. (1995) 'Bioremediation of a petroleum-contaminated cryic soil: Effects of phosphorus, nitrogen, and temperature', *Journal of Soil Contamination,* 4, (3), pp. 299 - 310.

Wang, G., Reckhorn, S. B. F. and Grathwohl, P. (2003) 'Volatile Organic Compounds Volatilization from Multicomponent Organic Liquids and Diffusion in Unsaturated Porous Media', *Vadose Zone J,* 2, (4), pp. 692-701.

Wang, Q., Garrity, G. M., Tiedje, J. M. and Cole, J. R. (2007) 'Naive Bayesian classifier for rapid assignment of rRNA sequences into the new bacterial taxonomy', *Applied and Environmental Microbiology,* 73, (16), pp. 5261-5267.

Ward, D. M., Ferris, M. J., Nold, S. C. and Bateson, M. M. (1998) 'A Natural View of Microbial Biodiversity within Hot Spring Cyanobacterial Mat Communities', *Microbiol. Mol. Biol. Rev.,* 62, (4), pp. 1353-1370.

Werner, D., Broholm, M. and Hohener, P. (2005) 'Simultaneous estimation of diffusive volatile organic compound (VOC) fluxes and non-aqueous phase liquid (NAPL) saturation in the vadose zone', *Ground Water Monitoring and Remediation*, 25, (2), pp. 59-67.

Werner, D., Ghosh, U. and Luthy, R. G. (2006) 'Modeling polychlorinated biphenyl mass transfer after amendment of contaminated sediment with activated carbon', *Environmental Science & Technology*, 40, (13), pp. 4211-4218.

Werner, D. and Hohener, P. (2003) 'In Situ Method To Measure Effective and Sorption-Affected Gas-Phase Diffusion Coefficients in Soils', *Environ. Sci. Technol.*, 37, (11), pp. 2502-2510.

Whyte, L. G., Bourbonniere, L. and Greer, C. W. (1997) 'Biodegradation of petroleum hydrocarbons by psychrotrophic Pseudomonas strains possessing both alkane (alk) and naphthalene (nah) catabolic pathways', *Applied and Environmental Microbiology*, 63, (9), pp. 3719-3723.

Widdowson, M. A., Molz, F. J. and Benefield, L. D. (1988) 'A numerical transport model for oxygen- and nitrate-based respiration linked to substrate and nutrient availability in porous media', *Water Resources Research*, 24, (9), pp. 1553-1565.

Wilson, J. T., Leach, L. E., Henson, M. and Jones, J. N. (1986) 'In Situ Biorestoration as a Ground Water Remediation Technique', *Ground Water Monitoring & Remediation*, 6, (4), pp. 56-64.

Wolicka, D., Suszek, A., Borkowski, A. and Bielecka, A. (2009) 'Application of aerobic microorganisms in bioremediation in situ of soil contaminated by petroleum products', *Bioresource Technology*, 100, (13), pp. 3221-3227.

Wu, Y., Li, Y., Hui, L., Tan, Y. and Jin, S. (2009) 'Effects of ethanol on benzene degradation under denitrifying conditions', *Bulletin of Environmental Contamination and Toxicology*, 82, (2), pp. 145-152.

Xu, R. and Obbard, J. P. (2003) 'Effect of Nutrient Amendments on Indigenous Hydrocarbon Biodegradation in Oil-Contaminated Beach Sediments', *J Environ Qual*, 32, (4), pp. 1234-1243.

Zhou, E. and Crawford, R. L. (1995) 'Effects of oxygen, nitrogen, and temperature on gasoline biodegradation in soil', *Biodegradation*, 6, (2), pp. 127-140.

9. APPENDIX

n-pentane flux (g min^{-1} cm^{-2})	n-hexane flux (g min^{-1} cm^{-2})	Methylcyclopentane flux (g min^{-1} cm^{-2})	Cyclolhexane flux (g min^{-1} cm^{-2})	Isooctane flux (g min^{-1} cm^{-2})	Methylcyclohexane flux (g min^{-1} cm^{-2})	Toluene flux (g min^{-1} cm^{-2})	n-octane flux (g min^{-1} cm^{-2})	m-xylene flux (g min^{-1} cm^{-2})	1,2,4 TMB flux (g min^{-1} cm^{-2})	n-decane flux (g min^{-1} cm^{-2})	n-dodecane flux (g min^{-1} cm^{-2})
$4.8x10^{-07}$	$9.8x10^{-07}$	$6.5x10^{-07}$	$5.1x10^{-07}$	$7.3x10^{-07}$	$4.3x10^{-07}$	0.0	$1.1x10^{-07}$	0.0	$1.7x10^{-08}$	$2.6x10^{-07}$	$6.4x10^{-08}$
$2.2x10^{-07}$	$9.7x10^{-07}$	$7.6x10^{-07}$	$6.0x10^{-07}$	$1.0x10^{-06}$	$6.4x10^{-07}$	0.0	$1.0x10^{-07}$	$1.2x10^{-08}$	$2.4x10^{-08}$	$1.6x10^{-07}$	$7.8x10^{-08}$
$1.6x10^{-07}$	$9.6x10^{-07}$	$8.0x10^{-07}$	$6.2x10^{-07}$	$1.0x10^{-06}$	$6.8x10^{-07}$	0.0	$1.2x10^{-07}$	$1.6x10^{-08}$	$2.6x10^{-08}$	$1.6x10^{-07}$	$7.6x10^{-08}$
$6.4x10^{-08}$	$9.1x10^{-07}$	$7.9x10^{-07}$	$6.3x10^{-07}$	$1.1x10^{-06}$	$7.6x10^{-07}$	$1.1x10^{-08}$	$1.7x10^{-07}$	$2.8x10^{-08}$	$3.9 x10^{-08}$	$2.3 x10^{-07}$	$5.7 x10^{-08}$
$4.0 x10^{-08}$	$8.0 x10^{-07}$	$7.0 x10^{-07}$	$5.6 x10^{-07}$	$1.2 x10^{-06}$	$7.8 x10^{-07}$	0.0	$2.9 x10^{-07}$	$5.1 x10^{-08}$	$6.4 x10^{-08}$	$4.8x10^{-07}$	$1.0x10^{-07}$
$2.0x10^{-09}$	$6.2x10^{-07}$	$5.2x10^{-07}$	$5.4x10^{-07}$	$1.3x10^{-06}$	$8.2x10^{-07}$	0.0	$4.7x10^{-07}$	$8.0x10^{-08}$	$1.0x10^{-07}$	$8.8x10^{-07}$	$1.7x10^{-07}$
$1.9x10^{-09}$	$4.0x10^{-07}$	$3.3x10^{-07}$	$4.4x10^{-07}$	$1.3x10^{-06}$	$8.5x10^{-07}$	0.0	$7.4x10^{-07}$	$1.3x10^{-07}$	$1.6x10^{-07}$	$1.5x10^{-06}$	$2.8x10^{-07}$
0.0	$2.8x10^{-07}$	$8.0x10^{-08}$	$2.8x10^{-07}$	$1.4x10^{-06}$	$8.4x10^{-07}$	0.0	$9.6x10^{-07}$	$2.0x10^{-07}$	$2.4x10^{-07}$	$1.6x10^{-06}$	$4.4x10^{-07}$
0.0	$4.0x10^{-08}$	0.0	$8.0x10^{-08}$	$1.5x10^{-06}$	$8.4x10^{-07}$	0.0	$1.2x10^{-06}$	$2.8x10^{-07}$	$3.6x10^{-07}$	$1.6x10^{-06}$	$5.6x10^{-07}$

Table 9.1 Measured and estimated diffusive flux (g min^{-1} cm^{-2}) during volatilization of PP constituents

n-pentane flux (g min^{-1} cm^{-2})	n-hexane flux (g min^{-1} cm^{-2})	Methylcyclopentane flux (g min^{-1} cm^{-2})	Cyclolhexane flux (g min^{-1} cm^{-2})	Isooctane flux (g min^{-1} cm^{-2})	Methylcyclohexane flux (g min^{-1} cm^{-2})	Toluene flux (g min^{-1} cm^{-2})	n-octane flux (g min^{-1} cm^{-2})	m-xylene flux (g min^{-1} cm^{-2})	1,2,4 TMB flux (g min^{-1} cm^{-2})	n-decane flux (g min^{-1} cm^{-2})	n-dodecane flux (g min^{-1} cm^{-2})
$1.4x10^{-07}$	$8.0x10^{-07}$	$4.6x10^{-07}$	$4.0x10^{-07}$	$3.6x10^{-07}$	$1.0x10^{-07}$	$4.0x10^{-08}$	0.0	0.0	$3.6x10^{-08}$	$4.6x10^{-08}$	$1.0x10^{-07}$
$8.0x10^{-08}$	$6.0x10^{-07}$	$3.8x10^{-07}$	$3.0x10^{-07}$	$4.0x10^{-07}$	$1.8x10^{-07}$	$2.0x10^{-08}$	0.0	0.0	$2.0x10^{-08}$	$4.8x10^{-08}$	$7.6x10^{-08}$
$7.3x10^{-08}$	$5.5x10^{-07}$	$3.6x10^{-07}$	$2.7x10^{-07}$	$4.1x10^{-07}$	$2.0x10^{-07}$	$1.7x10^{-08}$	0.0	0.0	$1.6x10^{-08}$	$4.6x10^{-08}$	$6.5x10^{-08}$
$4.8x10^{-08}$	$4.4x10^{-07}$	$3.1x10^{-07}$	$2.3x10^{-07}$	$4.4x10^{-07}$	$2.4x10^{-07}$	$1.6x10^{-08}$	$4.0x10^{-08}$	$2.0x10^{-08}$	$1.6x10^{-08}$	$4.5x10^{-08}$	$4.6x10^{-08}$
$1.8x10^{-08}$	$3.0x10^{-07}$	$2.4x10^{-07}$	$1.8x10^{-07}$	$4.8x10^{-07}$	$2.9x10^{-07}$	$1.4x10^{-08}$	$8.8x10^{-08}$	$4.8x10^{-08}$	$1.6x10^{-08}$	$4.5x10^{-08}$	$2.6x10^{-08}$
0.0	$1.9x10^{-07}$	$1.8x10^{-07}$	$1.8x10^{-07}$	$4.7x10^{-07}$	$3.0x10^{-07}$	$1.7x10^{-08}$	$1.2x10^{-07}$	$6.1x10^{-08}$	$1.7x10^{-08}$	$3.8x10^{-08}$	$9.4x10^{-09}$
$2.0x10^{-09}$	$1.0x10^{-07}$	$1.3x10^{-07}$	$2.7x10^{-07}$	$3.8x10^{-07}$	$2.0x10^{-07}$	$3.2x10^{-08}$	$8.7x10^{-08}$	$4.6x10^{-08}$	$2.4x10^{-08}$	$1.3x10^{-08}$	$2.0x10^{-10}$
$1.6x10^{-08}$	$7.0x10^{-08}$	$8.0x10^{-08}$	$3.7x10^{-07}$	$3.0x10^{-07}$	$9.0x10^{-08}$	$4.6x10^{-08}$	$5.2x10^{-08}$	$2.6x10^{-08}$	$3.0x10^{-08}$	0.0	$1.0x10^{-10}$
$2.5x10^{-08}$	$2.9x10^{-08}$	$5.6x10^{-08}$	$4.5x10^{-07}$	$2.2x10^{-07}$	0.0	$5.8x10^{-08}$	$1.8x10^{-08}$	$9.7x10^{-09}$	$3.5x10^{-08}$	0.0	0.0

Table 9.2 Measured and estimated diffusive flux (g min^{-1} cm^{-2}) during volatilization of E10 constituents

n-pentane flux (g min^{-1} cm^{-2})	n-hexane flux (g min^{-1} cm^{-2})	Methylcyclopentane flux (g min^{-1} cm^{-2})	Cyclolhexane flux (g min^{-1} cm^{-2})	Isooctane flux (g min^{-1} cm^{-2})	Methylcyclohexane flux (g min^{-1} cm^{-2})	Toluene flux (g min^{-1} cm^{-2})	n-octane flux (g min^{-1} cm^{-2})	m-xylene flux (g min^{-1} cm^{-2})	1,2,4 TMB flux (g min^{-1} cm^{-2})	n-decane flux (g min^{-1} cm^{-2})	n-dodecane flux (g min^{-1} cm^{-2})
$1.6x10^{-07}$	$8.0x10^{-07}$	$6.8x10^{-07}$	$6.4x10^{-07}$	$9.0x10^{-07}$	$6.4x10^{-07}$	$4.0x10^{-08}$	$1.0x10^{-08}$	0.0	$2.8x10^{-08}$	0.0	$6.0x10^{-09}$
$4.7x10^{-08}$	$5.9x10^{-07}$	$4.4x10^{-07}$	$4.3x10^{-07}$	$7.0x10^{-07}$	$4.3x10^{-07}$	$2.7x10^{-08}$	$4.3x10^{-08}$	$4.3x10^{-09}$	$1.5x10^{-08}$	$5.8x10^{-08}$	$1.3x10^{-08}$
$3.7x10^{-08}$	$5.0x10^{-07}$	$3.8x10^{-07}$ h$3.7x10^{-07}$	$3.7x10^{-07}$	$6.4x10^{-07}$	$3.9x10^{-07}$	$2.5x10^{-08}$	$6.4x10^{-08}$	$8.0x10^{-09}$	$1.2x10^{-08}$	$1.4x10^{-07}$	$2.0x10^{-08}$
$1.7x10^{-08}$	$3.0x10^{-07}$	$2.5x10^{-07}$	$2.6x10^{-07}$	$5.4x10^{-07}$	$3.0x10^{-07}$	$2.1x10^{-08}$	$1.2x10^{-07}$	$1.6x10^{-08}$	$6.8x10^{-09}$	$3.5x10^{-07}$	$3.7x10^{-08}$
$3.4x10^{-09}$	$1.7x10^{-07}$	$1.5x10^{-07}$	$1.8x10^{-07}$	$4.8x10^{-07}$	$2.6x10^{-07}$	$1.6x10^{-08}$	$1.5x10^{-07}$	$2.1x10^{-08}$	$4.1x10^{-09}$	$4.6x10^{-07}$	$4.6x10^{-08}$
0.0	$1.1x10^{-07}$	$1.1x10^{-07}$	$1.4x10^{-07}$	$5.0x10^{-07}$	$2.6x10^{-07}$	$1.3x10^{-08}$	$1.4x10^{-07}$	$2.2x10^{-08}$	$5.6x10^{-09}$	$4.3x10^{-07}$	$4.4x10^{-08}$
0.0	$1.0x10^{-07}$	$9.0x10^{-08}$	$1.2x10^{-07}$	$5.6x10^{-07}$	$3.0x10^{-07}$	$5.0x10^{-09}$	$1.4x10^{-07}$	$2.1x10^{-08}$	$1.0x10^{-08}$	$3.0x10^{-07}$	$3.7x10^{-08}$
0.0	$7.8x10^{-08}$	$7.5x10^{-08}$	$1.1x10^{-07}$	$6.1x10^{-07}$	$3.3x10^{-07}$	$1.4x10^{-09}$	$1.2x10^{-07}$	$1.9x10^{-08}$	$1.4x10^{-08}$	$2.1x10^{-07}$	$3.1x10^{-08}$
0.0	$6.0x10^{-08}$	$6.0x10^{-09}$	$1.0x10^{-07}$	$6.6x10^{-07}$	$3.6x10^{-07}$	0.0	$1.0x10^{-07}$	$2.1x10^{-08}$	$2.2x10^{-08}$	$1.2x10^{-07}$	$3.0x10^{-08}$

Table 9.3 Measured and estimated diffusive flux (g min-1 cm-2) during volatilization of B20 constituents

Band number [a]	**Closest relative and accession number**	**Percent identity**	**Origin**	**Reference (if it was published in a journal)**	**Classification according to RDP classifier** [c]
1	*Pseudomonas sp.* c1(2011) 16S ribosomal RNA gene, partial sequence (HQ652598.1)	100%	Magnetite mine drainage		**Pseudomonas 85%**
2	Bacterium ASFP-1 16S ribosomal RNA gene, partial sequence, pa (HQ018734.1) Pseudomonas fluorescens partial 16S rRNA gene, strain CNE 10 (FR749873.1)	99% 99%	stress ecosystems of Karnataka nuclear materials	**Alagawadi,A.R., Mudenoor,M.G., Krishnaraj,P.U., Doddagoudar,C.K., Jagadeesh,K.S., Patil,S.G. and Biradar,D.P.** Identification of salt tolerant AIMs isolated from stress ecosystems of Karnataka Unpublished **Forte Giacobone,A.F.** Microbiological induced corrosion in nuclear materials Thesis (2012) Universidad de Buenos Aires, Argentina	**Pseudomonas 100%**
3	Uncultured bacterium clone d27 16S ribosomal RNA gene, partial sequence (DQ103582.1) Uncultured bacterium clone ncd181d11c1 16S ribosomal RNA gene, partial	100% 99%	environmental samples environmental samples	**Dong,M.S. and Zhou,J.Z.** Direct Submission Submitted (23-JUN-2005) Food Microbiology Lab, College of Food Science and Technology, Nanjing Agricultural University, Wei Gang Nanjing, Jiangsu 210095, P.R. China **Kong,H.H., Grice,E.A., Conlan,S., Deming,C.B., Freeman,A.F., Beatson,M., Nomicos,E., Young,A.C., Bouffard,G.G., Blakesley,R.W., Candotti,F., Holland,S.M., Murray,P.R., Green,E.D. and Segre,J.A.** Direct Submission	**Pseudomonas 96%**

	sequence (JF015032.1)			Submitted (28-DEC-2010) National Human Genome Research Institute (NHGRI), National Institutes of Health (NIH), Bethesda, MD 20892, USA	
4	Pseudomonas sp. BW004 16S ribosomal RNA gene, partial sequence (HQ710831.1) Pseudomonas mosselii strain TZQ14 16S ribosomal RNA gene, partial sequence (HQ202559.1)	100% 100%	Nitrogen heterocyclic compounds degrading strain Soil	**Zhao,C., Li,X.B., Zhang,J., Zhang,Y., Wen,D.H. and Tang,X.Y.** Simultaneous Biodegradation of Three Nitrogen Heterocyclic Compounds by Different Bacterial Consortia and Interaction of the Strains and Compounds Unpublished **Jin,F. and Du,B.** Screening and Identification of PGPR Unpublished	**Pseudomonas 100%**
5	Pseudomonas sp. CNE 2 partial 16S rRNA gene, strain CNE 2 (FR749860.1) Uncultured bacterium clone ncd366f05c1 16S ribosomal RNA gene, partial sequence (JF019062.1)	100% 100%	nuclear materials environmental samples	**Forte Giacobone,A.F.** Microbiological induced corrosion in nuclear materials Thesis (2012) Universidad de Buenos Aires, **Kong,H.H., Grice,E.A., Conlan,S., Deming,C.B., Freeman,A.F., Beatson,M., Nomicos,E., Young,A.C., Bouffard,G.G., Blakesley,R.W., Candotti,F., Holland,S.M., Murray,P.R., Green,E.D. and Segre,J.A.** Direct Submission Submitted (28-DEC-2010) National Human Genome Research Institute (NHGRI), National Institutes of Health (NIH), Bethesda, MD 20892, USA	**Pseudomonas 100%**
6	Uncultured bacterium clone OM3-56 16S	100%	petroleum hydrocarbon	**Tancsics,A., Szabo,I., Baka,E., Szoboszlay,S., Kukolya,J.,** **Kriszt,B. and Marialigeti,K.**	**Pseudomonas 52%**

	ribosomal RNA gene, partial sequence (HM447076.1) Pseudomonas andersonii strain ARUPPA4 16S ribosomal RNA gene, partial sequence (HM581514.1)	 100%	contaminated groundwater pulmonary granulomas	Investigation of catechol 2,3-dioxygenase and 16S rRNA gene diversity in hypoxic, petroleum hydrocarbon contaminated groundwater Syst. Appl. Microbiol. 33 (7), 398-406 (2010) PUBMED 20970942 **Simmon,K.E., Fang,D.C., Tesic,V., Han,X.Y., Petti,C.A. and She,R.C.** Clinical and molecular support for Pseudomonas andersonii (ex Han 2005) as a validated microorganism associated with pulmonary granulomas Unpublished	
7	Uncultured bacterium clone OM3-56 16S ribosomal RNA gene, partial sequence (HM447076.1) Pseudomonas andersonii strain ARUPPA4 16S ribosomal RNA gene, partial sequence (HM581514.1)	100% 100%	petroleum hydrocarbon contaminated groundwater pulmonary granulomas	**Tancsics,A., Szabo,I., Baka,E., Szoboszlay,S., Kukolya,J., Kriszt,B. and Marialigeti,K.** Investigation of catechol 2,3-dioxygenase and 16S rRNA gene diversity in hypoxic, petroleum hydrocarbon contaminated groundwater Syst. Appl. Microbiol. 33 (7), 398-406 (2010) PUBMED 20970942 **Simmon,K.E., Fang,D.C., Tesic,V., Han,X.Y., Petti,C.A. and She,R.C.** Clinical and molecular support for Pseudomonas andersonii (ex Han 2005) as a validated microorganism associated with pulmonary granulomas Unpublished	**Pseudomonadaceae 95%**
8	Pseudomonas andersonii strain ARUPPA4 16S ribosomal RNA gene, partial sequence	99%	pulmonary granulomas	**Simmon,K.E., Fang,D.C., Tesic,V., Han,X.Y., Petti,C.A. and She,R.C.** Clinical and molecular support for Pseudomonas andersonii (ex Han 2005) as a validated microorganism associated with pulmonary granulomas Unpublished	**Pseudomonadaceae 96%**

	(HM581514.1) Pseudomonas andersonii strain ARUPPA3 16S ribosomal RNA gene, partial sequence (HM581513.1)	99%	pulmonary granulomas	**Simmon,K.E., Fang,D.C., Tesic,V., Han,X.Y., Petti,C.A. and She,R.C.** Clinical and molecular support for Pseudomonas andersonii (ex Han 2005) as a validated microorganism associated with pulmonary granulomas Unpublished	
9	Uncultured bacterium clone OM3-56 16S ribosomal RNA gene, partial sequence (HM447076.1) Pseudomonas andersonii strain ARUPPA4 16S ribosomal RNA gene, partial sequence (HM581514.1)	100% 100%	petroleum hydrocarbon contaminated groundwater pulmonary granulomas	**Tancsics,A., Szabo,I., Baka,E., Szoboszlay,S., Kukolya,J., Kriszt,B. and Marialigeti,K.** Investigation of catechol 2,3-dioxygenase and 16S rRNA gene diversity in hypoxic, petroleum hydrocarbon contaminated groundwater Syst. Appl. Microbiol. 33 (7), 398-406 (2010) PUBMED 20970942 **Simmon,K.E., Fang,D.C., Tesic,V., Han,X.Y., Petti,C.A. and She,R.C.** Clinical and molecular support for Pseudomonas andersonii (ex Han 2005) as a validated microorganism associated with pulmonary granulomas Unpublished	**Pseudomonadaceae 100%**
10	Uncultured marine bacterium clone SiDJun08M43 16S ribosomal RNA gene, partial sequence (GU326513.1)	99%	environmental samples	**Manes,C.L., West,N., Rapenne,S. and Lebaron,P.** Dynamic bacterial communities on reverse-osmosis membranes in a full-scale desalination plant Biofouling 27 (1), 47-58 (2011) PUBMED 21108068	**Pseudomonas 100%**

	Uncultured bacterium clone BL1289fO5 16S ribosomal RNA gene, partial sequence (HM445212.1)	99%	environmental samples	**Hathaway,J.J., Garcia,M.G., Moya,M., Spilde,M.N., Stone,F.D., Dapkevicius,L.M. and Northup,D.E**. Investigation of Novel Microbial Diversity in Azorean and Hawaiian Lava Tubes Unpublished	
11	Uncultured bacterium clone D70 16S ribosomal RNA gene, partial sequence (GQ389198.1) Uncultured bacterium clone D60 16S ribosomal RNA gene, partial sequence (GQ389188.1)	98% 98%	drinking water distribution system during serious red water outbreak drinking water distribution system during serious red water outbreak	**Li,D. and Yang,M.** Composition of bacterial communities of drinking water distribution system during water quality deterioration. Unpublished Direct Submission Submitted (16-JUL-2009) State Key Lab of Water Quality, Research Center for Eco-Environmental Science, Shuangqing 18, Haidian District, Beijing 100085, China **Li,D. and Yang,M.** Composition of bacterial communities of drinking water distribution system during water quality deterioration. Unpublished Direct Submission Submitted (16-JUL-2009) State Key Lab of Water Quality, Research Center for Eco-Environmental Science, Shuangqing 18, Haidian District, Beijing 100085, China	**Pseudomonadaceae 96%**
12	Uncultured bacterium clone F776O8Q01A4JRN 16S ribosomal RNA gene, partial sequence (GU775327.1) Uncultured bacterium	98% 98%	drinking water (treatment 3) drinking water (treatment 3)	**Kwon,S., Kim,T. and Park,H.** Direct Submission Submitted (11-FEB-2010) School of Civil, Environmental & Architectural Engineering, Korea University, Anam-Dong, Seoungbuk-Gu, Seoul 136-713, South Korea **Kwon,S., Kim,T. and Park,H.** Direct Submission Submitted (11-FEB-2010) School of Civil, Environmental	**Pseudomonas 63%**

	clone F776O8Q01AV4E3 16S ribosomal RNA gene, partial sequence (GU763439.1)			& Architectural Engineering, Korea University, Anam-Dong, Seoungbuk-Gu, Seoul 136-713, South Korea	

Table 9.4 Nearest neighbour of the cloned sequences from nutrient unamended and amended microcosms of pure and blended-fuel polluted soil

[a] *The numbers correspond to the band numbers in Figure 7.12*
[b] *Closest relative of the sequence obtained from the DGGE band and the sequence of the closest relative found in the GenBank database.*
[C] *Classification according to RDP classifier. For partial sequences of length shorter than 250 bps (longer than 50 bps), a bootstrap cutoff of 50% was shown to be sufficient to accurately classify sequences at the genus level, and to provide genus level assignments for higher percentage of sequences.*

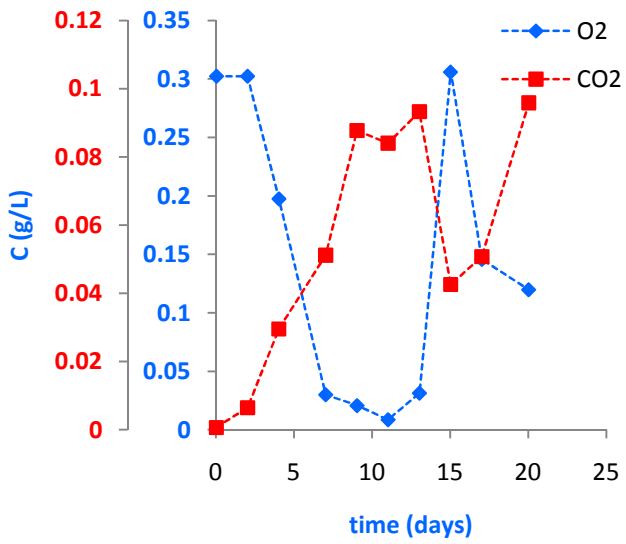

Figure 9.1 Correlation between O_2 consumption and CO_2 production for E10 mixture nutrient amended

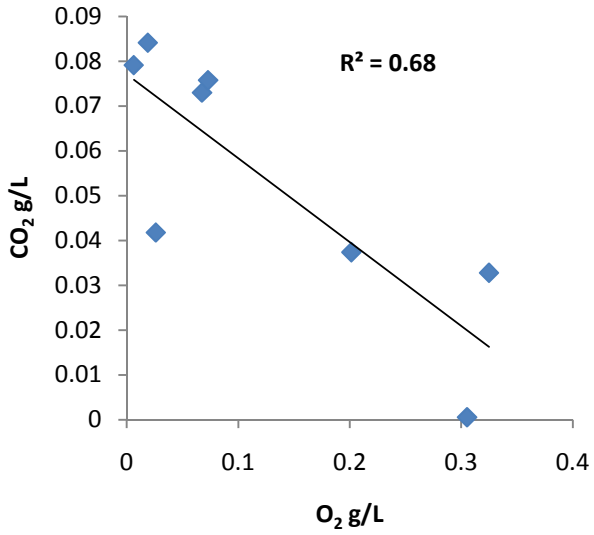

Figure 9.2 Degree of correlation between O_2 consumption and CO_2 production for PP nutrient amended

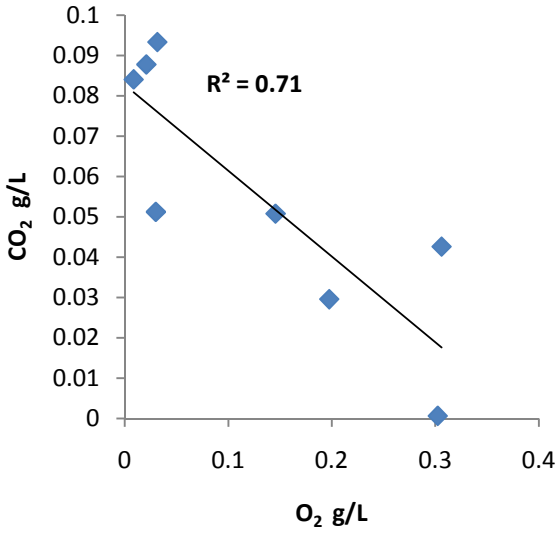

Figure 9.3 Degree of correlation between O_2 consumption and CO_2 production for E10 nutrient amended

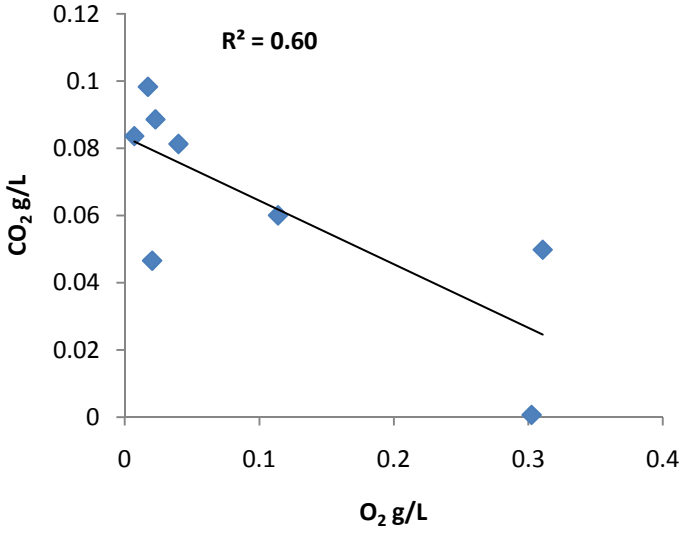

Figure 9.4 Degree of correlation between O_2 consumption and CO_2 production for B20 nutrient amended

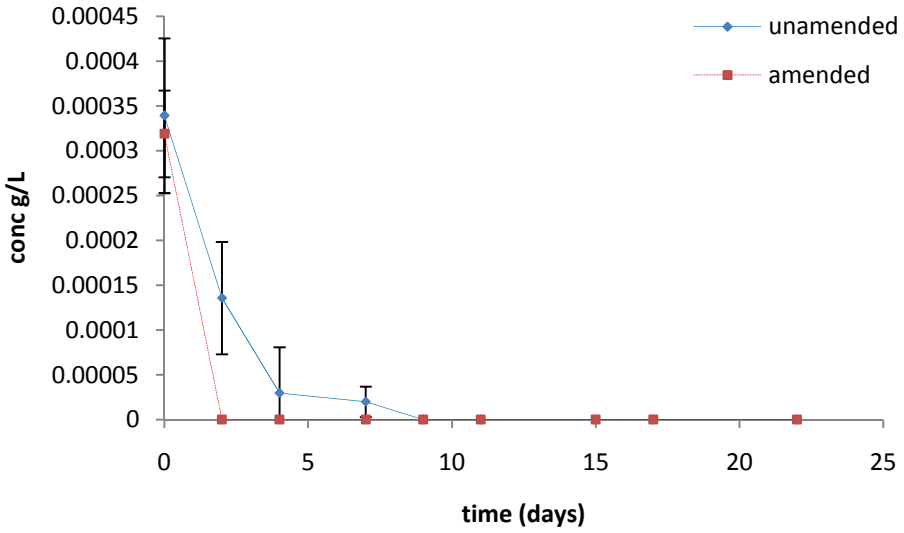

Figure 9.5 Changes in average vapour-phase concentrations for Ethanol in E10 mixtures during incubation, nutrient unamended (continuous line) and nutrient amended (dashed line). Error bars: ±1 standard deviation (SD, n=3).